Neuroimaging of human auditory cortex: data analysis and applications

THÈSE N^{O} 7672 (2017)

PRÉSENTÉE LE 23 MARS 2017

À LA FACULTÉ DES SCIENCES ET TECHNIQUES DE L'INGÉNIEUR
LABORATOIRE DE TRAITEMENT D'IMAGES MÉDICALES
PROGRAMME DOCTORAL EN NEUROSCIENCES

ÉCOLE POLYTECHNIQUE FÉDÉRALE DE LAUSANNE

POUR L'OBTENTION DU GRADE DE DOCTEUR ÈS SCIENCES

PAR

Naghmeh GHAZALEH

acceptée sur proposition du jury:

Prof. O. Blanke, président du jury
Prof. D. N. A. Van De Ville, Dr M. Saenz, directeurs de thèse
Prof. N. Golestani, rapporteuse
Prof. D. Bueti, rapporteuse
Prof. S. Micera, rapporteur

ÉCOLE POLYTECHNIQUE
FÉDÉRALE DE LAUSANNE
Suisse
2017

Your assumptions are your windows on the world.
Scrub them off every once in a while, or the light won't come in.
— Isaac Asimov

Acknowledgements

I would like to express my deepest gratitude and appreciation to my amazing PhD advisors, Dr. Melissa Saenz and Prof. Dimitri Van De Ville. Not only they have been tremendous mentors, they have also been great friends for me. Melissa, your enormous kindness and unlimited support fortified my passion for neuroscience; Dimitri, your bright mind, your brilliant ideas, and your cheerful inspiration in developing new ideas inspired me to fully enjoy my everyday work in research. Thank you both for your generous guidance and support. I could not have imagined having better advisors than you.

My sincere thanks also go to Dr. Raphael Maire for his precious support, guidance and collaboration that we had in working with tinnitus patients. Thanks as well to Dr. Wietske van der Zwaag for patiently training and helping me to use the high-resolution scanner at CIBM.

I would like to thank my defense jury committee, Prof. Narly Golestani, Prof. Domenica Bueti, Prof. Silvestro Micera and Prof. Olaf Blanke, for their encouragement and insightful comments about my dissertation and my research work. In addition, I would like to thank Giulia and Thomas for their kind and thorough proofreading of this dissertation.

I am also very grateful to Prof. Karl Friston and Dr. Adeel Razi for hosting me in the Functional Imaging Lab in UCL, for what was a truly inspiring academic visit.

I would like to thank EPFL and Swiss National Science Foundation and EPFL for providing the funding which allowed me to undertake this research.

My warmest thanks go to my current and former labmates in MIPLAB, for all our interesting scientific discussions, and above all, for the amazingly friendly laboratory environment that you have generated. For many delicious memories that were baked

by Giulia! as well as many good memories shared with Thomas, Zafer, Rotem, Nora, Daniela, Lorena, Anjali, Nicola, Jeff, Djalel, Valeria, Kirsten and Elvira; the warm and pleasant discussions shared with Yasaman; and the genuine moments of excitement illuminating the games played with them, as well as with Anais, Merel, Stefano, Antwnis, Helena and Luca. I also want to address special thanks to our joyful laboratory assistants Ruth and Manuela, for their kind and caring attitude.
Thanks to my students, who gave me the opportunity to practice my teaching skills. Thanks also to all the tinnitus patients and healthy subjects that participated in my studies.
I am also very thankful to Dr. Eleonora Fornari and Dr. Giovanni Batistela, who supervised me in my internship at CHUV as my first experience of working in the neuroimaging field, prior to my PhD; this sparked my interest for the domain, and made me interested to continue this field towards PhD.
My cordial thanks go to my friends that made my life in Switzerland more chocolaty. In particular, many thanks go to Dordaneh, Maryam, Amir, Natacha, Mohsen, and especially to Queen Elena! also special gratitude to Mahdad who was a great support for me in taking this journey and was the source of my inspiration.
Last but not least, my heartful thanks go to my family: my parents that have always believed in me and my sisters Nooshin and Nargess who are very special parts of my life, thank you for your unconditional and unlimited love, care, and support.

To love, the truest...

Abstract

Modern neuroimaging technologies provide us with non-invasive methods for studying structure and function, and plasticity of the human auditory cortex. Here we have acquired high spatial resolution functional magnetic resonance imaging (fMRI) data of the auditory cortex in patients with unilateral hearing loss and tinnitus. Compared to healthy controls, we found evidence of over-representation and hyperactivity in parts of cortical tonotopic map that correspond to low frequencies sounds, irrespective of the hearing loss and tinnitus range, which in most cases affected higher frequencies. These findings suggest that hearing loss has a destabilizing effect on the tonotopic organization in primary auditory cortex that is not restricted to the corresponding frequency range of hearing loss and tinnitus.

One of the challenges in tinnitus studies is the high relevance of the hyperacusis condition in these patients. The similarity and co-occurrence of these two disorders contributes to the debate about the specificity of findings associated with tinnitus alone. For classifying tinnitus patients with and without hyperacusis, we thus implemented partial least square correlation (PLSC) analysis that builds upon the cross-covariance information between audiogram and fMRI data. This method provides us with a multi modal measure to successfully detect the hyperacusis condition in tinnitus patients with 80% cross-validation accuracy, for the first time. The PLSC driven biomarker, also yields the brain area playing a major role in the condition.

There is a vast heterogeneity in the anatomy of auditory cortex across subjects, therefore individualized delineation the exact border between primary and secondary auditory cortex is a demanding research topic. Here we established a model of extrinsic connectivity of auditory cortex with the two other regions of the brain that have discriminative connectivity with primary and secondary auditory cortices. The

resting state fMRI connectivity features are used for segmentation and are performed exploiting two methods as dynamical causal modeling (DCM) of effective connectivity with 74% accuracy and functional connectivity with 71% accuracy. This data-driven segmentation method, not only facilitate the definition of auditory cortex subregions for fundamental research in the normal brain, but also yields a useful tool for following the modification in the functional anatomy of this region as a result of hearing disorders like tinnitus.

Key words: Auditory cortex, High-field fMRI, Tinnitus, Hyperacusis, Functional connectivity, Effective connectivity

Résumé

Les technologies de neuroimagerie moderne fournissent des méthodes non invasives pour l'étude de la structure, la fonction, et la plasticité du cortex auditif humain. Ici nous avons acquis, au moyen d'une imagerie par résonance magnétique fonctionnelle (IRMf) à haute résolution spatiale, des données sur le cortex auditif de patients présentant une perte auditive unilatérale associée à un acouphène. Par rapport à des témoins sains, nous avons trouvé des preuves d'une sur-représentation et d'une hyperactivité dans certaines parties de la carte tonotopique du cortex auditif qui correspondent au domaine des basses fréquences, indépendamment de la localisation de la perte auditive et de l'acouphène qui, dans la plupart des cas, touchent les fréquences plus élevées. Ces résultats suggèrent que la perte de l'audition a un effet déstabilisateur sur l'organisation tonotopique du cortex auditif primaire qui n'est pas limité aux fréquences de la perte auditive et des acouphènes.

Un des défis des études de l'acouphène est la grande incidence de l'hyperacousie rapportée chez les mêmes patients. La similitude et la co-occurrence de ces deux troubles contribuent au débat sur la spécificité des résultats associés à l'acouphène seul. Pour classer les patients atteints d'acouphènes associés ou non à de l'hyperacousie, nous avons utilisé la méthode « partial least square correlation (PLSC) » qui s'appuie sur l'information des covariance croisées entre audiogramme et données de l'IRMf. Cette méthode fournit pour la première fois une mesure multi modale permettant de détecter la condition d'hyperacousie chez les patients atteints d'acouphènes, avec une validation de 80%. La PLSC permet également d'identifer la/les région(s) du cerveau jouant un rôle majeur dans cet état.

Il y a une grande hétérogénéité inter-individuelle dans l'anatomie de cortex auditif et la délimitation de la frontière exacte entre les cortex auditifs primaire et secondaire

est un sujet de recherche actuel. Ici nous avons créé un modèle de connectivité extrinsèque du cortex auditif avec les deux autres régions du cerveau qui présentent une connectivité discriminante avec les cortex auditifs primaire et secondaire. Les caractéristiques de connectivité de l'état de repos données par l'IRMf sont utilisées pour la segmentation, exploitant deux méthodes comme la modélisation causale dynamique (DCM) de la connectivité efficace, avec une précision de 74%, ou la connectivité fonctionnelle avec une précision de 71%. Cette méthode de segmentation de données permet non seulement de définir les sous-régions du cortex auditif utiles pour l'étude du cerveau sain, mais représente également un outil puissant pour trouver une altération dans l'anatomie fonctionnelle de cette région à la suite de troubles auditifs tels que l'acouphène.

Mots clefs : Cortex auditif, l'IRMf à haut champ, acouphène, hyperacousie, connectivité fonctionnelle, connectivité efficace

Contents

1 Introduction

1.1 Motivation

Established before birth, our hearing sense shapes our connection to the external world in a remarkable manner: through the successive exposure to exquisitely rich and varied sounds, information about the environment in which we live can be gathered. Different types of hearing loss can interfere with the delicate auditory nervous system machinery, leading to unwanted plastic changes in the auditory cortex generation central hearing disorders. Tinnitus, the phantom perception of a sound in the absence of any external auditory stimulus, is one of the most common hearing disorders, affecting 10% of adults [Axelsson and Ringdahl, 1989]. In the most common type of tinnitus (subjective tinnitus), the phantom perception originates from aberrant activity of central auditory neurons [Roberts et al., 2010, Schaette and McAlpine, 2011, Eggermont and Tass, 2015, Elgoyhen et al., 2015]. Despite the potentially detrimental impact of tinnitus on the lives of affected individuals, no effective treatment is currently available [Langers et al., 2012].

Animal studies have consistently found a link between tinnitus and downstream neurophysiological changes in the central auditory system (midbrain, thalamic, and cortical areas). Distortions are seen in the tonotopic frequency maps of the primary auditory cortex. Many studies described this distortion as an overrepresentation of the hearing loss or hearing-loss edge and have interpreted this is as the causal factor

of tinnitus (maladaptive plasticity hypothesis) [Eggermont and Komiya, 2000, Seki and Eggermont, 2003, Noreña and Eggermont, 2003, Noreña and Eggermont, 2005]. On the other hand, other recent studies describe a broader pattern of neural activity changes, with map distortions occurring in relatively low-frequency areas away from hearing loss and presumed tinnitus range [Engineer et al., 2011, Yang et al., 2011]. In human neuroimaging studies of tinnitus, altered primary auditory cortex activity have been described [Langers et al., 2012, Wienbruch et al., 2006].In one such study analyzing functional magnetic resonance imaging (fMRI) data [Langers et al., 2012], in primary auditory cortex hyper-activity was detected, but a link to a specific part of the tonotopic map could not be established due to inter-subject brain averaging. High-resolution neuroimaging methods may thus be expected to provide a more potent tool for accurately studying the small primary auditory cortex area, permitting tonotopic mapping in individual subjects. Here we have happed high-resolution functional MRI imaging at 7 Tesla (ultra-high field strength) to test for plastic changes in the tonotopic maps of primary auditory cortex of hearing loss and tinnitus patients. This subject is investigated in the first study of this thesis.

One of the vivid challenges in tinnitus studies is the high co-occurrence of hyperacusis in these patients; i.e., decreased tolerance to normal environmental sounds. The co-occurrence of these two disorders demonstrates the inherent difficultly of disentangling the effects of tinnitus from other co-occurring effects of peripheral hearing loss [Salloum et al., 2016]. To date, there have been very few studies attempting to discriminate the potential sources of both conditions [Zeng, 2013] and for this purpose, finding a reliable method to detect hyperacusis in tinnitus patients is crucial. Here we present a novel application of a partial least square correlation (PLSC) analysis, which classifies the presence or absence of hyperacusis based on the cross-covariance between the patient's audiogram (behavioral) and fMRI data. This subject is investigated in the second study of this thesis.

The non-invasive identification and parcellation of auditory cortex subregions is another challenging issue in the field. Because of inter-individual anatomical differences, defining the exact border between primary and secondary auditory cortex is a

daunting task. Using common brain atlases that are based on the average anatomical properties of a group of subjects will not be accurate enough, and although parcellations of the auditory cortex based on myelin density or auditory tasks have been extracted in some studies [Dick et al., 2012, De Martino et al., 2015], they remain constrained by the experimental design parameters. Finding a reproducible parcellation method that uses features independent from any experimental setting appears an elegant strategy to bypass this complexity. Resting state functional connectivity consists of an appealing option towards this direction and is increasingly used for the parcellation of other regions of the brain [Shen et al., 2010, Chen et al., 2008, De Luca et al., 2006, Golland et al., 2008, Achard et al., 2006, Barnes et al., 2010, Kim et al., 2010, Li et al., 2015]. Resting state fMRI data can be acquired in a very short time and without any dependence on an experimental task. To harvest this potential, and at the same time enhance the ability to accurately model biological interactions between brain regions, features related to effective brain connectivity stand as ideal candidates to overcome the obstacles towards a precise auditory cortex parcellation method. This subject is investigated in the third study of the thesis.

1.2 Outline and contributions

This thesis is presented as the compiled version, of several journal articles. The following chapter presents an overview of the principles of fMRI data acquisition as a tool for acquiring data for studying auditory cortex functional activity and also an overview of auditory nervous system and related disorders. After this background, we present the journal articles in chapters three to five. The sixth chapter concludes the thesis and conveys outlooks for the future studying. My contribution in the journal papers are as below:

Chapter 3: ***High-Resolution fMRI of Auditory Cortical Map Changes in Unilateral Hearing Loss and Tinnitus.*** N. Ghazaleh, W. Van der Zwaag, R. Maire, D. Van De Ville S. Clarke and M. Saenz, Brain topography, in press.

Contribution: The main author, contributed to all aspects of the work: Data acquisi-

tion with 7T MRI scanner, Data analysis and writing.

In this work, ultra high-field fMRI at 7 Tesla is applied to investigate the altered functional activity in the primary auditory cortex of patients with unilateral hearing loss and tinnitus. We used 7T fMRI scanner to acquire high-resolution fMRI data. This data with higher signal to noise ratio comparing to the recent human study [Langers et al., 2012] that has acquired fMRI data at 3 Tesla, allows tonotopic mapping of primary auditory cortex on an individual subject basis. Eleven patients with unilateral hearing loss and tinnitus were compared to normal- hearing controls. Patients showed an over-representation and hyperactivity in the part of the cortical map that corresponds to low frequencies sounds, irrespective of the hearing loss and tinnitus range, which in most cases affected higher frequencies. This large low-frequency distortion is consistent with the previous findings in animal models. Overall, the findings suggest that hearing-loss has a destabilizing effect on the tonotopic organization of primary auditory cortex that is not restricted to the hearing loss and tinnitus frequency range.

Chapter 4: ***Detection of hyperacusis condition in tinnitus patients based on PLSC features that link audiogram and fMRI tonotopy responses***. N. Ghazaleh, W. Van der Zwaag, R. Maire, M. Saenz and D. Van De Ville, Front. Syst. Neurosci, submitted.

Contribution: The main author, contributed to all aspects of the work: Data acquisition with 7T MRI scanner, Data analysis and writing.

Our goal in this study is detection of hyperacusis condition in tinnitus patients. To this purpose ,from the same tinnitus patients as in the study of chapter three, we acquire audiogram measurements that involve peripheral auditory system and for central auditory systems we acquired high-resolution fMRI at 7T to picture the tonotopic maps of the primary auditory cortex as a meaningful measure of brain activity. These measures do not provide sufficient information for spotting the hyperacusis condition when considered separately. To get meaningful biomarkers for classifying tinnitus patients with and without hyperacusis, we implemented for the first time partial least square correlation analysis (PLSC) that builds upon the cross-covariance information between audiogram and fMRI data. The cross-covariance of these two sets of data

proved to provide us with metrics for successfully detecting this condition in tinnitus patients with 80% of accuracy and it is the first classifier that can detect hyperacusis condition in tinnitus patients.The PLSC obtained biomarkers, also localize the brain area playing a major role in the condition. These findings provide precious insight for the clinical study of hyperacusis and its treatment.

Chapter 5: ***Subject-specific parcellation of auditory cortex based on resting state fMRI functional and effective connectivity.***. N. Ghazaleh, A. Razi, S. Kumar, G. Pretti, K. Friston, M. Saenz and D. Van De Ville, Neuroimage, in preparation.

Contribution: The main author, contributed to all aspects of the work: Data analysis and writing.

Segmentation of auditory cortex based on anatomical atlases is not enough precise because of the huge differences in the topography of auditory cortex among individuals. Here we are going to use the pattern of extrinsic connectivity of auditory cortex as the segmentation feature and exploit two methods of effective connectivity and functional connectivity. The problem is defined as segmentation of auditory cortex as the target region in two subregions of primary and the secondary auditory cortex. For this purpose, we have built the model of effective connectivity of the voxels inside the auditory cortex with two other regions of the brain that have discriminative connections with primary and secondary auditory cortex. These source regions of interests are basolateral amygdala and hippocampus. Auditory cortex has been divided smaller auditory patches, for each of them, we derive DCM effective connectivity with three ROIs: auditory patch and the two source regions. Similarly, for functional connectivity approach, we make drive the correlation of the resting state activity of each auditory patch with the source regions. Spectral clustering of the graph model of auditory cortex represents the two subregions of primary and secondary auditory cortex with 74% accuracy for DCM based and 71% for FC based segmentation, in average for both hemispheres. This segmentation method built upon effective connectivity take advantage of the information about the influence of the neurons on each other versus the functional connectivity parameters which is a measure of statistical dependencies

and leads to the lower clustering accuracy. This successful data-driven segmentation method, not only ease defining the subregions of the auditory cortex for studying healthy brain but also yields a powerful tool for following the modification in the functional anatomy of this region in the result of hearing disorders like tinnitus.

2 Background

2.1 Brain imaging

Human beings have always been curious about unraveling the mysteries of the brain, with motivations ranging from understanding of its underlying biological working principles, medical diagnosis, or mind reading. To those aims a large panel of non-invasive neuroimaging techniques can be used for human brain imaging. Different types of magnetic resonance imaging (MRI) techniques have enabled investigation of the structures and functions in the central nervous system, in normal or pathological condition. Structural MRI techniques are used to study the anatomy of the brain and functional MRI (fMRI) is used to study functional activity of the brain. The first fMRI data get acquired in early 1991 in NMR Center at the Massachusetts General Hospital (Fig.2.1) and led to remarkable findings in neuroscience research. This technique provides a relatively high spatial resolution and is used in the data acquisition of the projects, discussed in this dissertation. In this section, after an overview of the principles of MRI, we describe the fMRI technique, and how it reflects neuronal activity. Later on, we tackle the issues of ultra-high field MRI, as well as task based and resting state fMRI [Ashburner, 2009].

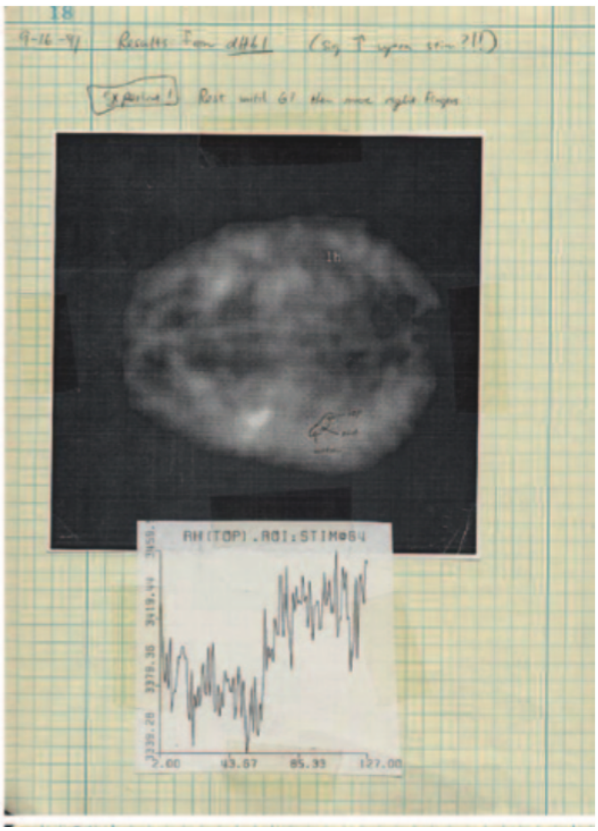

Figure 2.1 – Notes of Peter Bandettini on analyzing the result of the first human fMRI data, acquired in 1991in Massachusetts General Hospital. Reprinted with permission from [Bandettini, 2015].

2.1.1 Magnetic resonance imaging (MRI)

Magnetic resonance imaging is a tool used to picture different organs of the body and their activity thanks to magnetic fields. MRI acquisition is based on the science of nuclear magnetic resonance (NMR).

When the subject is inside the magnetic field (B) of the scanner, magnetic moments of the hydrogen protons of the body share a similar direction parallel to the field (low energy state), while a few of them point in an anti parallel direction (high energy state) forced by the magnetic field that creates a net magnetic moment M. The nuclear magnetic moment oscillates, around the axis of the direction of the magnetic field. This oscillatory motion is called *precession*. The frequency of the precession is directly proportional to the strength of the magnetic field. It means that nuclei can be tuned to

a different frequency by changing the strength of the magnetic field. When applying a radio-frequency (RF) pulse with the same frequency as precession, a resonance phenomenon occurs and nuclei flip into the high energy state. By changing alignment, the direction of the protons towards the transverse plane is increased. When the RF pulse stops, transverse magnetization vanishes. Nuclei then start emitting the radio frequency pulse and go back to the equilibrium state over the duration of a relaxation time. This emitted signal provides the measure that drives the intensity of the images. Different relaxation times characterize different tissues. $T1$ is the longitudinal relaxation time, which corresponds to the time period that the excited proton requires to return to equilibrium, and is also the time taken by the spinning protons to re-align with the external magnetic field [Dougherty et al., 2008]. $T2$ is the transverse relaxation time and is defined as the rate at which excited protons reach the equilibrium state, and also as the time for loss of coherence phase of the spinning protons. Spatial localization is obtained by applying magnetic gradients, which are magnetic fields whose strength changes gradually across an axis; hence, depending on the field strength, the precession frequency of protons varies as a function of their location. Acquisition of anatomical images is mostly based on $T1$values with a short repetition time (TR) to maximize the difference in longitudinal relaxation during the return to equilibrium, and a short echo time (TE) to minimize $T2$ relaxation effects. In $T1$ weighted images, tissues with high fat content (e.g. white matter) appear bright and regions filled with water (e.g. cerebrospinal fluid) appear darker [Dougherty et al., 2008, Weishaupt et al., 2008].

2.1.2 Functional magnetic resonance imaging (fMRI)

Functional magnetic resonance provides us with an indirect measure of neural activity, which is based on metabolic coupling (Fig.2.2). This form of MRI is blood oxygenation level dependent (BOLD) imaging. Changes in the BOLD signal happen with a 1 to 2 second delay after neural activity, and follows three phases (Fig.2.3). In hemodynamic response (HR), glucose and oxygen (O_2) are constantly supplied by cerebral blood flow to the brain to maintain neural activity. It means that in the active areas of the

brain, glucose metabolism, O_2 metabolism, blood flow and blood volume all increase. The increase in oxygenated hemoglobin occurs in the capillary beds near the region of neural activity. Increased oxygenated hemoglobin and increased blood flow lead to a momentary decrease of deoxygenated hemoglobin during the initial phase. Then, a large increase is observed during the overcompensation of oxygenated blood 4-6 seconds later, before a decrease back to below baseline and an eventual return to baseline level following another 5-10 seconds. Deoxygenated hemoglobin is greatly paramagnetic (unlike oxygenated hemoglobin), and thus, its increase introduces an inhomogeneity into the nearby magnetic field and increases the intensity of the image [Heeger and Ress, 2002].

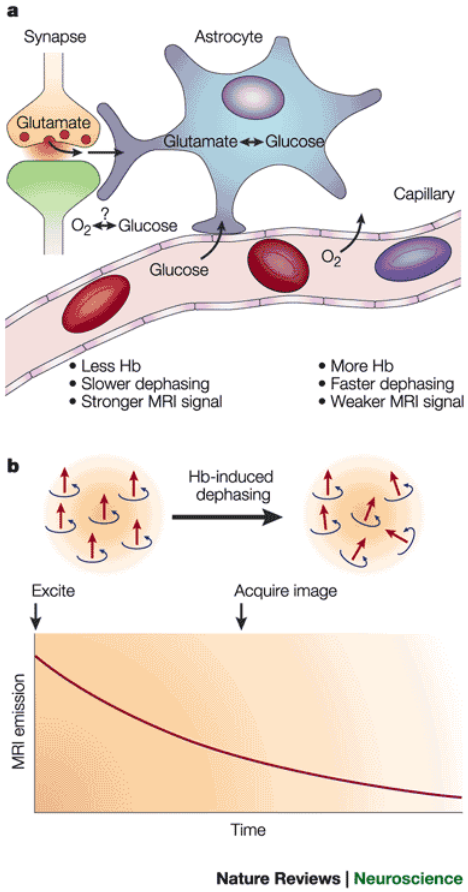

Figure 2.2 – Neurovascular coupling in response to neural activity. Reprinted with permission from [Heeger and Ress, 2002]

Acquiring fMRI data is done by consecutive sampling of the BOLD signal. Here, TR

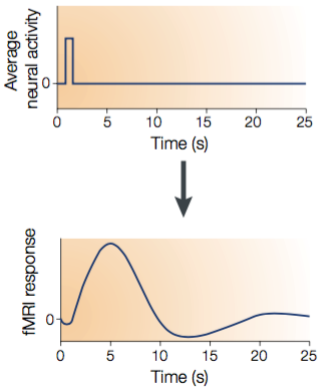

Figure 2.3 – Hemodynamic response function in response to the stimuli with the above experimental design timing. Reprinted with permission from [Heeger and Ress, 2002]

should be short enough to capture as many different activations as possible that happen in the brain over time, and at the same time, long enough to properly resolve the BOLD response resulting from the neural activity, which is prolonged in time [Faro and Mohamed, 2010, Buxton, 2009] In most of the tissues in the brain, $T1$ is around 10 times larger than $T2$. Although imaging based on $T1$ provides us with higher resolution, because TR in fMRI experiments is particularly short (between 0.5 and 4 sec), imaging is carried out based on $T2^*$, which is short enough to fit between two consecutive repetitions. As explained before, T2 is the transverse relaxation time. However, in practice, the transverse magnetization decays much faster than would be predicted for a tissue due to the inherent inhomogeneity of the magnetic field, and this rate is denoted as $T2^*$ ("T2-star"). Having a perfectly uniform magnet and an object without susceptibility effects, the $T2$ and $T2^*$ would be the same [Huettel et al., 2004].

2.1.3 Ultra high-field fMRI

Neuroimaging has provided a profound tool for studying the human brain. Although compared to the other non-invasive brain imaging methods, such as electroencephalogram (EEG), MRI excels in terms of spatial resolution, it remains very far from reaching the precision of data acquired with invasive methods such as neural recordings.

Strengthening magnetic field power in high field MRI scanners is a an attempt towards improving the quality of MRI data. The ultra high field terminology is assigned to the scanners with 7T or higher magnetic field comparing to high field as 3T and lower field as 1.5 T. Increasing the field strength leads to longer $T1$ and shorter $T2^*$, making the BOLD signal change stronger and providing the possibility of scanning at shorter TR, with the requirement of higher performance gradients to prevent artifacts. As it is shown in Fig.2.4, 7T imaging, comparing to 3T and 1.5T imaging, make it possible to acquire images with higher resolution (in similar signal to noise ratio acquisition in lower fields), and greater sensitivity to BOLD effects.

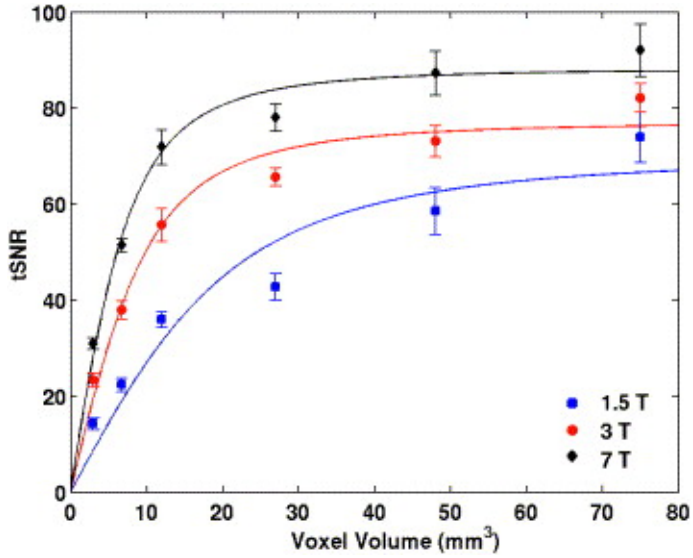

Figure 2.4 – Time course signal to noise ratio (tSNR) as a function of voxel volume (spatial resolution). Averaged measures on different areas of cortical gray matter for five subjects at each field strength. Reprinted with permission from [Triantafyllou et al., 2005].

At higher resolution, the voxel size is smaller, meaning that each voxel includes a smaller number of neurons. Therefore, physiological noise is decreased per voxel in comparison to signal acquisition noise [Robitaille and Berliner, 2007, Zwaag et al., 2015, Triantafyllou et al., 2005]. Because of these properties, high field imaging is ideal for the detailed investigation of the functional organization of small brain regions. A good example of its application is the highly accurate tonotopic of the primary auditory cortex [Da Costa et al., 2011]. Furthermore, there are proven evidence for 7T

benefits over 3T for discovering anatomical and functional changes is the human brain as a result of neurological disorders [Beisteiner et al., 2011]. These properties make 7T scanning a profound tool for studying the functional or anatomical changes in primary auditory cortex of patients with hearing disorders. And we have successfully taken advantage of it for studying the auditory cortical map in tinnitus patients [Ghazaleh et al., 2017]. A summary of the advantages and challenges of scanning with high field fMRI is shown in Table.2.5.

Difference 7 T with lower field	Advantage	Challenge
Magnetization M_0 increases with field ($\propto B_0$)	Increased available signal $\propto B_0$ (2)	
Shorter wavelength of resonance radio frequency (~30 cm in tissue @ 3 T, ~13 cm in tissue @ 7 T) (217)	B_1 inhomogeneity: more spatial differentiation for parallel reception and transmission Electrical property mapping (90)	B_1 inhomogeneity: inhomogeneous tissue contrasts (10)
Higher resonance frequency (128 MHz @ 3 T, 300 MHz @ 7 T)	Increased electromotive force responsible for signal detection $\propto B_0$ (2)	Increased SAR $\propto B_0^2$ (11,12), required higher bandwidth increases noise $\propto B_0^{0.5}$ (2)
Magnetic-field-susceptibility-induced variations $\propto B_0$	Increased PC, increased BOLD contrast $\Delta R_2^* \propto B_0^{1-1.5}$ (13,14)	Increased susceptibility-induced distortions (EPI)
Longer T_1 (gray matter, 1300 ms @ 3 T, 2000 ms @ 7 T; white matter, 800 ms @ 3 T, 1200 ms @ 7 T (4,104); blood, 1650 ms @ 3 T, 2100 ms @ 7 T (7))	Increased T_1 contrast, longer-lasting label and therefore longer possible transfer times in perfusion imaging	Longer T_R if T_1-weighting/inflow is to be avoided
Shorter T_2, decrease $\propto B_0^1$ (gray matter, 72 ms @ 3 T, 47 ms @ 7 T; white matter, 71 ms @ 3 T, 47 ms @ 7 T (5))	Increased T_2-weighting at fixed T_E	Need to acquire T_2-weighted data with shorter T_E (require stronger gradients, more pulses/second)
Shorter T_2^* (gray matter, 66 ms @ 3 T, 33 ms @ 7 T; white matter, 53 ms @ 3 T, 27 ms @ 7 T (6))	Increased T_2*/BOLD contrast	Need to acquire T_2*-weighted data with shorter T_E (require stronger gradients; possibly more blurring in EPI)
Shorter venous T_2* (20–29 ms @ 3 T, 7 ms @ 7 T (140); note that the gray matter/veins difference increases at 7 T)	Increased BOLD specificity to tissue BOLD signal changes (14) Simplified identification of veins in T_2*-weighted data as regions of no signal (140)	

Figure 2.5 – The advantages and challenges of scanning with high field fMRI. Reprinted with permission from [Zwaag et al., 2015]

2.1.4 Topographic mapping with task based fMRI

In task based fMRI, the goal is to discover the brain functionality when it is engaged in a specific task. As the BOLD response is an indirect measure of neural activity, the evaluation of activity is done by contrasting this measure between active and resting

periods, or by comparing different active conditions. This involves the design of an experimental paradigm with defined time periods for each condition. The ideally expected BOLD response will be the convolution of the task time course with the hemodynamic response function. The amount of similarity of this signal with the fMRI signal of each voxel defines the association of that voxel to the task. One specific experimental design that is used for topographic mapping is phase encoding [Engel, 2012] [Li, 2014]. A topographic map is the sorted illustration of sensory input on the cortex. In this experiment, the stimulus is presented similar to a traveling wave and continuously changes. The task based fMRI data that is used in the chapters 3 and 4 of this thesis are acquired with a phase encoding experimental design for tonotopic mapping. In this case, the traveling waves are continuous presentations of different sounds with pure tone frequencies that are played with different time delays. The regressors matching those tones can be expressed as similar waves, corresponding to each tone with a phase shift associated with its order of play in different time lags. To find out the best frequency match of each voxel, the linear cross-correlation of its time course with all of the regressors is calculated and the highest value defines the best frequency fit. A more detailed explanation of the experiment shown in Fig.2.6.

2.1.5 Resting state fMRI for discovering functional connectivity

Resting state fMRI data is acquired while the subject is not performing any specific task, and is a measure of spontaneous brain activity. Analyzing this data has shown the close correlation of activity time courses of spatially distant regions of the brain [Biswal et al., 1995] that has been demonstrated in different sensory networks as auditory, visual and somatosensory and high-level ones as default mode network (DMN), attentional and salience network (Fig.2.8) [Seeley et al., 2007, Hampson et al., 2002]. There are different methods for analyzing resting state data for detecting the functional connectivity networks. The simplest form is *seed-correlation analysis*, where the correlation of the average time course of an ROI with the other voxels in the brain is calculated and the similarity of the connectivity pattern between neighboring voxels in not taking into the account. The similarity matrix is obtained by calculating

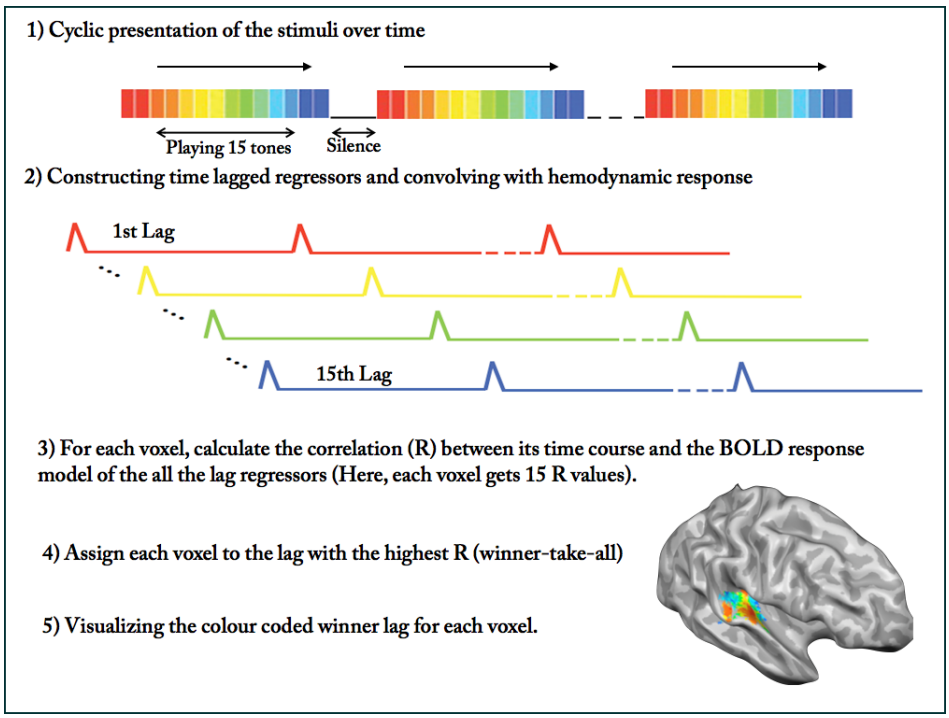

Figure 2.6 – Phase encoding experiment for sensory mapping.

the temporal correlation between the activity time courses of different regions of the brain. Depending on the selection of the seed region, different resting state networks (RSNs) can be detected [Cordes et al., 2000, Lowe et al., 1998, Greicius et al., 2009]. Seed-correlation, as an univariate method, is also used in cortical parcellation based on the similarity in functional connectivity pattern, known as *connectivity fingerprint* [Margulies et al., 2007, Barnes et al., 2010, Kim et al., 2010]. An example of exploiting functional connectivity for defining the subregions of human medial frontal cortex (MFC) [Kim et al., 2010] is shown in Fig.2.7. We have exploited this method for parcellation of auditory cortex in chapter 5.

There are more advanced analysis methods that are suitable for *multivariate* data driven analysis of fMRI data that also take into the account a priori assumption of a network pattern [Van Den Heuvel and Pol, 2010]. Using these methods there is no need for pre-defining a seed region and are used for discovering the whole brain connectivity network. Examples are principle component analysis (PCA) [Van Den Heuvel and Pol, 2010], Laplacian graph cut clustering [Thirion et al., 2006], modularity clus-

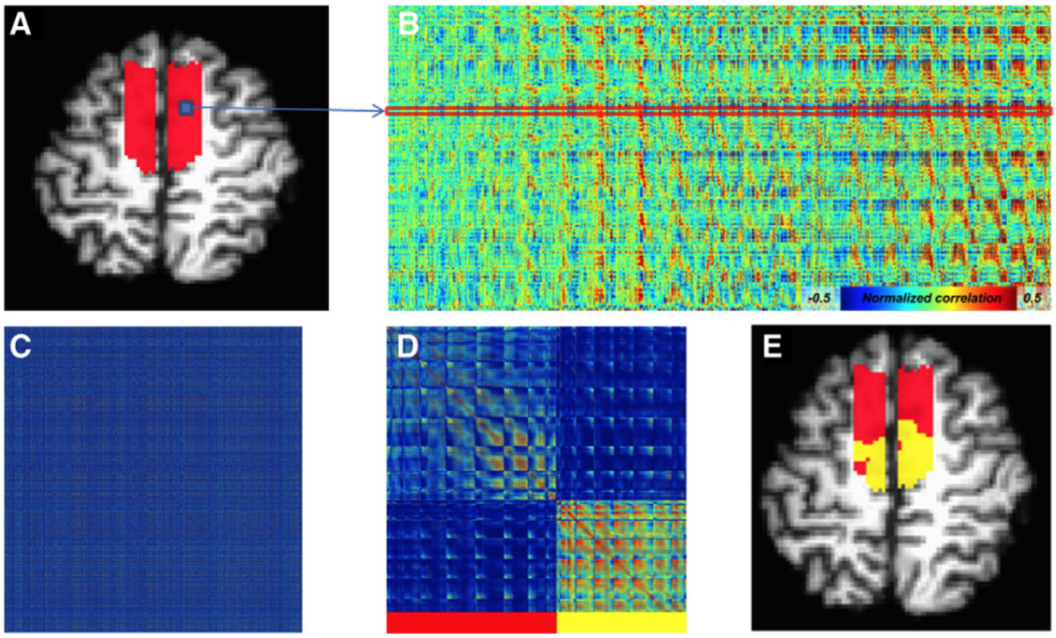

Figure 2.7 – Cortical parcellation based on resting state functional connectivity. a)Manually defined target area. b)Normalized correlation matrix of the voxels inside target region with all the voxels in gray matter. c)Similarity matrix of functional connectivity. d)Reordered similarity matrix based on the clustering of similarity values. e)Color coded projection of clusters on the brain. Reprinted with permission from [Kim et al., 2010]

tering [Newman, 2006] and Independent component analysis (ICA). Applying ICA on fMRI time-courses identifies non-overlapping spatially and temporally independent components that can be used for data de-noising as well as identifying RSNs (Fig.2.8) as DMN [Beckmann et al., 2005, **?**].

Following the changes of resting state functional connectivity networks is used as a tool for diagnosing brain disorders as detection of an early stage of Alzheimer's disease [Wang et al., 2006] or detection of major depression [Greicius et al., 2007].

While functional connectivity based on the cross-correlation of time-courses is widely used, this model has limitations in terms of revealing the detailed biological principles of brain interactions. Defining a more accurate model to link the BOLD signal with neural activity can improve the accuracy [Stephan et al., 2004, Breakspear, 2008].

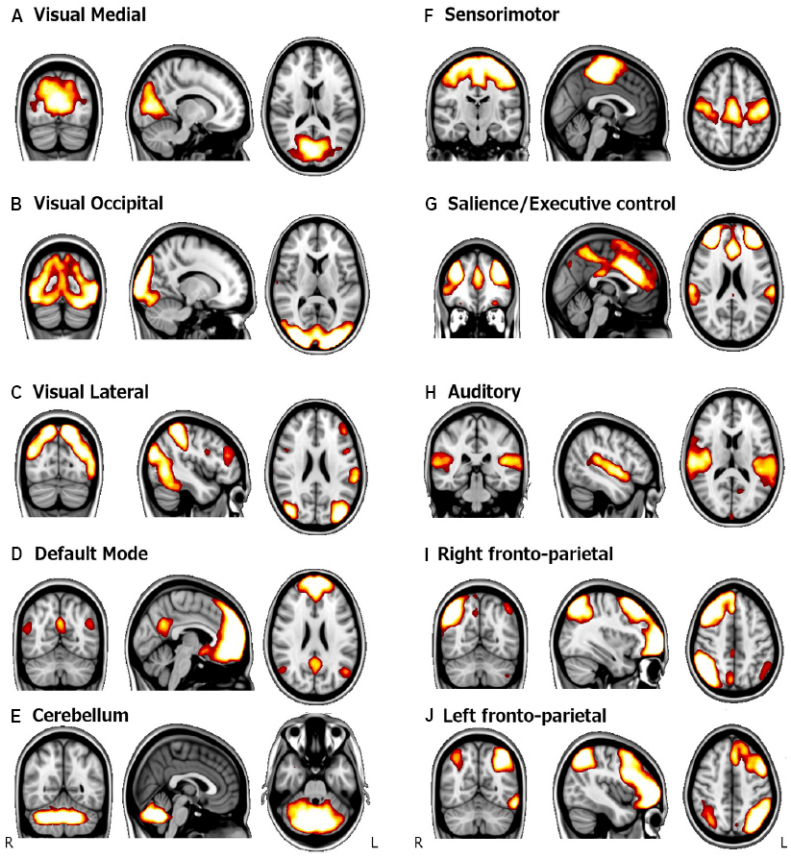

Figure 2.8 – RSNs, derived from group ICA analysis on young healthy subjects. Reprinted with permission from [Palacios et al., 2013]

2.1.6 Dynamical causal modeling of effective connectivity

The ultimate goal of working on fMRI data is to find out the underlying neuronal activity. The success of this goal is dependent on the accuracy of the hemodynamic response in reflecting neural activity. DCM creates a fairly accurate neuronal model of interacting cortical regions, based on hemodynamic time courses. and a forward model that shows how the neural activity is represented in the measured signal as fMRI. This makes it possible to estimate the neural activity parameter from observed data (as fMRI data). This approach provides a more precise model of brain functional networks called effective connectivity [Friston et al., 2003]. DCM originally is used to model evoked brain responses.In defined regions of interest (ROIs), the experimental design matrices of each stimulus serve as the inputs of this model. The outputs are the

observed time courses corresponding to the inputs. Five state variables are estimated for each ROI. Four of them are related to the different parameters of hemodynamic modeling [Friston et al., 2003] and are not affected by the state of the other ROIs and one other state variable for each ROI (z_i), is related to the modeling of the neural activity and is influenced by the neural state of the other ROIs. A summary of this states modeling is shown in Fig.2.9. As it is depicted, DCM takes the direction of the coupling between ROIs into the account and the excitatory and inhibitory effects of regions on each other are modeled as a directed graph. Effective connectivity has recently been translated into a use on resting state data [Friston et al., 2014]. In chapter 5, we have exploited effective connectivity-based modeling of the voxels in the auditory cortex to generate features for the segmentation of this region of the brain. In

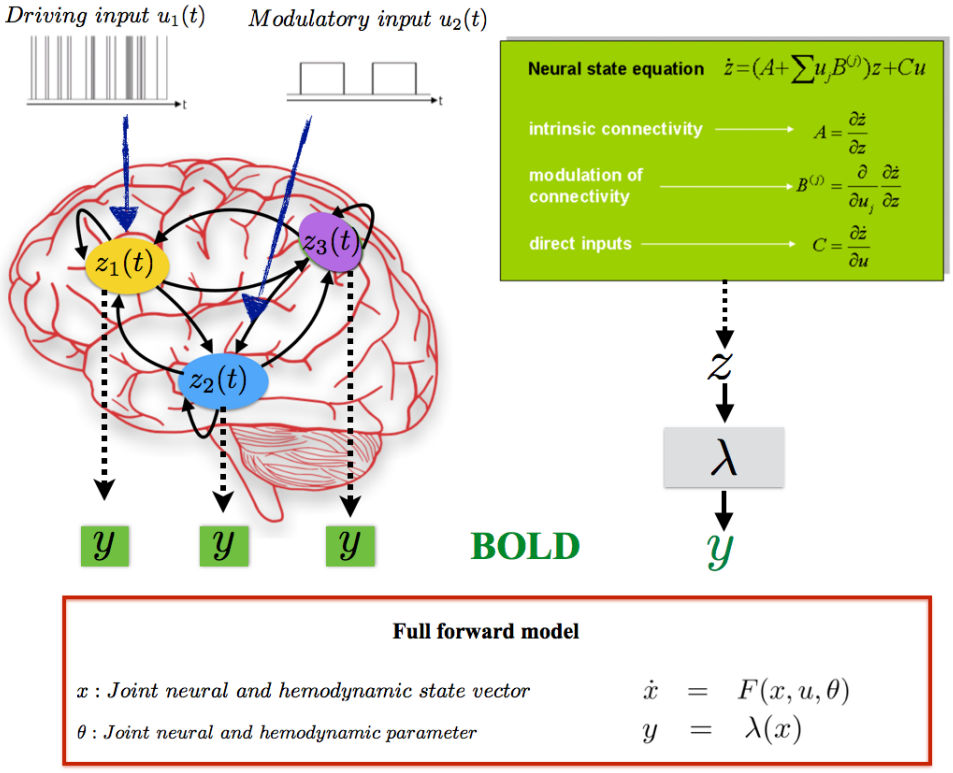

Figure 2.9 – Schematic of predicting the neural state vector (z) that is used as the input of a hemodynamic model (λ) to predict the BOLD response y. The experimental (driving) input influence the neural state dynamic locally and its effect gets propagated into the network [Friston et al., 2003]. The strength of the network edges gets affected by modulatory inputs. The full forward model x is obtained by combining neural and hemodynamic states based on their joint parameter, θ.

addition to some theoretical limitation of DCM of effective connectivity [Daunizeau et al., 2011], the practical limitation of this model compared to functional connectivity is its higher computational complexity. This limitation makes DCM more suitable for studying the network that is composed of a small number of brain ROIs, comparing to the functional connectivity that is appropriate for the whole brain resting state connectivity modeling.

2.2 Auditory system

2.2.1 From acoustic wave to tonotopy

Our ears are one of our most important organs for providing us with information regarding our environment. Fig.2.10 shows the structure of the ear. The acoustic waves, which are manifestations of air pressure, enter the ear canal and pass to the middle ear via pressure on the eardrum. Mechanical sound wave are transmitted via the ossicles of the middle ear to the round window of the cochlea. Here the mechanical waves are transfered to fluid waves in the liquid-containing cochlea.

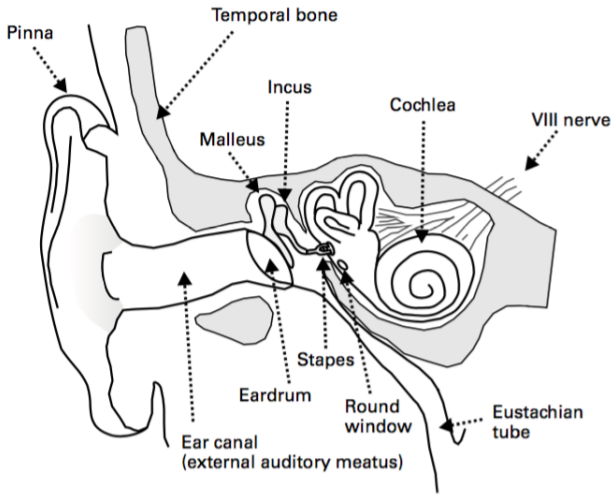

Figure 2.10 – Anatomical structure of the outer, middle, and inner ear. Reprinted with permission from Auditory Neuroscience book [Schnupp et al., 2011]

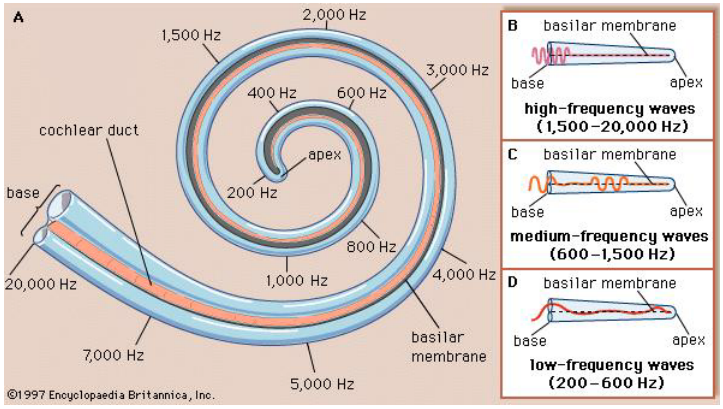

Figure 2.11 – Cochlea as the frequency filter bank. Reprinted with permission from Neuroscience book. [Schnupp et al., 2011]

Cochlea is one the most important parts of the inner. The spiral shaped cavity that is turned 2.5 rounds around its axis. In the cochlear, the fluid waves are transduced to neural signals via stimulation of the hair cells lining the basilar membrane. The basilar membrane is the main element within the cochlea; its fibers get progressively wider from the base of the cochlea to its apex. Each area, depending on the width of the basilar membrane, vibrates preferentially in response to a specific sound frequency from high frequencies at the basal end to low frequencies at the apical end, This property generates a continuous spatial mapping of sound frequencies called the tonotopic organization (Fig.2.11).

Conversion of the mechanical vibration into neuronal electrical excitation occurs by stimulation of the hair cells in the organ of corti. These neural action potentials travel along the auditory nerve through structures in the brainstem to reach the auditory cortex for further processing. Fig.2.12 shows the auditory pathway. The tonotopic organization of the cochlea is retained all the way to the auditory cortex.

The auditory cortex is located in the temporal lope, and is composed of two general subdivisions: the primary and the secondary auditory cortex. Inputs from the ventral division of the medial geniculate complex get forwarded to the primary auditory cortex (PAC), located on the superior temporal gyrus, with an orderly tonotopic mapping. Depending on the anatomy of Heschl's gyri (HG) in different individuals, PAC contains

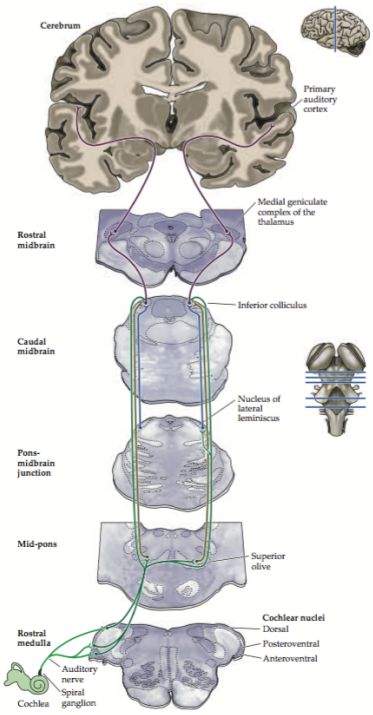

Figure 2.12 – Human auditory pathway. Reprinted with permission from Neuroscience book [Schnupp et al., 2011] .

at least two mirror symmetric tonotopic maps as high to low to high frequency representations in the A1 and R areas. The tonotopic map imaged using high-resolution 7 Telsa fMRI [Da Costa et al., 2011] is shown in Fig.2.13. The neurons of the primary auditory cortex project to surrounding secondary auditory cortex, which is less clearly tonotopically organizated.

2.2.2 Tinnitus and hyperacusis

One the most common hearing disorders is tinnitus. It is characterized by the perception of a sound (ringing or other sounds) in the absence of an identifiable sound source. One third of all adults experience tinnitus at some time in their lives. 40% of veterans suffer from tinnitus, and 10-15% of people above 50 years old have prolonged tinnitus, requiring medical evaluation [Roberts et al., 2010, Eggermont and Tass, 2015, Schaette, 2014]. People suffering from tinnitus are sometimes unable to

sleep, sustain relationships, or hold employment. The sound is distracting, and can have a significant impact on the quality of life. [Melcher et al., 2000, Kaltenbach, 2011]. There are two types of tinnitus: objective tinnitus and subjective tinnitus. Objective tinnitus is a rare disorder, and is related to a physical sound source in the inner ear and can be heard by someone else. Most of the time, the noise has some vascular source, with other possible causes being palatal myoclonus, myoclonus of the tensor tympani, tubal patency, or cochlear activity [Guinchard et al., 2016]. Subjective tinnitus is, by far, the more common type of tinnitus, and is mostly associated with sensorineural hearing loss of various types. Therefore, the ear itself does not generate tinnitus, but it is a phantom perception resulting from plastic changes in the central auditory system as a result of peripheral hearing loss. Recent animal studies [Yang et al., 2011, Engineer et al., 2011] link tinnitus to tonotopic map reorganization and reduced inhibitory neurotransmission in the auditory cortex of mice Fig.2.14, showing that reversal of the A1 pathology eliminated tinnitus symptoms.

Human studies also support reorganization of the tonotopic map, but until now lacked spatial resolution for fine-scale imaging in individual subjects. In [Wienbruch et al., 2006], Using MEG the reorganization of tonotopic mapping in the human has been reported in tinnitus patients, suggesting a maladaptive plasticity hypothesis for tinnitus generation. However, as MEG is limited for studying the tonotopic maps of auditory cortex, where multiple mappings converge at angles that are unresolvable by this imaging method. In another human study [Langers et al., 2012], the hyperactivity in the primary auditory cortex is detected in tinnitus patients without hearing loss, but the allocation of these hyperactive voxels in the tonotopic map is not defined. Hence, the investigation of the issue of the map cortical plasticity in tinnitus requires a more precise data acquisition method such as high-resolution fMRI, as discussed in the next section. Around 70% of tinnitus patients additionally suffer from loudness hyperacusis. Hyperacusis is characterized by increased loudness discomfort and decreased tolerance to normal sound levels, and is additionally a common symptom of age-related hearing loss. Persons suffering from hyparacusis .experiencing trouble in tolerating ordinary sounds that are neither threatening nor uncomfortably loud to a

normal hearing person [Baguley, 2003]. Hyperacusis has been the subject of relatively few studies and its underlying mechanism is unknown. It has been shown that animal models of tinnitus show the same behavioral response compared to the hyperacusis condition [Salloum et al., 2014]. The co-occurrence with tinnitus symptoms brings complexity to the interpretation of results claimed to be related to tinnitus alone; therefore, determining a method to discriminate both conditions appears essential.

2.2.3 Brain plasticity in tinnitus

The neural wiring network of the human brain is in constant modification to adapt behavior to sensory input, due to multiple mechanisms collectively called brain plasticity. Sometimes this plasticity leads to a pathological response, as in phantom limb pain following neural deafferentation due to the loss of a limb [Flor et al., 2006]. Similarly, auditory neural deafferentation associated with cochlear damage, are thought to lead to changes in central neural activity in the auditory cortex leading to tinnitus generation. [Langers et al., 2012]. Some animal studies support a maladaptive plasticity hypothesis which proposes that an overrepresentation and/or hyperactivity of the hearing loss or hearing-loss edge frequencies in the cortex generates tinnitus (analogous to the leading phantom pain hypothesis). [Eggermont and Komiya, 2000, Seki and Eggermont, 2003, Noreña and Eggermont, 2005, Noreña and Eggermont, 2003]. Other studies describe a broader pattern of tonotopic map distortions in the primary auditory cortex, with large effects away from the hearing loss and tinnitus range. These proposed changes may be described in the context of *homeostatic plastic mechanisms*. Homeostatic plasticity refers to modifications in neural wiring and synaptic activity to maintain a stable pattern of activity [Yang et al., 2011, Engineer et al., 2011]. This group of studies notably found prominent hyperactivity in low frequency areas, away from the hearing-loss and presumed tinnitus range. Thus based on animal studies, it appears that tinnitus is associated with an alteration in the normal cortical mappings of neuronal sound frequency preference in the primary auditory cortex, but the exact pattern of changed to expect is unclear. Here, we applied high-resolution functional MRI imaging at 7 Tesla (ultra-high field strength) to the primary auditory cortex in

human patients with hearing loss and tinnitus, to better understand the neural basis of this disorder.

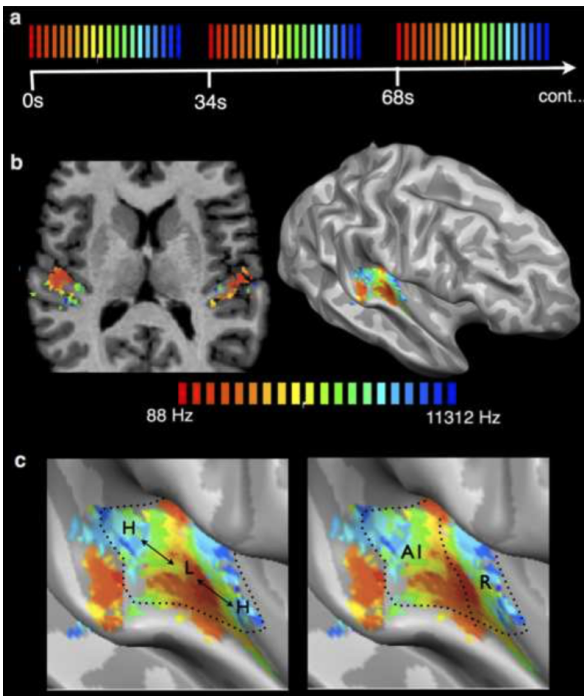

Figure 2.13 – Tonotopic mapping in auditory cortex with 7T fMRI. (a) Presented sound stimuli as pure tone bursts ranging from 88 to 11312 Hz. tones are presented in slow cyclical sweeps from low frequencies to high (or in reverse order). These frequency sweeps are designed to induce a traveling wave of response across the tonotopic maps of primary auditory cortex. The time-to-peak, or phase, of the response in the measured fMRI time series of each voxel reveals its preferred frequency. Color- coded maps (red = low, blue = high) of preferred frequency are shown (b, left) in volumetric anatomical space and (b, right) on a cortical surface mesh of one sample control subject. A close-up of the temporal plane shows the outlined mirror-symmetric frequency gradients from high to low and back to high (c, left). The same maps are relabeled (c, right) to show how the two gradient correspond to anatomical fields A1 and R which together comprise the primary auditory cortex in each brain hemisphere.

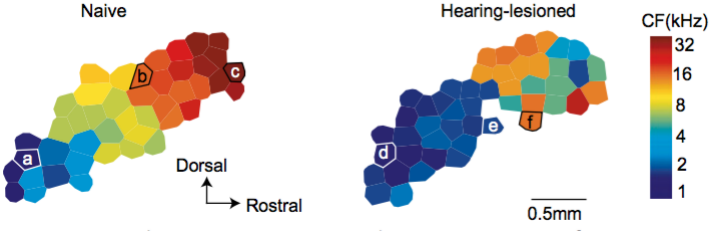

Figure 2.14 – Cortical map and receptive fields in naive and hearing-lesioned animals. Reprinted with permission from [Yang et al., 2011]

3 High-Resolution fMRI of Auditory Cortical Map Changes in Unilateral Hearing Loss and Tinnitus

This article is publication in the journal of Brain Topography.

Brain Topogr
DOI 10.1007/s10548-017-0547-1

ORIGINAL PAPER

High-Resolution fMRI of Auditory Cortical Map Changes in Unilateral Hearing Loss and Tinnitus

Naghmeh Ghazaleh[1,2] · Wietske van der Zwaag[3,4] · Stephanie Clarke[5] · Dimitri Van De Ville[1,2] · Raphael Maire[6] · Melissa Saenz[1,7]

Received: 30 June 2016 / Accepted: 18 January 2017

Abstract Animal models of hearing loss and tinnitus observe pathological neural activity in the tonotopic frequency maps of the primary auditory cortex. Here, we applied ultra high-field fMRI at 7 T to test whether human patients with unilateral hearing loss and tinnitus also show altered functional activity in the primary auditory cortex. The high spatial resolution afforded by 7 T imaging allowed tonotopic mapping of primary auditory cortex on an individual subject basis. Eleven patients with unilateral hearing loss and tinnitus were compared to normal-hearing controls. Patients showed an over-representation and hyperactivity in a region of the cortical map corresponding to low frequencies sounds, irrespective of the hearing loss and tinnitus range, which in most cases affected higher frequencies. This finding of hyperactivity in low frequency map regions, irrespective of hearing loss range, is consistent with some previous studies in animal models and corroborates a previous study of human tinnitus. Thus these findings contribute to accumulating evidence that gross cortical tonotopic map reorganization is not a causal factor of tinnitus.

Keywords Tinnitus · fMRI · Primary auditory cortex · Neural plasticity

✉ Naghmeh Ghazaleh
naghmeh.ghazaleh@epfl.ch

[1] Institute of Bioengineering, École Polytechnique Fédérale de Lausanne (EPFL), Lausanne, Switzerland

[2] Department of Radiology and Medical Informatics, University of Geneva, Geneva, Switzerland

[3] Spinoza Centre for Neuroimaging, Royal Netherlands Academy for Arts and Sciences, Amsterdam, Netherlands

[4] Center for Biomedical Imaging, University of Lausanne, Lausanne, Switzerland

[5] Service of Neuropsychology and Neurorehabilitation, Department of Clinical Neurosciences, Lausanne University Hospital, Lausanne, Switzerland

[6] Department of Otorhinolaryngology, Head and Neck Surgery, Lausanne University Hospital, Lausanne, Switzerland

[7] Neuroimaging Research Lab (LREN), Department of Clinical Neurosciences, Lausanne University Hospital, Lausanne, Switzerland

Introduction

Tinnitus, or 'ringing in the ear', is a common and potentially debilitating hearing disorder for which treatment options are lacking. Tinnitus is estimated to affect at least 10% of adults, and approximately 2% of adults to the degree that it negatively impacts quality of life, potentially contributing to stress, anxiety, and insomnia (Axelsson and Ringdahl 1989). In the vast majority of cases, tinnitus is not generated in the ear itself, but rather stems from pathological activity in auditory centers of the brain (Roberts et al. 2010; Schaette and McAlpine 2011a; Eggermont 2015; Elgoyhen et al. 2015). Peripheral hearing loss triggers downstream central neural activity that generates a "phantom" sound perception, ranging from tonal to broadband, of which the center frequency tends to occur in the hearing loss range (Norena et al. 2002; Schecklmann et al. 2012). Treatment options are currently limited and a better understanding of central auditory changes is needed to guide treatment strategies.

In animal models of tinnitus, induced cochlear damage is associated with behavioral evidence of tinnitus symptoms. These studies consistently report numerous downstream neurophysiological changes in the central auditory system (midbrain, thalamic, and cortical areas) including

Published online: 06 February 2017

increased spontaneous and driven neural activity, increased neural synchrony, and reduced inhibitory synaptic activity. However, it remains inherently difficult to disentangle changes related to tinnitus from other co-occurring effects of peripheral hearing loss, including hyperacusis (decreased sound tolerance) (Sheldrake et al. 2015).

In the primary auditory cortex, animal studies have shown distortions in the normal mapping of sound frequency preference, known as the tonotopic map. Some studies describe an overrepresentation of the hearing loss or hearing-loss edge frequencies (Eggermont and Komiya 2000; Seki and Eggermont 2003; Noreña and Eggermont 2003, 2005), and this finding has been taken to support a hypothesis that map distortion causes tinnitus (*maladaptive reorganization hypothesis)*. Other studies, quite differently, describe a broader pattern of distortions that favors hyperactivity in low frequency areas, notably away from the hearing-loss and presumed tinnitus range (Engineer et al. 2011; Yang et al. 2011).

Based on animal models, it is likely that hearing loss and tinnitus in humans is associated with altered activity in the tonotopic maps of primary auditory cortex, although the exact pattern of changes to expect is unclear. We have tested for such changes by applying high spatial resolution fMRI at ultra-high field (7 T) to measure tonotopic maps of the primary auditory cortex in human patients suffering from unilateral hearing loss and tinnitus. 7 T imaging offers distinct advantages for imaging small functional subunits in the cortex and facilitates fine-scale tonotopic mapping at the individual subject level, as we have previously shown in normal hearing adults. The increased signal-to-noise ratio and available BOLD signal associated with ultra-high magnetic field imaging at 7 T allows the use of smaller voxel sizes. Additionally, the BOLD signal is better restricted to cortical gray matter because the signal strength of blood in draining veins is reduced due to shortened T_2* relaxation time at higher fields, thus improving spatial localization (van der Zwaag et al. 2009, 2015).

In this clinical investigation, we studied patients with unilateral sensorineural hearing loss and tinnitus of at least 6-months duration (n = 11) compared to normal hearing controls (n = 7). The inclusion of patients with only unilateral hearing loss allowed the presentation of sound stimuli via the normal hearing ear, thus side-stepping the problem of unequal peripheral stimulation between hearing-loss and control groups. High-resolution 7 T fMRI imaging (1.5 mm isotropic voxels) was acquired over the auditory cortex to assess the organization of the primary tonotopic maps bilaterally. Notably, we observed map distortion and hyperactivity in a region of primary auditory cortex corresponding to relatively low frequency sounds, peaking at 250–354 Hz, irrespective of the patient's hearing loss and tinnitus frequency range. These results do not support the hypothesis that tinnitus is caused by the overrepresentation of hearing loss (or near) frequencies, but do corroborate recent findings from animal models (Engineer et al. 2011; Yang et al. 2011) and a previous human neuroimaging study of tinnitus (Langers and Kleine 2012).

Materials and Methods

Patients

All subjects gave written, informed consent. Experimental procedures were approved by the Ethics Committee of the Faculty of Biology and Medicine of the University of Lausanne.

Patients (n = 11, age 37.5 ± 12 years, age range 26–49 years, 6 male, 5 female) were recruited from the outpatient clinic of Otolaryngology of the Lausanne University Hospital and underwent a complete ear, nose, and throat (ENT) assessment including standard pure tone audiometry (PTA) and evaluation of tinnitus characteristics. Selected patients had chronic subjective non-pulsatile tinnitus associated with moderate to severe unilateral sensorineural hearing loss (SHL) in one ear only with a decrease in hearing thresholds of at least 40dB on three consecutive frequencies between 1 and 4 kHz, duration >6 months; and normal age-adjusted hearing thresholds in the unaffected ear. Age-matched control subjects (n = 7, 39.2 ± 10 years, age range 29–50 years, 3 male, 4 female) (Newman et al. 1996) had normal bilateral hearing. Exclusion criteria for all subjects included a history of neurological or psychiatric illness and standard MRI contraindications. Hearing loss originated from acoustic neuroma (noncancerous tumor of the auditory nerve), Meniere's disease (disorder of the inner ear typically affecting one side only), or unilateral cochlear damage caused by head trauma, infection, or blood clot. Some patients subjectively reported hyperacusis—a decreased tolerance to sounds—which often co-occurs with tinnitus. Table 1 provides an overview of patient characteristics.

Tinnitus pitch was assessed by matching external tones presented to the unaffected ear from 125 Hz to 12 kHz in half-octave steps. Tinnitus loudness was subsequently assessed by matching the selected tinnitus pitch to sound levels starting at 15 dB above auditory threshold and increasing by 5 dB increments. Tinnitus discomfort was assessed by the French version the Tinnitus Handicap Inventory (Newman et al. 1996). Patients reported THI rankings from 2 to 5 indicating mild to severe tinnitus discomfort (Table 1).

The recruitment of patients with unilateral hearing loss allowed for the unimpaired delivery of sound stimuli via the unaffected ear. As such, both patient and control groups

Table 1 Tinnitus patients' characteristics

ID	Sex	Age	Hearing loss side	Hearing loss degree and frequency range	Tinnitus center frequency	THi grade (1–5)	Tinnitus duration	Hyper-acusis	Hearing loss origin
P1	F	54	L	>40 dB, >1000 Hz	Noise 8000 Hz	3	>1 year	Yes	Cochear
P2	M	35	R	>90 dB, full spectrum	Noise 8000 Hz	3	>2 year	No	Cochlear
P3	M	44	R	>60 dB, full spectrum	Noise 1000 Hz	2	>2 year	No	Acoustic neuroma
P4	M	46	L	>60 dB, full spectrum	Noise 2000 Hz	4	>1 year	Yes	Cochlear
P5	F	46	L	>40 dB, full spectrum	Noise 1000 Hz Tone 6000 Hz	3	>5 year	Yes	Meniere's disease
P6	M	48	R	>50 dB, full spectrum	Noise 6000 Hz	3	>7 year	No	Meniere's disease
P7	F	20	L	>40 dB, <1000 Hz	Noise 1000 Hz	2	>3 year	No	Acoustic neuroma
P8	M	46	R	>50 dB, >2000 Hz	Tone 6000 Hz	5	>6 month	Yes	Cochlear
P9	F	26	L	>50 dB, >2000 Hz	Noise 1000 Hz	4	>5 year	Yes	Acoustic neuroma
P10	M	27	L	>90 dB, full spectrum	Tone 8000 Hz	2	>10 year	No	Cochlear
P11	F	20	R	>90 dB, full spectrum	Noise 1000 Hz	3	>2 year	No	Cochlear

(both stimulated unilaterally) received the equivalent stimulation and any eventual differences in the measured fMRI response could be attributed to altered cortical rather than to altered peripheral processing. Note that a different effect of background scanner noise may remain between groups (See Discussion). Stimulation of either ear activates auditory cortex bilaterally (van der Zwaag et al. 2011) allowing measurement of tonotopic maps in both brain hemispheres (See Discussion).

MRI Data Acquisition

Blood oxygenation level dependent (BOLD) functional imaging was performed with an actively shielded 7 T Siemens MAGNETOM scanner (Siemens Medical Solutions) at the Centre d'Imagerie BioMedicale in Lausanne, Switzerland. fMRI data were acquired with an 8-channel head volume RF-coil (RAPID Biomedical GmbH) (Salomon et al. 2014) large enough to comfortably fit the headphones used for auditory stimulation, and a continuous EPI pulse sequence with sinusoidal read-out (1.5×1.5 mm in-plane resolution, slice thickness = 1.5 mm, TR = 2000 ms, TE = 25 ms, flip angle = 47 deg, slice gap = 0.07 mm (5%), matrix size = 148×148, field of view 222×222, 30 oblique slices covering the superior temporal plane). A T_1-weighted high-resolution 3D anatomical image (resolution = $1 \times 1 \times 1$ mm, TR = 5500 ms, TE = 2.84 ms, slice gap = 1 mm, matrix size = 256×240, field of view = 256×240) was acquired for each subject using the MP2RAGE pulse sequence optimized for 7 T MRI (Marques et al. 2010). Susceptibility induced distortions are small in the area of the brain covered by our imaging slab (van der Zwaag et al. 2009) and were further limited by the use of a limited matrix size in combination with parallel imaging to keep the read-out duration short. As a result co-registration between the functional images and the MP2RAGE was successful for all subjects, as verified by visual inspection.

fMRI data preprocessing steps were performed with BrainVoyager QX software including linear trend removal, temporal high-pass filtering (2 cycles), and motion correction. Spatial smoothing and slice-timing correction were not applied. Functional time-series data were interpolated into a $1 \times 1 \times 1$ mm volumetric space and registered to each subject's own 3D Talairach normalized anatomical dataset. Cortical surface meshes were generated from each subject's anatomical dataset using automated segmentation tools in BrainVoyager QX.

Sound Stimulation (General Parameters)

Sound stimuli were generated on a laptop computer using Matlab and The Psychophysics Toolbox (www. Psychtoolbox.org) with a sampling rate of 44.1 kHz, and were delivered via MRI-compatible optical headphones (Audio-System, Nordic NeuroLab). Sound level intensities were between 82 and 97 dB SPL, and were adjusted per frequency to approximate equal perceived-loudness of 85 phon according to standard equal-loudness curves (ISO 226). Stimulus intensities were further attenuated approximately 24 dB by the required use of protective earplugs. Earplugs inevitably attenuate sound spectrum unevenly, affecting high frequencies more than low. All subjects reported hearing all tone frequencies at a clear and comfortable level, and were instructed to listen passively with eyes closed. Patients were stimulated in the unaffected ear only (Table 1) and control subjects were equivalently stimulated in one ear only, randomly selected. Overall time in the scanner including set-up, two fMRI tonotopy runs, and

an anatomical scan was approximately 45 min, sufficiently brief for patient comfort.

Tonotopic Mapping Paradigm and Analysis

Tonotopy refers to the spatial layout of auditory neurons in gradients of sound frequency preference. Tonotopy originates on the basilar membrane of the cochlea which due to mechanical properties resonates best to high-frequency sound waves on the basal end and to progressively lower sound frequencies towards the apical end, hence creating a spatial gradient of sound frequency selectivity along its length. Tonotopic organization of auditory neurons is maintained in the auditory nerve, mid-brain, thalamus, and cortex. In human primary auditory cortex, two tonotopic gradients with mirror-symmetry ('high-to-low' followed by 'low-to-high' preferences) are found running across Heschl's gyrus in each brain hemisphere, along an overall posterior-to-anterior axis. Figure 1 illustrates the primary auditory cortex tonotopic gradients with a color spectrum: red shows where neurons respond best to low frequency tones, and blue to high frequency tones.

These two mirror-symmetric gradients appear to correspond to primary auditory cortex fields A1 and R, (Da Costa et al. 2011; Langers and Dijk 2012b; Saenz and Langers 2014). In monkeys, both of these fields are considered part of the core koniocortical cortex along with a third smaller field RT which has not yet been reliably confirmed in humans (Hackett 2011; Baumann et al. 2013). In humans, visualizing the two tonotopic gradients with fMRI allows localization of primary auditory cortex in individual human subjects (Saenz and Langers 2014), although the exact lateral border remains difficult to define (See Discussion). No difference in function is known between fields A1 and R and they are treated together here as primary auditory cortex.

To map tonotopy in the cortex, we employed a "phase-encoded" mapping paradigm, a technique commonly used in the visual system for retinotopic mapping (Engel 2012), as well as in the somatosensory cortex for somatotopic mapping (Sanchez-Panchuelo et al. 2010). Briefly, the mapping stimulus is designed to sweep the parameter space of the map (in this case, low to high sound frequencies), thus generating a wave of response across the cortical surface. Recorded activity peaks earliest at the low frequency map endpoint and progressively later in parts of the map preferring higher frequencies. The phase of the response reveals the preferred frequency of each responsive voxel.

The mapping stimulus (Fig. 1a) cycled through tones of 15 different sound frequencies (88, 125, 177, 250, 354, 500, 707, 1000, 1414, 2000, 2828, 4000, 5657, 8000, and 11,312 Hz, half-octave spacing), as in our previously described methods (Da Costa et al. 2011). During each cycle, pure tone bursts of the first frequency were presented during a 2 s block before stepping to the next frequency until all 15 frequencies were presented, followed by a 4 s silent pause (Fig. 1a). During each 2 s block, pure tone bursts of the given frequency had variable onset times (50 and 250 ms duration randomly interspersed with 50 ms inter-stimulus intervals) to avoid a fixed periodicity. Each 34 s cycle (sounds plus silent pause) was repeated 14 times for a scan run duration of 7 min and 56 s. Each subject participated in two scan runs (one with stimulus sweeps from low-to-high, and one in reverse order) since tonotopic preferences should be independent of stimulus order, and the resulting maps of the two runs were averaged. Linear cross-correlation analysis was used to determine the response phase that best fit the measured fMRI time course of each

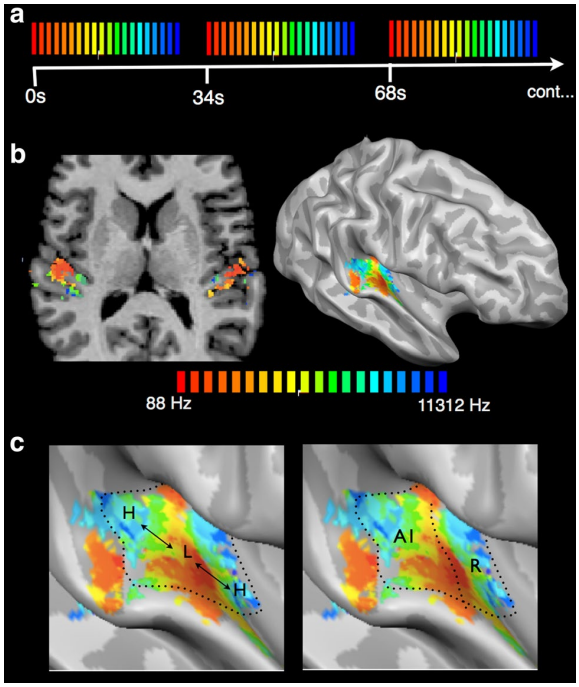

Fig. 1 Tonotopic mapping in auditory cortex with 7 T fMRI. **a** Sound stimuli were pure tone bursts ranging from 88 to 11,312 Hz. As illustrated, tones were presented in *slow cyclical sweeps* from low frequencies to high (or in reverse order). These frequency sweeps are designed to induce a traveling wave of response across the tonotopic maps of primary auditory cortex. The time-to-peak, or phase, of the response in the measured fMRI time series of each voxel reveals its preferred frequency. Color-coded maps (*red* = low, *blue* = high) of preferred frequency are shown (**b**, *left*) in volumetric anatomical space and (**b**, *right*) on a cortical surface mesh of one sample control subject. A close-up of the temporal plane shows the outlined mirror-symmetric frequency gradients from high to low and back to high (**c**, *left*). The same maps are relabeled (**c**, right) to show how the two gradients correspond to anatomical fields A1 and R which together comprise the primary auditory cortex in each brain hemisphere. (Color figure online)

responsive voxel. The assigned frequency preferences are color-coded from red-to-blue to indicate low-to-high.

Data analysis was performed in 3-D volumetric space in each subject individually (Fig. 1b, left). Resulting maps were projected onto cortical surface meshes to facilitate viewing (Figure b, right). On the cortical surface, contiguous areas containing the two primary gradients of auditory cortex (high-to-low followed by low-to-high) were manually selected using drawing tools within BrainVoyager QX, as illustrated with dotted lines (Fig. 1c). Anterior and posterior borders were drawn along the outer edges of the high-frequency zones. Lateral and medial borders were conservatively drawn to include approximately the medial two-thirds of Heschl's gyrus, in accordance with human architectonics (Rivier and Clarke 1997; Hackett 2011) (See "Discussion") and as in our previous studies (Da Costa et al. 2011, 2013). The exact borders did not depend upon the particular correlation threshold used for display since the overall pattern was observable across a large range of display thresholds. Figure 2 displays the selected surface regions for all subjects. Next, the selected regions were projected into each subjects $1 \times 1 \times 1$ mm volumetric space width of 2 mm (−1 mm to +1 mm from the white/gray matter boundary). Our relatively thin gray matter projection was effectuated in order to avoid contamination by voxels from abutting cortical folds.

The data analysis of Fig. 3 included all volumetric fMRI voxels ($1 \times 1 \times 1$ mm interpolated) falling within this 2 mm thick region-of-interest (ROI) in each subject's hemisphere. Relative frequency histograms show the percentage of the total number of voxels in the volumetric ROI assigned to each sound frequency (%voxels). Response amplitudes were measured as the maximal signal change in the average fMRI signal of all voxels assigned to each sound frequency within the volumetric ROI, as in (Da Costa et al. 2015).

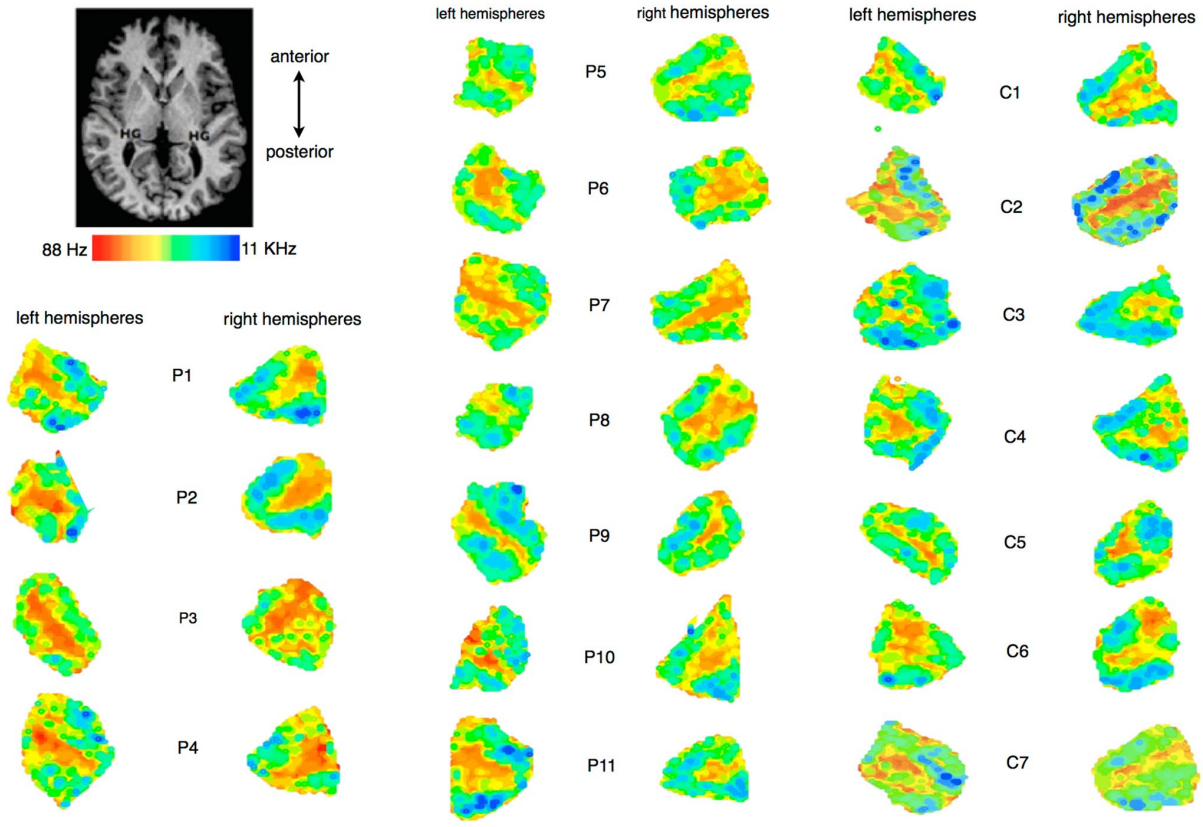

Fig. 2 All individual subject tonotopic maps from the cortical surface meshes are shown for patients with unilateral heaing loss and tinnitus (P1-P11) and normal hearing control subjects (C1–C7) in left and right hemispheres. The *upper-left inset* is provided as a reference of the anatomical orientation of all the plots (HG = Heschl's gyrus). At a macroscopic level, patient maps were normal in terms of location and orientation, running along a posterior-to-anterior axis across Heschl's gyrus

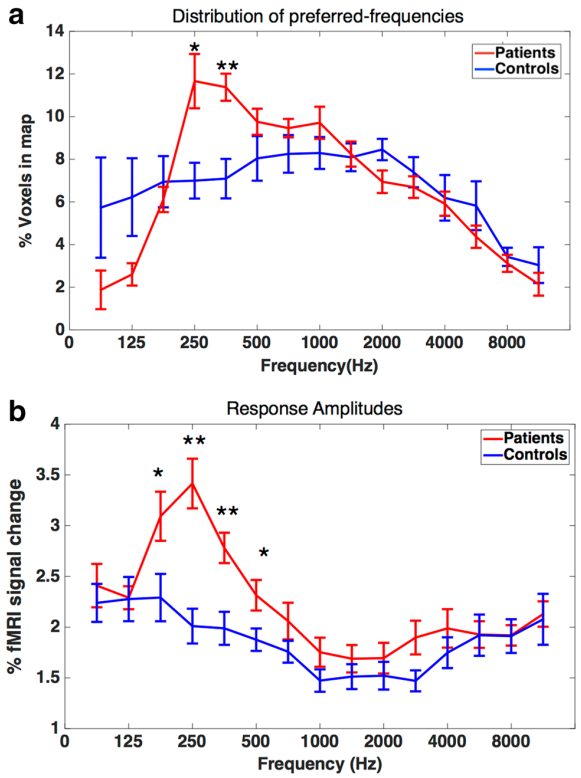

Fig. 3 Quantitative comparison of maps reveals differences between tinnitus patients and healthy control subjects. **a** Distribution of preferred-frequencies. Patients had a higher proportion of voxels preferring low frequencies peaking at 250–354 Hz indicating an enlarged representation of those sound frequencies. **b** Response amplitudes at each frequency. Patients had higher response amplitudes also peaking in the low-frequency range indicating hyperactivity in that part of the map. (*$p<0.05$ Mann–Whitney U test uncorrected, **$p<0.05$ following FDR correction for multiple comparisons, *error bars* = SEM across subjects and hemispheres)

Results

Tonotopic maps of the primary auditory cortex, consisting of two mirror-symmetric frequency gradients (high-to-low followed by low-to-high) running across Heschl's gyrus, could be identified in both hemispheres of all patients and controls (Fig. 2). At a macroscopic level, the mappings in patients were normal in terms of location and orientation, running along a posterior-to-anterior axis across Heschl's gyrus on the temporal plane in both left and right brain hemispheres, and were consistent with the maps of control subjects and with expectations based on our previous studies in normal hearing subjects (Da Costa et al. 2011; Da Costa et al. 2013; Da Costa et al. 2015).

Quantitative differences between patients and controls were observed. Figure 3a compares the distribution of preferred-frequencies across the maps in both groups. Patients showed a higher proportions of voxels preferring a range of low frequencies peaking at 250–354 Hz (*Mann–Whitney U test uncorrected*: $p<0.05$ at 250 and 354 Hz; *following FDR correction for multiple comparisons*: $p<0.05$ at 354 Hz), indicating an enlarged representation of those sound frequencies. Next, Fig. 3b compares response amplitudes at each frequency in both groups. Patients showed higher response amplitudes peaking in the same low-frequency range (*Mann–Whitney U test uncorrected*: $p<0.05$ at 117, 250, 354 and 500 Hz; *following FDR correction for multiple comparisons*: $p<0.05$ at 250 Hz and 354 Hz) indicating a hyperactivity in that part of the map. These patterns were observed in both hemispheres, ipsilateral and contralateral to the hearing ear, and both sides are combined in Fig. 3a, b. In Fig. 4, map frequency distributions and response amplitudes are re-plotted separately for both hemispheres, ipsilateral and contralateral to the normal hearing ear (i.e. the side of sound presentation). As can be seen, the low-frequency over-representation and hyperactivity are common to both hemispheres.

The low-frequency area of over-representation and hyperactivity in patients did not correspond with the ranges of hearing loss, which were either across the full spectrum or limited to higher-frequencies (Table 1); nor did they correspond with tinnitus pitch judgments which ranged form 1000–8000 Hz (Table 1). No significant correlation was found between response amplitudes at 250 Hz and tinnitus center frequency ($R=-0.49$, $p>0.05$), THI score ($R=$-0.36, $p>0.05$), years of tinnitus duration ($R=-0.03$, $p>0.05$), or patient age ($R=-0.01$, $p>0.05$), nor was there an association with hearing loss side, or presence of hyperacusis ($p>0.05$). The occurrence of Heschl's gyrus duplications (See Discussion) was similar across both groups: 10 partial duplications out of 22 hemispheres in patients: 6 partial and 1 complete duplication out of 14 hemispheres in normal hearing controls.

Discussion

We applied high-resolution fMRI at 7 T to image the tonotopic sound frequency maps of primary auditory cortex in individual patients with unilateral hearing loss and tinnitus, and in normal hearing controls. Evidence of cortical map distortion in patients was two-fold: increased representation and increased response amplitudes of low frequency sites in primary auditory cortex. These changes peaked at 250–354 Hz, considerably lower than the tinnitus frequency ranges of the patients. Given this mismatch, we do not interpret these map distortions as a causal factor of tinnitus, and consider them more likely to be a co-occurring effect of hearing loss. As discussed below, the finding of low-frequency hyperactivity, irrespective of the

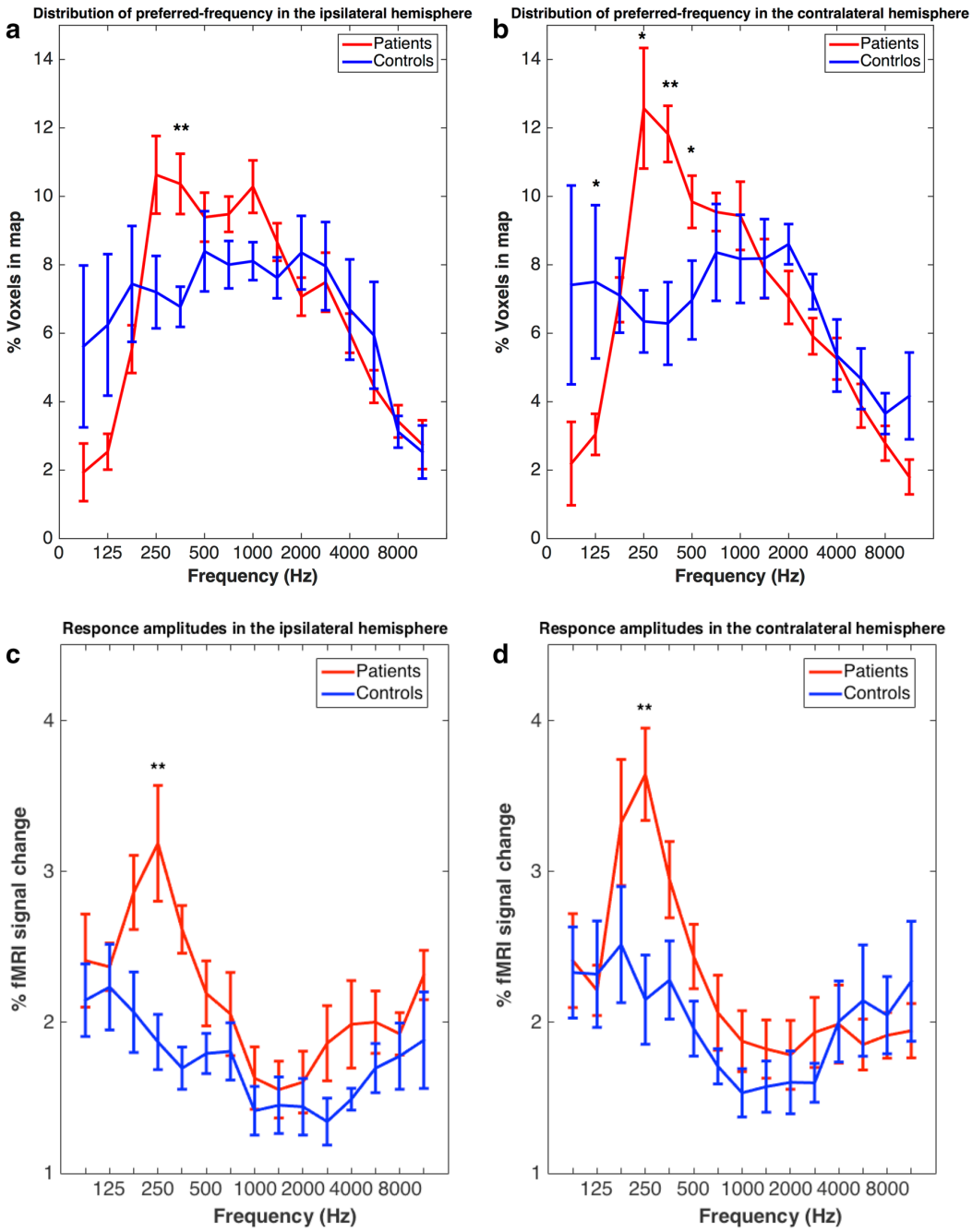

Fig. 4 Distribution of preferred frequencies re-plotted separately for both hemispheres **a** ipsilateral and **b** contralateral to the normal hearing ear (the side of sound presentation). Response amplitudes at each frequency re-plotted separately for both hemispheres, **c** ipsilateral and **d** contralateral to the normal hearing ear. As can be seen, the patterns of low-frequency map over-representation and hyperactivity are common to both hemispheres. (*$p < 0.05$ Mann–Whitney U test uncorrected, **$p < 0.05$ following FDR correction for multiple comparisons, *error bars* = SEM across subjects)

hearing loss or tinnitus range, is consistent with recent studies in animal models (Engineer et al. 2011; Yang et al. 2011) and corroborates a previous human fMRI study in tinnitus patients with normal hearing thresholds (Langers and Kleine 2012a). Our results do not rule out the possibility, and indeed likelihood, of other changes in the

functional properties of neurons within the hearing loss and tinnitus range, which may not have been detected by our methodology.

Neurophysiological Mechanisms

The pathological mechanisms underlying tinnitus have not been resolved, however many clues have emerged from research in humans and in animal models. A key observation is that tinnitus perception typically corresponds to the side and frequency range of maximum hearing loss (Norena et al. 2002; Schecklmann et al. 2012), an association that implicates neurons within the hearing loss range are responsible for tinnitus generation (Roberts et al. 2010). Although some tinnitus patients present with a normal audiogram, these cases may be accompanied by "hidden" hearing loss, occurring at high intensity levels not detected by standard audiometry (Schaette and McAlpine 2011b). Other consequences of hearing loss, namely hyperacusis, are not necessarily limited to the hearing loss range and thus might stem different from mechanisms than tinnitus (Sheldrake et al. 2015).

Animal studies associate cochlear damage (induced by noise exposure or drug induction) with increases in spontaneous activity, driven activity, neural synchrony, and excitatory glutamatergic neurotransmission, with cortical tonotopic map distortions, and with reductions in inhibitory GABAergcic and glycinergic neurotransmission across auditory midbrain (Brozoski et al. 2002; Kaltenbach et al. 2004), collicular (Ma et al. 2006), thalamic, and cortical sites (Seki and Eggermont 2003; Noreña and Eggermont 2003, 2005; Engineer et al. 2011; Yang et al. 2011). Overall, these physiological effects of cochlear damage generally implicate the involvement of homeostatic plasticity mechanisms (Turrigiano and Nelson 2004) and are in some cases correlated with behavioral evidence of tinnitus in the hearing loss range (Brozoski et al. 2002; Kaltenbach et al. 2004; Middleton et al. 2011). Notably, increased neural synchrony appears to localize well with the hearing loss and presumed tinnitus range (Noreña and Eggermont 2003; Eggermont and Roberts 2012). It has been recently demonstrated, however, that the gap-detection behavioral test for tinnitus commonly used in animal studies can confounded by hearing loss and hyperacusis, evoking the difficulty in disentangling the effects specifically related to tinnitus (Salloum et al. 2016).

Regarding cortical tonotopic maps, some studies describe an overrepresentation of sound frequencies within or at the edge of the hearing loss range (Eggermont and Komiya 2000; Seki and Eggermont 2003; Noreña and Eggermont 2003, 2005), leading to the hypothesis that cortical map reorganization is a causal factor of tinnitus (maladaptive plasticity hypothesis). That hypothesis predicts that an overrepresentation of hearing loss or hearing loss-edge frequencies coupled with spontaneous activity would lead to a frequency-specific tinnitus percept. However, other studies describe a broader pattern of neural activity changes, with map distortions occurring in relatively low frequency areas away from hearing loss and presumed tinnitus range (Engineer et al. 2011; Yang et al. 2011). These latter results do not support the idea that map reorganization is the cause of tinnitus.

In Yang et al. hearing-lesioned animals displayed evidence of high-frequency hearing-loss and tinnitus, and these were associated with distinct changes in different zones of the cortical map: (1) decreased inhibitory neurotransmission in the hearing-loss zone, and (2) increased inhibitory and excitatory neurotransmission in the low frequency normal-hearing zone (Yang et al. 2011). In these animals, there was an enlarged cortical representation of low-frequency sound that was, at least partly, a result of enhanced cortical responses to low-frequency tones. While, the receptive fields of high-frequency neurons tended to be discontinuous, rendering the corresponding cortical area less tonotopic. Interestingly, pharmaceutical manipulations that enhanced inhibition, and not those that reduced excitation, appeared to alleviate the tinnitus percept, thus implicating the neurons in the hearing-loss zone as having a causal role in tinnitus. In Engineer et al. 2011, the data also suggested over-representation at lower frequencies, with lower neuronal thresholds and higher amplitudes, in the noise-exposed animals (Engineer et al. 2011).

We compare these results in animal models to our findings in human patients, keeping in mind the important differences in species, etiology, and methodology. Of the multiple cortical pathologies seen in animal models, the low frequency hyper-excitability was relatively prominent in magnitude and thus perhaps the most likely to be detectable by non-invasive BOLD fMRI. We do not provide evidence nor claim that tonotopic map distortions are causal of tinnitus perception. Hyper-excitability could be related to hyperacusis, which commonly occurs with tinnitus and might be due to a generalized increase in auditory gain (Sheldrake et al. 2015). Some patients reported subjective complaints of hyperacusis which, in our study, did not correlate with response amplitudes. Future studies could utilize quantitative measures of loudness discomfort levels to more directly test this possibility (Knudson et al. 2016). Tonotopic distortions and tinnitus perception may be parallel consequences of a common underlying cause, namely neural deafferentation due to hearing loss.

It is important to note the difference in how tonotopic maps are measured in animal compared to human neuroimaging studies. In animal research, tonotopic maps are based on the spatial mapping of characteristic frequencies (CF), which are the best frequency response at threshold sound

levels (Rajan et al. 1993). In human neuroimaging, high intensity sounds are required to evoke measurable BOLD responses and tuning is thus based on the best frequency response at highly suprathreshold sound levels. In the normal brain, these two maps (threshold and suprathreshold tuning) appear to correspond well (Joly et al. 2014). However, in cases of hearing loss, which are likely associated with neural gain changes, differences could arise, thus imposing limitations in the comparison of human and animal mapping data.

Our findings contribute to increasing evidence against the idea that tinnitus is caused by maladaptive reorganization of hearing loss edge frequencies in tonotopic maps. Observational studies indicate that tinnitus tends to occur at the peak rather than the edge of the hearing loss range (Schecklmann et al. 2012), and studies of map reorganization have found either a lack of it (Langers and Kleine 2012, 2014), or that it occurs mostly in non-hearing loss regions (Yang et al. 2011; Engineer et al. 2011). Maladaptive map plasticity has also been much discussed in the context of phantom limb pain, and interestingly, its role there is also currently under question (Makin et al. 2013, 2015). It is unknown to what extent these two phenomena, tinnitus and phantom pain, share common neurophysiological origins.

More generally, auditory map plasticity has been studied in a broad context of behavioral and environmental manipulations (Schreiner and Polley 2014) and there are different mechanisms by which auditory maps could reorganize. Changes in neurophysiological properties of auditory neurons that could contribute to map plasticity include changes in: spectral tuning, response magnitudes, and dependence on sound intensity, tuning to sound location, response timing and neural synchrony. Inhibitory synapses have been indicated as 'critical gatekeepers' of plasticity and have also been implicated in tinnitus pathology (Middleton et al. 2011; Yang et al. 2011).

Human Studies

Human neuroimaging findings emphasize a broad anatomical network of tinnitus related pathology (Elgoyhen et al. 2015). Studies have shown altered responses in the auditory thalamus and cortex (Gu et al. 2010; Leaver et al. 2011; Langers and Kleine 2012; Melcher et al. 2000), and also implicate limbic and other non-auditory brain areas in modulating tinnitus perception and distress (Leaver et al. 2011; Seydell-Greenwald et al. 2012; Emmert et al. 2014; Lanting et al. 2014; Boyen et al. 2014). Alterations in functional connectivity patterns between auditory cortex and other brain regions emphasize increased interaction with attentional and limbic networks and possible impairments in thalamocortical gating (Maudoux et al. 2012; Schmidt et al. 2013; Lanting et al. 2014; Boyen et al. 2014). In contrast, a recent neuroimaging study of patient with a rare, high-intensity, tonal objective tinnitus (stemming from a physical sound generated in the ear) found a lack of changes in brain activity, underscoring the difference from centrally generated tinnitus (Guinchard et al. 2016). In Weisz et al. 2007, tinnitus patients showed a marked increase in auditory cortex gamma-band oscillations, thought to reflect underlying neural synchrony (Weisz et al. 2007). This evidence is compelling in that the oscillatory activity correlated with the laterality of the tinnitus percept and may relate to neural synchrony findings in animals, however see Sedley et al. 2012 for an alternate interpretation (Sedley et al. 2012).

Our results corroborate previous fMRI findings from a cohort of tinnitus patients with normal hearing thresholds (Langers and Kleine 2012a). That study used high-resolution 3 T fMRI to assess the integrity of the primary tonotopic maps and reported an overall lack of macroscopic changes in tinnitus sufferers (thus not supporting the maladaptive plasticity hypothesis). Additionally, using a conventional linear regression model, they reported increased activation in patients in the region of the low-frequency part of the tonotopic map in left lateral Heschl's gyrus. The authors note that this low-frequency response did not agree with the typical high-pitched tinnitus of their patients. It is encouraging that our studies converge upon coherent findings in two, rather different, patient groups. The bilaterality of the effect in our study could be related to the more extensive hearing loss in our patients, and also potentially to methodological differences.

It should be noted that the boundaries of primary auditory cortex are not fully discernable with human neuroimaging. The anterior and posterior borders are revealed by frequency reversals, but the lateral and medial borders cannot be distinguished by tonotopy alone (Da Costa et al. 2011). In monkeys, isofrequency bands of the primary (core) gradients extend continuously into lateral and medial non-primary (belt) auditory fields (Hackett 2011). As in our previous work (Da Costa et al. 2013), medial and lateral borders were manually drawn to include the medial-two-thirds of Heschl's gyrus in accordance with expectations from human architectonics (Rivier and Clarke 1997; Hackett 2011). We thus cannot rule out the inclusion of voxels belonging to non-primary auditory cortex in some subjects, particularly on the lateral end of Heschl's gyrus. The search for complementary measures to parcellate human auditory cortex such as myelin density (Dick et al. 2012; Martino et al. 2015) and tuning width or other spectral properties (Moerel et al. 2012; Thomas et al. 2015) is an active area of research. However, as yet no other solution has emerged as a gold standard.

Tonotopic maps were measured bilaterally based on ipsilateral stimulation, in both patients and controls. Unilateral stimulation induces clear bilateral activation of BOLD responses in the auditory cortex (van der Zwaag et al. 2011), although more strongly in contralateral cortex (Scheffler et al. 1998). In our study the same pattern of response was observed on contralateral and ipsilateral sides, and so both sides were combined in the analysis. The extent to which map accuracy differs given contralateral vs. ipsilateral stimulation is unknown, and this could be assessed by future studies, for example, designed to estimate population receptive fields (Thomas et al. 2015).

We included patients with unilateral hearing loss so that sound stimuli could be presented to unaffected ear, equivalently to control subjects. However, there remains an unequal effect of scanner noise since controls are more exposed to it in both ears. The effect of scanner noise on the mapping aren't known, but the most likely consequence would be sound masking which could lower BOLD response amplitudes in controls relative to patients. The acoustic resonance of the scanning protocol peaks strongly at approximately 1700 Hz (corresponding to the pulse sequence bandwidth) and does not have substantial energy in the 250–500 Hz range. We suspect that this may contribute to the dip in response amplitudes that we see here in both groups in the 1000–2000 Hz range, and in our previous studies with the same 7 T protocol (Da Costa et al. 2011; Da Costa et al. 2015). However, it is not obvious that this could account for the difference in patients and controls that peaks at 250–354 Hz range. Another approach to equating sound stimuli is to study the subgroup of tinnitus sufferers with normal hearing thresholds; however these patients are likely to suffer from 'hidden', high-intensity hearing-loss not assessed by standard audiograms (Schaette and McAlpine 2011b). Adequate sound delivery and, indeed, the broader problem of dissociating the effects of hearing loss and tinnitus are among the main challenges of human tinnitus studies. Utilizing sparse fMRI protocols and including tinnitus patients without hearing loss are among the methods that have been used to address these issues (Langers et al. 2012a).

Previous anatomical MRI studies have associated tinnitus with structural brain changes in the auditory cortex (Schneider et al. 2009; Boyen et al. 2013) and non-auditory areas (Mühlau et al. 2006). Heschl's gyrus is known for high anatomical variability in the normal population (Da Costa et al. 2011; Marie et al. 2013). The variability in the presence of an intermediate sulcus along its length that can divide the gyrus and make partially or complete duplications. Here, the rate of Heschl's gyrus divisons was similar in patients and controls, and within the previously reported range (Leonard et al. 1998; Da Costa et al. 2011; Marie et al. 2013). Thus, gross anatomical changes are not an obvious explanation for the functional changes we observed.

Comparing Findings from Humans and Animal Models

Tinnitus is an inherently subjective phenomenon and it is difficult to assess whether animal models (primarily rodent) have the same perceptual experience as human tinnitus sufferers. Hence there is a clear need to assess tinnitus-related pathology in humans. Our findings indicate a potential parallel in neurophysiological changes across human and animal models of tinnitus. In light of the observed hyperexcitability, treatments which aim to reinstate the balance between neuronal excitation and inhibition in auditory brain centers may help to alleviate tinnitus (Richardson et al. 2012). Experimental sound exposure therapies, and also neurofeedback, based on restoring normal activity levels in auditory cortex have shown potential in human patients (Haller et al. 2009; Okamoto et al. 2010; Tass et al. 2012) and may also induce changes in large-scale networks (Van De Ville et al. 2012; Haller et al. 2013).

Caution needs to be taken however in comparing findings from animal models and humans as there are many differences. Our patients had different etiologies and none of the patients presented hearing loss due to acoustic trauma or to sound exposure as in the majority of animal models. Indeed, investigations of tinnitus many challenges because the disorder is heterogeneous in terms of multiple factors including: etiology, loudness and quality of the percept, degree of hearing loss, level of associated distress, co-occurrence of hyperacusis, and potential interaction with age-related brain changes. Hearing loss is not always accompanied by tinnitus and the discriminating factors are not known (Schecklmann et al. 2012). Approximately 15% of tinnitus cases present without detectable changes in hearing thresholds but these cases may present hearing loss which is not detected by standard audiometry (Weisz et al. 2007; Schaette and McAlpine 2011a). Tinnitus risk factors may interact with age-related factors such as down-regulation of neural inhibition in the cortex (Caspary et al. 2008; Llano et al. 2012). Additionally human studies must consider differences in neuroimaging and data analysis methods.

Clinical Applications at 7T

Ultra-high field fMRI imaging offers a bridge between clinical and basic neuroscience research. Mapping of small functional subunits such as ocular dominance columns in the human visual cortex (Yacoub et al. 2007), tonotopic organization in human auditory cortex (Da Costa et al. 2011; Da Costa et al. 2013) and inferior colliculus (De Martino et al. 2013), or finger somatotopy in somatosensory

cortex (Martuzzi et al. 2012) and cerebellum (van der Zwaag et al. 2013) requires high-spatial resolution which is more easily achieved with ultra high field fMRI (van der Zwaag et al. 2009, 2015; Da Costa et al. 2015). Our study demonstrates the applicability of high-resolution mapping methods to clinical groups with auditory neurological disorders. We further illustrate the applicability of individual subject assessments, as opposed to group brain-averaged based analysis, in order to take full advantage of the spatial resolution achievable at ultra high field and to facilitate the relation of results to neurophysiological studies in animal models.

Conclusions

Here, we successfully employed high spatial resolution ultra-high field fMRI to demonstrate functional changes in primary auditory cortex related to hearing loss and tinnitus. In future studies, high-resolution imaging could be applied to track potential renormalization of auditory cortex during the testing of tinnitus treatments.

Acknowledgements This work was supported by Swiss National Science Foundation Grant 320030_143989 and by the Centre d'Imagerie BioMédicale (CIBM) of the Université de Lausanne, Université de Genève, Hôpitaux Universitaires de Genève, Lausanne University Hospital, École Polytechnique Fédérale de Lausanne, and the Leenaards and Louis-Jeantet Foundations.

Compliance with Ethical Standards

Conflict of interest The authors declare that they have no conflict of interest.

References

Axelsson A, Ringdahl A (1989) Tinnitus—a study of its prevalence and characteristics. Br J Audiol 23:53–62

Baumann S, Petkov CI, Griffiths TD (2013) A unified framework for the organization of the primate auditory cortex. Front Syst Neurosci 7:11.

Boyen K, Langers DRM, de Kleine E, van Dijk P (2013) Gray matter in the brain: differences associated with tinnitus and hearing loss. Hear Res 295:67–78

Boyen K, de Kleine E, van Dijk P, Langers DRM (2014) Tinnitus-related dissociation between cortical and subcortical neural activity in humans with mild to moderate sensorineural hearing loss. Hear Res 312:48–59

Brozoski TJ, Bauer CA, Caspary DM (2002) Elevated fusiform cell activity in the dorsal cochlear nucleus of chinchillas with psychophysical evidence of tinnitus. J Neurosci 22:2383–2390

Caspary DM, Ling L, Turner JG, Hughes LF (2008) Inhibitory neurotransmission, plasticity and aging in the mammalian central auditory system. J Exp Biol 211:1781–1791

Da Costa S, Zwaag W van der, Marques JP et al (2011) Human Primary Auditory Cortex Follows the Shape of Heschl's Gyrus. J Neurosci 31:14067–14075

Da Costa S, Zwaag W van der, Miller LM et al (2013) Tuning In to sound: frequency-selective attentional filter in human primary auditory cortex. J Neurosci 33:1858–1863

Da Costa S, Saenz M, Clarke S, van der Zwaag W (2015) Tonotopic gradients in human primary auditory cortex: concurring evidence from high-resolution 7 T and 3 T fMRI. Brain Topogr 28:66–69

De Martino F, Moerel M, van de Moortele P-F et al (2013) Spatial organization of frequency preference and selectivity in the human inferior colliculus. Nat Commun 4:1386

Dick F, Tierney AT, Lutti A et al (2012) In vivo functional and myeloarchitectonic mapping of human primary auditory areas. J Neurosci Off J. Soc Neurosci 32:16095–16105

Eggermont JJ (2015) Animal models of spontaneous activity in the healthy and impaired auditory system. Front Neural Circuits 9:19.

Eggermont JJ, Komiya H (2000) Moderate noise trauma in juvenile cats results in profound cortical topographic map changes in adulthood. Hear Res 142:89–101

Eggermont JJ, Roberts LE (2012) The neuroscience of tinnitus: understanding abnormal and normal auditory perception. Front Syst Neurosci 6:53.

Eggermont JJ, Roberts LE (2015) Tinnitus: animal models and findings in humans. Cell Tissue Res 361:311–336

Elgoyhen AB, Langguth B, De Ridder D, Vanneste S (2015) Tinnitus: perspectives from human neuroimaging. Nat Rev Neurosci 16:632–642

Emmert K, Ville DVD, Bijlenga P et al (2014) Auditory cortex activation is modulated by somatosensation in a case of tactile tinnitus. Neuroradiology 56:511–514

Engel SA (2012) The development and use of phase-encoded functional MRI designs. NeuroImage 62:1195–1200.

Engineer ND, Riley JR, Seale JD et al (2011) Reversing pathological neural activity using targeted plasticity. Nature 470:101–104

Gu JW, Halpin CF, Nam E-C et al (2010) Tinnitus, diminished sound-level tolerance, and elevated auditory activity in humans with clinically normal hearing sensitivity. J Neurophysiol 104(6):3361–3370. doi:10.1152/jn.00226.2010.

Guinchard AC, Ghazaleh N, Saenz M, Fornari E, Prior JO, Maeder P, Adib A, Maire R (2016) Study of tonotopic brain changes with functional MRI and FDG-PET in a patient with unilateral objective cochlear tinnitus. Hear Res 341:232–239

Hackett TA (2011) Information flow in the auditory cortical network. Hear Res 271:133–146

Haller S, Birbaumer N, Veit R (2009) Real-time fMRI feedback training may improve chronic tinnitus. Eur Radiol 20:696–703

Haller S, Kopel R, Jhooti P, et al (2013) Dynamic reconfiguration of human brain functional networks through neurofeedback. NeuroImage 81:243–252.

Joly O, Baumann S, Balezeau F, Thiele A, Griffiths TD (2014) Merging functional and structural properties of the monkey auditory cortex. Front Neurosci 8:198

Kaltenbach JA, Zacharek MA, Zhang J, Frederick S (2004) Activity in the dorsal cochlear nucleus of hamsters previously tested for tinnitus following intense tone exposure. Neurosci Lett 355:121–125

Knudson IM, Melcher JR (2016) Elevated acoustic startle responses in humans: relationship to reduced loudness discomfort level, but not self-report of hyperacusis. J Assoc Res Otolaryngol 17(3):223–235

Langers DRM (2014) Assessment of tonotopically organised subdivisions in human auditory cortex using volumetric and surface-based cortical alignments. Hum Brain Mapp 35:1544–1561

Langers DRM, van Dijk P (2012b) Mapping the tonotopic organization in human auditory cortex with minimally salient acoustic stimulation. Cereb Cortex 22:2024–2038

Langers DRM, Kleine E de (2012a) Tinnitus does not require macroscopic tonotopic map reorganization. Front Syst Neurosci 6:2.
Lanting CP, de Kleine E, Langers DRM, van Dijk P (2014) Unilateral tinnitus: changes in connectivity and response lateralization measured with fMRI. PLoS ONE 9(10):e110704
Leaver AM, Renier L, Chevillet MA et al (2011) Dysregulation of limbic and auditory networks in tinnitus. Neuron 69:33–43
Leonard CM, Puranik C, Kuldau JM, Lombardino LJ (1998) Normal variation in the frequency and location of human auditory cortex landmarks. Heschl's gyrus: where is it? Cereb Cortex 8:397–406
Llano DA, Turner J, Caspary DM (2012) Diminished cortical inhibition in an aging mouse model of chronic tinnitus. J Neurosci 32:16141–16148.
Ma W-LD, Hidaka H, May BJ (2006) Spontaneous activity in the inferior colliculus of CBA/J mice after manipulations that induce tinnitus. Hear Res 212:9–21
Makin TR, Scholz J, Filippini N et al (2013) Phantom pain is associated with preserved structure and function in the former hand area. Nat Commun 4:1570
Makin TR, Scholz J, Henderson Slater D et al (2015) Reassessing cortical reorganization in the primary sensorimotor cortex following arm amputation. Brain 138:2140–2146
Marie D, Jobard G, Crivello F, et al (2013) Descriptive anatomy of Heschl's gyri in 430 healthy volunteers, including 198 left-handers. Brain Struct Funct 220:729–743.
Marques JP, Kober T, Krueger G, et al (2010) MP2RAGE, a self bias-field corrected sequence for improved segmentation and T1-mapping at high field. NeuroImage 49:1271–1281.
Martino FD, Moerel M, Xu J et al (2015) High-resolution mapping of myeloarchitecture in vivo: localization of auditory areas in the human brain. Cereb Cortex 25:3394–3405
Martuzzi R, van der Zwaag W, Farthouat J et al (2012) Human finger somatotopy in areas 3b, 1, and 2: A 7 T fMRI study using a natural stimulus. Hum Brain Mapp 35(1):213–226
Maudoux A, Lefebvre P, Cabay J-E et al (2012) Auditory resting-state network connectivity in tinnitus: a functional MRI study. PLoS ONE 7:e36222
Melcher JR, Sigalovsky IS, Guinan JJ, Levine RA (2000) Lateralized tinnitus studied with functional magnetic resonance imaging: abnormal inferior colliculus activation. J Neurophysiol 83:1058–1072
Middleton JW, Kiritani T, Pedersen C, et al (2011) Mice with behavioral evidence of tinnitus exhibit dorsal cochlear nucleus hyperactivity because of decreased GABAergic inhibition. Proc Natl Acad Sci 108:7601–7606.
Moerel M, De Martino F, Formisano E (2012) Processing of natural sounds in human auditory cortex: tonotopy, spectral tuning, and relation to voice sensitivity. J Neurosci 32:14205–14216
Mühlau M, Rauschecker JP, Oestreicher E, et al (2006) Structural brain changes in tinnitus. Cereb Cortex 16:1283–1288.
Newman CW, Jacobson GP, Spitzer JB (1996) Development of the tinnitus handicap inventory. Arch Otolaryngol Head Neck Surg 122:143–148
Norena A, Micheyl C, Chéry-Croze S, Collet L (2002) Psychoacoustic characterization of the tinnitus spectrum: implications for the underlying mechanisms of tinnitus. Audiol Neurootol 7:358–369
Noreña AJ, Eggermont JJ (2003) Changes in spontaneous neural activity immediately after an acoustic trauma: implications for neural correlates of tinnitus. Hear Res 183:137–153
Noreña AJ, Eggermont JJ (2005) Enriched acoustic environment after noise trauma reduces hearing loss and prevents cortical map reorganization. J Neurosci 25:699–705
Okamoto H, Stracke H, Stoll W, Pantev C (2010) Listening to tailor-made notched music reduces tinnitus loudness and tinnitus-related auditory cortex activity. Proc Natl Acad Sci 107:1207–1210.
Rajan R, Irvine DR, Wise LZ, Heil P (1993) Effect of unilateral partial cochlear lesions in adult cats on the representation of lesioned and unlesioned cochleas in primary auditory cortex. J Comp Neurol 338(1):17–49
Richardson BD, Brozoski TJ, Ling LL, Caspary DM (2012) Targeting inhibitory neurotransmission in tinnitus. Brain Res 1485:77–87
Rivier F, Clarke S (1997) Cytochrome oxidase, acetylcholinesterase, and NADPH-diaphorase staining in human supratemporal and insular cortex: evidence for multiple auditory areas. NeuroImage 6:288–304.
Roberts LE, Eggermont JJ, Caspary DM et al (2010) Ringing ears: the neuroscience of tinnitus. J Neurosci 30:14972–14979
Saenz M, Langers DRM (2014) Tonotopic mapping of human auditory cortex. Hear Res 307:42–52
Salloum RH, Sandridge S, Patton DJ, Stillitano G, Dawson G, Niforatos J, Santiago L, Kaltenbach JA (2016) Untangling the effects of tinnitus and hypersensitivity to sound (hyperacusis) in the gap detection test. Hear Res 331:92–100
Salomon R, Darulova J, Narsude M, van der Zwaag W (2014) Comparison of an 8-channel and a 32-channel coil for high-resolution FMRI at 7 T. Brain Topogr 27:209–212
Sanchez-Panchuelo RM, Francis S, Bowtell R, Schluppeck D (2010) Mapping human somatosensory cortex in individual subjects with 7 T functional MRI. J Neurophysiol 103:2544–2556
Schaette R, McAlpine D (2011) Tinnitus with a normal audiogram: physiological evidence for hidden hearing loss and computational model. J Neurosci 31:13452–13457
Schecklmann M, Vielsmeier V, Steffens T et al (2012) Relationship between audiometric slope and tinnitus pitch in tinnitus patients: insights into the mechanisms of tinnitus generation. PLoS ONE
Scheffler K, Bilecen D, Schmid N et al (1998) Auditory cortical responses in hearing subjects and unilateral deaf patients as detected by functional magnetic resonance imaging. Cereb Cortex 8:156–163
Schmidt SA, Akrofi K, Carpenter-Thompson JR, Husain FT (2013) Default mode, dorsal attention and auditory resting state networks exhibit differential functional connectivity in tinnitus and hearing loss. PLoS ONE 8:e76488
Schneider P, Andermann M, Wengenroth M, et al (2009) Reduced volume of Heschl's gyrus in tinnitus. NeuroImage 45:927–939.
Schreiner CE, Polley DB (2014) Auditory map plasticity: Diversity in causes and consequences. Curr Opin Neurobiol 24:143–156
Sedley W, Teki S, Kumar S, Barnes GR, Bamiou D-E, Griffiths TD (2012) Signle-subject oscillatory gamma responses in tinnitus. Brain 135(10):3089–3100
Seki S, Eggermont JJ (2003) Changes in spontaneous firing rate and neural synchrony in cat primary auditory cortex after localized tone-induced hearing loss. Hear Res 180:28–38
Seydell-Greenwald A, Leaver AM, Turesky TK et al (2012) Functional MRI evidence for a role of ventral prefrontal cortex in tinnitus. Brain Res 1485:22–39
Sheldrake J, Diehl PU, Schaette R (2015) Audiometric characteristics of hyperacusis patients. Front Neurol 15(6):105
Tass PA, Adamchic I, Freund H-J et al (2012) Counteracting tinnitus by acoustic coordinated reset neuromodulation. Restor Neurol Neurosci 30:137–159
Thomas JM, Huber E, Stecker GC, et al (2015) Population receptive field estimates of human auditory cortex. NeuroImage 105:428–439.
Turrigiano GG, Nelson SB (2004) Homeostatic plasticity in the developing nervous system. Nat Rev Neurosci 5:97–107
Van De Ville D, Jhooti P, Haas T, et al (2012) Recovery of the default mode network after demanding neurofeedback training occurs in spatio-temporally segregated subnetworks. NeuroImage 63:1775–1781.

van der Zwaag W, Francis S, Head K, et al (2009) fMRI at 1.5, 3 and 7 T: characterising BOLD signal changes. NeuroImage 47:1425–1434.

van der Zwaag W, Gentile G, Gruetter R, et al (2011) Where sound position influences sound object representations: A 7-T fMRI study. NeuroImage 54:1803–1811.

van der Zwaag W, Kusters R, Magill A, et al (2013) Digit somatotopy in the human cerebellum: a 7 T fMRI study. NeuroImage 67:354–362.

van der Zwaag W, Schäfer A, Marques JP et al (2015) Recent applications of UHF-MRI in the study of human brain function and structure: a review. NMR Biomed 29(9):1274–1288

Weisz N, Müller S, Schlee W et al (2007) The neural code of auditory phantom perception. J Neurosci 27:1479–1484

Yacoub E, Shmuel A, Logothetis N, Uğurbil K (2007) Robust detection of ocular dominance columns in humans using Hahn Spin Echo BOLD functional MRI at 7 T. NeuroImage 37:1161–1177.

Yang S, Weiner BD, Zhang LS, et al (2011) Homeostatic plasticity drives tinnitus perception in an animal model. Proc Natl Acad Sci 108:14974–14979.

4 Detection of hyperacusis condition in tinnitus patients based on PLSC features that link audiogram and fMRI tonotopy responses.

This article is submitted in Frontiers journal.

frontiers

Detection of hyperacusis condition in tinnitus patients based on PLSC features that link audiogram and fMRI tonotopy responses.

Naghmeh Ghazaleh [1,4*], Wietske van der Zwaag2 [2,3],Raphael Maire [2,5], Melissa Saenz [1,6], Dimitri Van de Ville [1,4],

[1] *Medical image processing Laboratory (MIPLAB), Institute of Bioengineering, Ecole Polytechnique Federale de Lausanne (EPFL), Geneva , Switzerland*
[2] *Spinoza Centre for Neuroimaging, Royal Netherlands Academy for Arts and Sciences, Amsterdam, Netherlands*
[3] *Center for Biomedical Imaging, University of Lausanne, Switzerland*
[4] *Department of Radiology and Medical Informatics, University of Geneva, Geneva, Switzerland*
[5] *Department of Otorhinolaryngology, Head and Neck Surgery, Lausanne University Hospital, Lausanne, Switzerland*
[6] *Department of Clinical Neurosciences, Lausanne University Hospital, Lausanne,Switzerland*

Correspondence*:
Naghmeh Ghazaleh
Medical image processing Laboratory (MIPLAB), Institute of Bioengineering, Ecole Polytechnique Federale de Lausanne (EPFL), Geneva ,1004, Switzerland,
Naghmeh.Ghazaleh@epfl.ch

ABSTRACT

Our goal in this study is detection of hyperacusis condition in tinnitus patients. To this purpose, we acquire audiogram measurements of tinnitus patients that has information from peripheral auditory systems and also apply high-resolution fMRI at 7T to picture the tonotopic maps of primary auditory cortex as a meaningful measure of brain activity in the central auditory system. These measures do not provide sufficient information for spotting the hyperacusis condition when considered separately. To get meaningful biomarkers for classifying tinnitus patients with and without hyperacusis, we implemented for the first time partial least square correlation analysis (PLSC) that builds upon the cross-covariance information between audiogram and fMRI data. The cross-covariance of these two sets of data proved to provide us with metrics for successfully detecting this condition in tinnitus patients with 80% of accuracy and it is the first classifier that can detect hyperacusis condition in tinnitus patients.The PLSC obtained biomarkers, also yield the brain area playing a major role in the condition.

These findings provide precious insight for clinical study of hyperacusis and its treatment.

Keywords: Hyperacusis, Tinnitus, fMRI, Audiogram, PLSC, tonotopy, classification

1 INTRODUCTION

Hyperacusis is a condition of having difficulty in tolerating environmental sounds (Baguley (2003)).This term has been used in 1938 for the first time in medical literature (Baguley and McFerran (2011)). In some studies it is one type of a of the more general condition of decreased sound tolerance (Jastreboff and Jastreboff (2004)). Potential sources have been referred to the problem in peripheral auditory system, diseases in the central nervous system, infectious disease or hormonal imbalance (Katzenell and Segal (2001)). Hyperacusis patients show exaggerated reaction to the ordinary sounds that are neither threatening nor uncomfortably loud to a typical person. As a consequence, this condition can have a severe negative impact on the quality of life, like avoiding social gathering, crowded places, public transports and unveiling psychiatric disorders related to anxiety (Jüris et al. (2013)).

Hyperacusis emerges from the way that the central brain auditory system processes sounds, and its symptoms often overlap with tinnitus, which is instead the perception of a phantom sound in the absence of an external sound source. In fact, a great percentage of tinnitus patients report hyperacusis, according to the literature: 79.1% (Dauman and Bouscau-Faure (2005)), 40% (Baguley (2003); Levine (2013)), and, vice versa, tinnitus is very common in hyperacusis patients: reported as 86% (Baguley (2003)), 79% (Jüris et al. (2013))and 40% (Jastreboff et al. (1998); Jastreboff (1999)). For some of patients reporting both conditions are more bothered by hyperacousis than tinnitus (Chen et al. (2015); Levine (2013)).

The cause of hyperacusis is still not clear and to date there is no method that can examine objectively neither the existence nor the level of the disease. The current examination protocols are based on the response of the subject to questionnaires that are based on the subject perception of the sound, such as the uncomfortable loudness level (ULL) (Fackrell et al. (2015)) and the German questionnaire on hypersensivity to sound (G U F) (Nelting and Finlayson (2004)). Multiple-activity scale for hyperacusis (MASH) is also another subjective questionnaire introduced by (Dauman and Bouscau-Faure (2005)) to provide a scale for assessment of hyperacusis and determining the severity and prevalence of this condition in tinnitus patient based on the level of annoyance that the subjects feel during different activities; e.g., attending a concert. The evaluation of hyperacusis based on these questionnaires does not take into account the neurological changes in the brain and is just based on the subjective perception of the examined patients.

Few studies attempted to relate the loudness of the perceived sound stimuli with brain signal recordings (Gu et al. (2010); Langers et al. (2007)) but grouping tinnitus and hyperacusis patients in the same study population. One of the rare studies that

has considered hyperacusis and tinnitus as separate groups, investigates the effect of sodium salicylate on the functional connectivity of the tinnitus-hyperacusis network in rats, including behavioral, electrophysiological and functional magnetic resonance imaging (fMRI) measurements. However, their findings do not show any difference in functional connectivity between the two groups. Zeng (2013) adopted a systematic engineering approach to compare the quantified measures for input output ratio in tinnitus, hyperacusis and hearing loss, and to model the central and peripheral changes on the auditory system, as a result of these disorders. Their model predicts two different origins for hyperacusis and tinnitus, respectively, claiming that tinnitus is the result of increased central noise, whereas hyperacusis is due to increased nonlinear gain. This model offers precious insights to explain the origin of these disorders, but still it does not allow to discriminate the two conditions based on the clinical data acquired from patients. In many literature it has been concluded that hyperacusis problem is more complex to be solved just considering central or peripheral auditory nerves system separately. Therefore a method that is derived based on the data of both part of auditory nervous system could be stronger in diagnosing hyperacusis (Jastreboff and Jastreboff (2004); Jastreboff (1999)).
With the goal of objectively detecting the hyperacusis condition in tinnitus patients, we implemented for the first time partial least square correlation analysis (PLSC) (Krishnan et al. (2011)) that builds upon the cross-covariance information between audiogram and fMRI data, to get meaningful features for classifying tinnitus patients with and without hyperacusis. This approach is also useful for identifying hyperacusis symptoms in the auditory cortex where there is no access to the fMRI data of patients.

2 MATERIAL & METHODS

2.1 Subjects

All the patients gave written, informed consent. The ethics committee of the Faculty of Biology and Medicine of the University of Lausanne approved the experimental procedures. Patients (n=10, age 37.5 +/- 12 yrs, 6 male, 4 female) were recruited from the Otolaryngology Clinic of the Lausanne University Hospital and underwent a complete ear, nose, and throat (ENT) assessment including standard pure tone audiometry (PTA) and evaluation of tinnitus characteristics including the question about whether they have hyperacusis or not. Included patients had chronic subjective non-pulsatile tinnitus and moderate to severe unilateral sensorineural hearing loss (SHL) only in one ear with a decrease in hearing thresholds of minimum 40dB on three successive frequencies between 1 and 4 kHz, for a duration of at least 6 months; and normal age-adjusted hearing thresholds in the unaffected ear. None of the patients had history of neurological or psychiatric illness or standard MRI contraindications. Hearing loss caused from acoustic neuroma (noncancerous tumor of the auditory nerve), Merniere's disease (disorder of the inner ear typically affecting one side only), or unilateral cochlear damage caused by head trauma, infection, or

blood clot. Table.1 provides an overview of patient characteristics. French version the Tinnitus Handicap Inventory Newman et al. (1996) was used for Tinnitus discomfort assessment. The selection of patients with only unilateral hearing loss allowed for the unimpaired delivery of sound stimuli via the unaffected ear and any differences in the measured fMRI response could be asigned to altered cortical rather than to altered peripheral processing. Auditory cortex gets activated bilaterally (Van der Zwaag et al. (2011)) with stimulation of either ear so the fMRI data is measured from both brain hemispheres(Ghazaleh et al. (2017)).

Table 1. The characteristic of tinnitus patients that have been conducted in this study

ID	sex	age	Hearing loss side	hearing loss degree and frequency range	tinnitus center frequency	THi grade (1-5)	tinnitus duration	hyper-acusis	hearing loss origin
P1	F	54	L	>40 dB, >1000 Hz	noise 8000 Hz	3	>1 yr	yes	cochear
P2	M	35	R	>90 dB, full spectrum	noise 8000 Hz	3	>2 yr	no	cochlear
P3	M	44	R	>60 dB, full spectrum	noise 1000 Hz	2	>2 yr	no	acoustic neuroma
P4	M	46	L	>60 dB, full spectrum	noise 2000 Hz	4	>1 yr	yes	cochlear
P5	F	46	L	>40 dB, full spectrum	noise 1000 Hz, tone 6000 Hz	3	>5 yr	yes	Meniere's disease
P6	M	48	R	>50 dB, full spectrum	noise 6000 Hz	3	>7yr	no	Meniere's disease
P7	F	20	L	>40 dB, < 1000 Hz	noise 1000 Hz	2	>3 yr	no	acoustic neuroma
P8	M	46	R	>50dB, > 2000 Hz	tone 6000 Hz	5	>6 m	yes	cochlear
P9	F	26	L	>50 dB, >2000 Hz	noise 1000 Hz	4	>5 yr	yes	acoustic neuroma
P10	M	27	L	>90 dB, full spectrum	tone 8000 Hz	2	>10 yr	no	cochlear

2.2 Audiogram data acquisition

Audiogram of each patient is acquired by measuring the audible threshold of 9 different presenting frequencies starting from 125 Hz with steps of half octave and continues till 8 kHz. Making 9 in 10 matrix A representing the audiogram data for 10 subjects.

2.3 fMRI Data acquisition

An actively shielded 7 Tesla Siemens MAGNETOM scanner (Siemens Medical Solutions) was employed for Blood oxygenation level dependent (BOLD) functional imaging, performed at the Centre d'Imagerie BioMedicale in Lausanne, Switzerland. An 8-channel head volume RF-coil (RAPID Biomedical GmbH) (Salomon et al. (2014)) is used for scanning that is large enough to fit the headphones used for auditory stimulation, and a continuous EPI pulse sequence with sinusoidal read-out (1.5 × 1.5 mm in-plane resolution, slice thickness = 1.5 mm, TR = 2000 ms, TE = 25 ms, flip angle = 47 deg, slice gap = 0.07 mm (5%), matrix size = 148 × 148, field of view 222 × 222, 30

oblique slices covering the superior temporal plane). A T1-weighted high-resolution 3D anatomical image (resolution = 1 × 1 × 1 mm, TR = 5500ms, TE = 2.84 ms, slice gap = 1mm, matrix size = 256 × 240, field of view = 256 × 240) was acquired for each subject using the MP2RAGE pulse sequence optimized for 7T MRI (Marques et al. (2010)). The area of the brain covered by our imaging slab (van der Zwaag et al. (2009)) has a very small susceptibility induced distortions therefore co-registration between the functional images and the MP2RAGE was successful for all subjects, as aproved by visual inspection.

2.4 Sound stimuli

Sound stimuli were generated with Matlab and The Psychophysics Toolbox (www.Psychtoolbox.org) on a laptop computer with a sampling rate of 44.1 kHz, and were delivered via MR-compatible optical headphones (AudioSystem, Nordic NeuroLab). Sound intensities per frequency were between 82-97 dB SPL to get perceived equaly loud based on the standard equal-loudness curves (ISO 226, Phon 85 dB). Stimulus intensities were further reduced approximately 24 dB by the protective earplugs. Earplugs inevitably reduced sound spectrum unevenly, with more effect on high frequencies than low. All subjects reported hearing all tone frequencies at a clear and comfortable level and were stimulated in the unaffected ear only Table.1. Overall time in the scanner including set-up, two fMRI tonotopy runs, and an anatomical scan was approximately 45 minutes, sufficiently brief for patient comfort.

2.5 fMRI data preprocessing

fMRI data preprocessing steps, including linear trend removal, temporal high-pass filtering (2 cycles), and motion correction were done with BrainVoyager QX software. We didn't apply any Spatial smoothing to preserve the advantages of high-resolution acquisition. Slice-timing correction was not applied. Data of fMRI runs were interpolated into a 1 × 1 × 1 mm volumetric space and registered to each subject's own 3D Talairach normalized anatomical data. Foreach subject, cortical surface meshe was generated from its anatomical dataset using automated segmentation tools in BrainVoyager QX.

2.6 Tonotopic mapping task

Initiated in the basilar membrane of the cochlea, tonotopy is the spatial positioning of auditory neurons in gradients of sound frequency preference. These arrangement is maintained in the auditory nerve, mid-brain, thalamus, and cortex. In human primary auditory cortex, two tonotopic gradients with mirror-symmetry ('high-to-low' followed by 'low-to-high' preferences) are detected across Heschl's gyrus, along an overall posterior-to-anterior axis. These two mirror-symmetric gradients appear to correspond to primary auditory cortex fields A1 and R,(Da Costa et al. (2011); Langers and van Dijk (2011); Ghazaleh et al. (2017); Guinchard et al. (2016)). Following the method of Da Costa et al. (2011), we use tonotopic gradients for localization of

primary auditory cortex (PAC). We employed a *phase-encoded* mapping paradigm to define tonotopic maps in the cortex, this technique is commonly used for retinotopic mapping (Engel (2012)), and also for somatotopic mapping (Sanchez-Panchuelo et al. (2010)). Tonotopic mapping stimulus is designed to sweep the parameter space of the map (in this case, low to high), and generates a wave of best responses to different sound frequencies across the cortical surface. The initial peaks of the recorded activity placed in the low frequency map endpoint and progressively later in parts of the map preferring higher frequencies. The phase of the response defines the preferred frequency of each responsive voxel. The mapping stimulus is periodic presentation of 15 different sound frequencies (88, 125, 177, 250, 354, 500, 707, 1000, 1414, 2000, 2828, 4000, 5657, 8000, and 11312 Hz, half-octave spacing). For each period, pure tone bursts of each frequency were presented for 2 sec and stepping to the next frequency until all 15 frequencies were presented followed by a 4 sec silent pause. During each 2 sec block, pure tone bursts of the given frequency had different onset times (50 ms and 250 ms duration randomly interspersed with 50 ms inter-stimulus intervals) to avoid a fixed periodicity. Each period of 34 sec (14 times 2 seconds sec plus 4 sec silent pause) was repeated 14 times for a scan run duration of 7 min and 56 sec. Each subject participated in two scan runs (one with stimulus sweeps from low-to-high, and one in reverse order). The resulting maps of the two runs were averaged to keep the tonotopic preferences independent of stimulus order. Linear correlation analysis was used to discern the response phase that best fitted the measured fMRI time course of each responsive voxel. Response amplitudes were measured as the maximal signal change of voxels in the volumetric ROI assigned to each sound frequency. So for each frequency tones per subject we get the measure of activity for that frequency that makes the 15 in 10 matrix B for the brain activity data.

2.7 Partial least square correlation analysis

Partial least square correlation analysis is a multivariate method applied to neuroimaging data for the first time by McIntosh (McIntosh and Lobaugh (2004)). PLSC analyzes associations between two sets of data, and is often used in the field to explore the correlation between brain activity and behavioral data in one or more groups of subjects. Here, we adopted this method to analyze the correlation between the tonotopic mapping (our brain data matrix A) and the audiograms measurements (our behavioral data matrix B). Both matrices are Z-score normalized for each variable, and then the cross-covariance of all the brain and behavioral activities is calculated as $R = B^T A$. The singular value decomposition (SVD) of R is then performed as $R = U \nabla V$, to yield the behavioral salience matrix U, including the behavioral profiles that best characterize the correlation R, and the brain salience matrix V, highlighting instead the brain activity patterns that best characterize R. By projecting the original matrices A and B on their saliences, we obtain the PLS components or latent variables $L_A = AV$ and $L_B = BU$, representing a new set of dimensions, along which the data correlation is maximized. The significance of the latent variables is assessed by

permutation testing (Higgins (2003)), where we randomly permute the order of the fMRI and behavioral data 1'000 times, and extract singular values from the permuted data. Only one *LV* was found to be significant ($p < 0.05$). The stability of the calculated saliences is then tested by bootstrapping, that is sampling with replacement of the measurements (Kohavi et al. (1995)) in matrix A and B. The standard error of salience values is calculated from the bootstrapping distribution and used to normalize them for their stability. Fig.1 shows the pipeline for extracting PLSC features.

2.8 Classifier design

We design a support vector machine (SVM) based classifier Vapnik and Vapnik (1998) to detect hyperacusis condition in tinnitus patients. SVM is a supervised classifier that gets trained on labeled data to find a hyperplane for categorizing a new data. Here, the SVM classifier is trained on the brain and behavioral scores. As it is shown in Fig.1, PLSC makes one set of brain *LV* and two sets of audiogram *LV*s, for the two groups of hyperacusis and non hyperacusis patients, respectively. These two set of features are used for training SVM.

2.9 Validation

Using leave-one-out cross-validation (Kohavi et al. (1995)), the audiogram and fMRI measurements of a test subject not included in the training set serve as the input for the classifier to evaluate detection of the hyperacusis condition. Leave one out cross validation is applied on the set of 10 patients. For each subject, the SVM is trained on the PLS scores of the other 9 subjects and tested on the selected subject. To assess the advantages of using PLSC-derived features as inputs to the classifier, we compare the performance of our designed classifier with a SVM classifier that is trained on brain and behavioral data (A and B) directly and perform leave-one-out cross validation accordingly.

3 RESULTS

We applied PLSC method on the two sets of audiogram measures and fMRI measures for two applications: first to use audiogram data to infer the differences in fMRI measurement and second to extract biomarkers from combining the two datasets to make a classifier for detecting hyperacusis condition.
Fig.2.a illustrates the behavioral saliencies of the hyperacusis and non-hyperacusis conditions. Those saliencies of the audiogram measures that have different signs (positive and negative values) per each group (the last four saliences) can be used to discriminate fMRI data saliencies of the two group of study. These results imply that audiogram measures in high frequency band can be used to predict the difference in fMRI measurement and therefore plays more important role in detecting hyperacusis condition. The brain saliencies related to the fMRI data of the both groups are shown in Fig.2.b these measures explain how much is the contribution of fMRI measure

Table 2. Performance of the classifier, trained with different data types

Training data	PLSC saliences	fMRI and audiogram data	fMRI data	Audiogram data
Accuracy (%)	80	60	50	40

related to each frequency tone, in explaining the relation between brain (fMRI) and behavioral (audiogram) data. Where the saliencies related to middle high frequency (2800Hz) have the most contribution in explaining the information derived from cross-covariance between the two sets of data. Fig.3 displays the projection of the brain saliences of Fig.2.b on the auditory cortex of all the subjects, using their tonotopy map as the reference of the voxels label. In the classification task, we compare the accuracy of the PLS made classifier, trained with brain scores L_A and behavioral scores L_B with the classifier that is trained with brain and behavioral data, A and B matrix, together and also each of them alone. The accuracy is calculated as(Powers (2011)):

$$Accuracy = \frac{TruePositive + TrueNegative}{TotalPopulation} \tag{1}$$

The classification accuracy, built based on different data types is shown in Table.2.

4 DISCUSSION

Hyperacusis is a very common condition among tinnitus patients, which has been rarely studied independently from tinnitus (Nelson and Chen (2004)). Both conditions are subjective phenomenon and usually it is not possible to be assessed objectively. As it is discussed in Eggermont (2013), the similarity in behavioral response of animals to hyperacusis and tinnitus declines the specificity of the result for diagnosing one of this condition alone.

In human hyperacusis, the only existing method for the evaluation is based on the scores obtained from the answer of patients to different questionnaires (Fackrell et al. (2015); Nelting and Finlayson (2004)) and because of their subjective nature, can not provide a reliable measure for this disorder (Wallén et al. (2012)). Here, we introduce audiogram and imaging data, with the aim of finding an objective way to detect hyperacusis. To this purpose, we acquire audiogram measurements of tinnitus patients that involve peripheral and central auditory systems and also apply high-resolution fMRI at 7T to picture the tonotopic maps of primary auditory cortex as a meaningful measure of brain activity. These measures do not provide sufficient information for spotting the hyperacusis condition when considered separately, but the cross-covariance of these two sets of data proved to provide us with metrics for successfully detecting this condition in tinnitus patients.

We extract these metrics by applying PLSC on the sets of data to get brain and behavioral saliences. Firstly, the two sets of behavioral saliences reveal that the audiogram measurements related to the high frequency tones have different contributions to the fMRI activity profiles of the tinnitus patients with and without hyperacusis (Fig.2.a). This can facilitate the prediction of information about the fMRI data of auditory cortex for a new subject just with audiogram measurements.
The brain saliences projected on the auditory cortex (Fig.2.b) show that the information obtained from the responses of the voxels with best responses in the higher frequency range can describe most of the relationship between the brain activity in the auditory cortex and the audiogram, which is closer to the subjective report of the patients about their hyperacusis condition. These findings can stimulate the research towards investigating the underlying neurological disorder of hyperacusis and providing useful information about the areas of the brain that are affected.
We provided therefore a more powerful method for objectively detecting the hyperacusis condition in a fully data driven approach, by using a classifier that we designed based on the information extracted from PLSC. The classifier can detect the existence of the hyperacusis condition in an unknown subject with 80% of accuracy. This outcome cannot be achieved using the audiogram measures or fMRI measures alone, and neither using both of them directly, rather than based on their joint information in the saliences extracted from PLSC. Among the very limited number of studies distinguishing hyperacusis from tinnitus condition, one of them (Zeng (2013)) has differentiated the origin of hyperacusis and tinnitus, by making different models for predicting the source and effect of the two conditions and the hearing loss on the nervous system from peripheral to central level. This model gives a good understanding about the possible reason of these disorders, but does not resolve the need for having an objective method to diagnose the hyperacusis condition in tinnitus patients, that has resolved with our suggested method.
Even though our proposed clustering technique is able to detect hyperacusis condition for a new subject, in an unsupervised way, the training phase of the classifier has been made with supervised and subjective assessment of sustaining hyperacusis disorder. As the training is done on a limited number of sample patients it is possible to use different methods of assessment to obtain a reliable data for making a precise classifier. Therefore the focus of this study is not on the initial subjective way of detecting hyperacusis condition for training data, rather we are proposing an efficient method for feature extraction from multi modal data and training a classifier that is built based on this features. This classifier can therefore detect hyperacusis condition in a new subject without any subjective evaluation as the first study that targets this goal and successfully achieved it. This result can get improved by increasing the number of subject and having more heterogeneous type of hyperacusis and tinnitus patients.

5 CONCLUSION

Loudness hyperacusis is a very common hearing disorder among tinnitus patients, but has been rarely studied independently from tinnitus. The reason could be that none of the existing clinical measurements have been sufficient for detecting this condition in tinnitus patients and so just relies on the patients' subjective perceptions. Here, we made the objective detection of hyperacusis possible, by introducing a PLSC-based feature extraction for classification that uses the combination of audiogram and fMRI measures. By applying PLSC on these data, we find a biomarker that can differentiate hyperacusis condition among tinnitus patients and also yields the brain area playing a major role in the condition. This approach shows therefore to be worth exploring for further clinical study of hyperacusis and its treatment.

DISCLOSURE/CONFLICT-OF-INTEREST STATEMENT

The authors declare that the research was conducted in the absence of any commercial or financial relationships that could be construed as a potential conflict of interest.

Funding: This work was supported by Swiss National Science Foundation Grant 320030_143989 and by the Centre d'Imagerie BioMedical (CIBM) of the Universite de Lausanne, Universite de Geneve, Hopitaux Universitaires de Geneve, Lausanne University Hospital and Ecole Polytechnique Federale de Lausanne school of engineering.

REFERENCES

Baguley, D. M. (2003). Hyperacusis. *Journal of the Royal Society of Medicine* 96, 582–585

Baguley, D. M. and McFerran, D. J. (2011). Hyperacusis and disorders of loudness perception. In *Textbook of tinnitus* (Springer). 13–23

Chen, Y.-C., Li, X., Liu, L., Wang, J., Lu, C.-Q., Yang, M., et al. (2015). Tinnitus and hyperacusis involve hyperactivity and enhanced connectivity in auditory-limbic-arousal-cerebellar network. *Elife* 4, e06576

Da Costa, S., van der Zwaag, W., Marques, J. P., Frackowiak, R. S., Clarke, S., and Saenz, M. (2011). Human primary auditory cortex follows the shape of heschl's gyrus. *The Journal of Neuroscience* 31, 14067–14075

Dauman, R. and Bouscau-Faure, F. (2005). Assessment and amelioration of hyperacusis in tinnitus patients. *Acta oto-laryngologica* 125, 503–509

Eggermont, J. J. (2013). Hearing loss, hyperacusis, or tinnitus: what is modeled in animal research? *Hearing research* 295, 140–149

Engel, S. A. (2012). The development and use of phase-encoded functional mri designs. *Neuroimage* 62, 1195–1200

Fackrell, K., Fearnley, C., Hoare, D. J., and Sereda, M. (2015). Hyperacusis questionnaire as a tool for measuring hypersensitivity to sound in a tinnitus research population. *BioMed research international* 2015

Ghazaleh, N., Zwaag, W. v. d., Clarke, S., Ville, D. V. D., Maire, R., and Saenz, M. (2017). High-resolution fmri of auditory cortical map changes in unilateral hearing loss and tinnitus. *Brain Topography* , 1–13doi:10.1007/s10548-017-0547-1

Gu, J. W., Halpin, C. F., Nam, E.-C., Levine, R. A., and Melcher, J. R. (2010). Tinnitus, diminished sound-level tolerance, and elevated auditory activity in humans with clinically normal hearing sensitivity. *Journal of Neurophysiology* 104, 3361–3370

Guinchard, A.-C., Ghazaleh, N., Saenz, M., Fornari, E., Prior, J., Maeder, P., et al. (2016). Study of tonotopic brain changes with functional mri and fdg-pet in a patient with unilateral objective cochlear tinnitus. *Hearing research* 341, 232–239

Higgins, J. J. (2003). Introduction to modern nonparametric statistics

Jastreboff, P. (1999). The neurophysiological model of tinnitus and hyperacusis. In *Sixth International Tinnitus Seminar* (The Tinnitus and Hyperacusis centre London), 32–38

Jastreboff, P., Gray, W., and Mattox, D. (1998). Tinnitus and hyperacusis. *Otolaryngology Head & Neck Surgery* 165, 3198–222

Jastreboff, P. J. and Jastreboff, M. M. (2004). Decreased sound tolerance. *Tinnitus: Theory and management* , 8–15

Jüris, L., Andersson, G., Larsen, H. C., and Ekselius, L. (2013). Psychiatric comorbidity and personality traits in patients with hyperacusis. *International Journal of Audiology* 52, 230–235

Katzenell, U. and Segal, S. (2001). Hyperacusis: review and clinical guidelines. *Otology & Neurotology* 22, 321–327

Kohavi, R. et al. (1995). A study of cross-validation and bootstrap for accuracy estimation and model selection. In *Ijcai* (Stanford, CA), vol. 14, 1137–1145

Krishnan, A., Williams, L. J., McIntosh, A. R., and Abdi, H. (2011). Partial least squares (pls) methods for neuroimaging: a tutorial and review. *Neuroimage* 56, 455–475

Langers, D. R. and van Dijk, P. (2011). Mapping the tonotopic organization in human auditory cortex with minimally salient acoustic stimulation. *Cerebral Cortex* , bhr282

Langers, D. R., van Dijk, P., Schoenmaker, E. S., and Backes, W. H. (2007). fmri activation in relation to sound intensity and loudness. *Neuroimage* 35, 709–718

Levine, R. A. (2013). Tinnitus: diagnostic approach leading to treatment. In *Seminars in neurology* (Thieme Medical Publishers), vol. 33, 256–269

Marques, J. P., Kober, T., Krueger, G., van der Zwaag, W., Van de Moortele, P.-F., and Gruetter, R. (2010). Mp2rage, a self bias-field corrected sequence for improved segmentation and t 1-mapping at high field. *Neuroimage* 49, 1271–1281

McIntosh, A. R. and Lobaugh, N. J. (2004). Partial least squares analysis of neuroimaging data: applications and advances. *Neuroimage* 23, S250–S263

Nelson, J. J. and Chen, K. (2004). The relationship of tinnitus, hyperacusis, and hearing loss. *Ear, nose & throat journal* 83, 472

Nelting, M. and Finlayson, N. K. (2004). *Geräuschüberempfindlichkeits-Fragebogen: GÜF; Manual* (Hogrefe)

Newman, C. W., Jacobson, G. P., and Spitzer, J. B. (1996). Development of the tinnitus handicap inventory. *Archives of Otolaryngology–Head & Neck Surgery* 122, 143–148

Powers, D. M. (2011). Evaluation: from precision, recall and f-measure to roc, informedness, markedness and correlation

Salomon, R., Darulova, J., Narsude, M., and Van Der Zwaag, W. (2014). Comparison of an 8-channel and a 32-channel coil for high-resolution fmri at 7 t. *Brain topography* 27, 209–212

Sanchez-Panchuelo, R. M., Francis, S., Bowtell, R., and Schluppeck, D. (2010). Mapping human somatosensory cortex in individual subjects with 7t functional mri. *Journal of neurophysiology* 103, 2544–2556

van der Zwaag, W., Francis, S., Head, K., Peters, A., Gowland, P., Morris, P., et al. (2009). fmri at 1.5, 3 and 7 t: characterising bold signal changes. *Neuroimage* 47, 1425–1434

Van der Zwaag, W., Gentile, G., Gruetter, R., Spierer, L., and Clarke, S. (2011). Where sound position influences sound object representations: a 7-t fmri study. *Neuroimage* 54, 1803–1811

Vapnik, V. N. and Vapnik, V. (1998). *Statistical learning theory*, vol. 1 (Wiley New York)

Wallén, M. B., Hasson, D., Theorell, T., and Canlon, B. (2012). The correlation between the hyperacusis questionnaire and uncomfortable loudness levels is dependent on emotional exhaustion. *International journal of audiology* 51, 722–729

Zeng, F.-G. (2013). An active loudness model suggesting tinnitus as increased central noise and hyperacusis as increased nonlinear gain. *Hearing Research* 295, 172–179

FIGURES

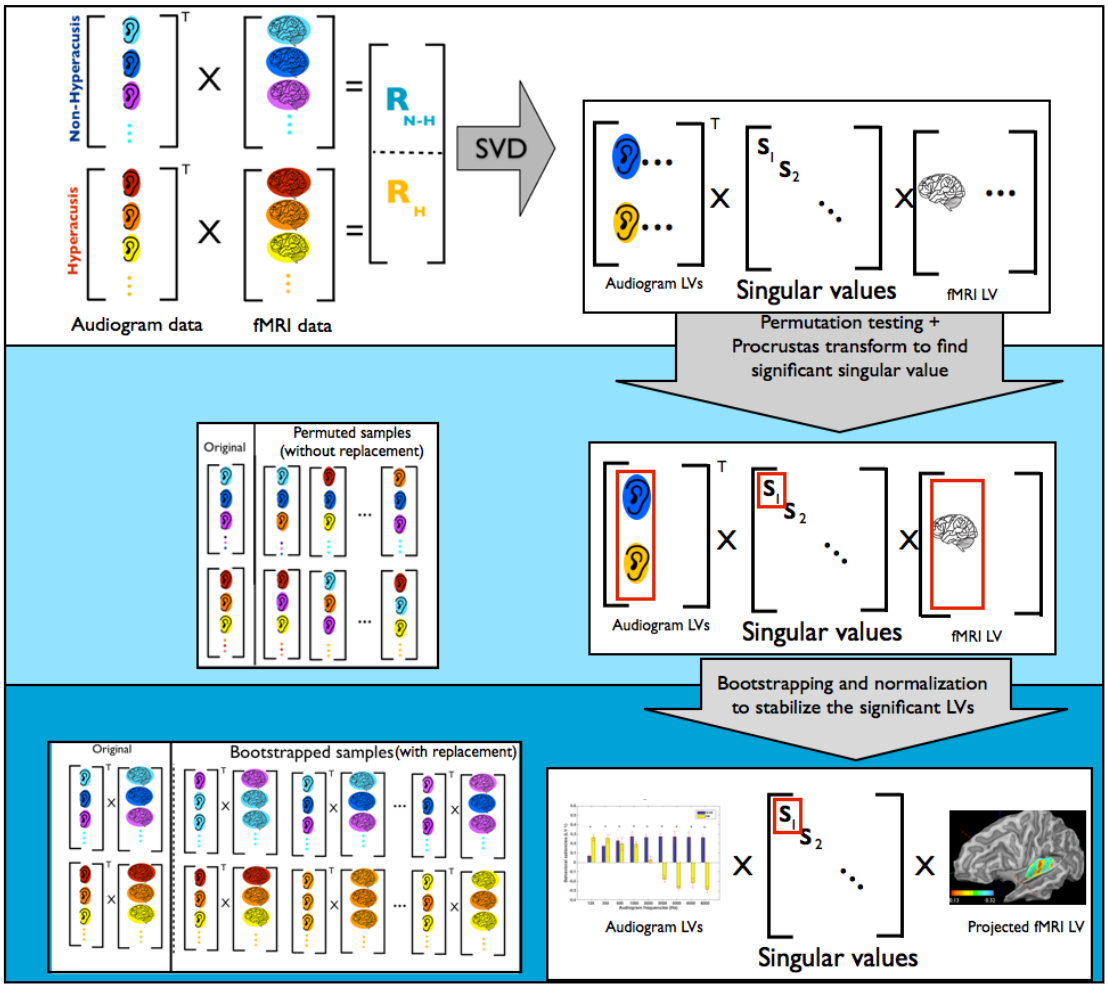

Figure 1. Pipeline of applying PLSC method on the data. Applying SVD on cross product matrix of Audiogram and fMRI data. Permutation testing is applied on the data to extract the significant eigenvalue and related significant LVs. After repeating the procedure on bootstapped data the stable output is extracted.

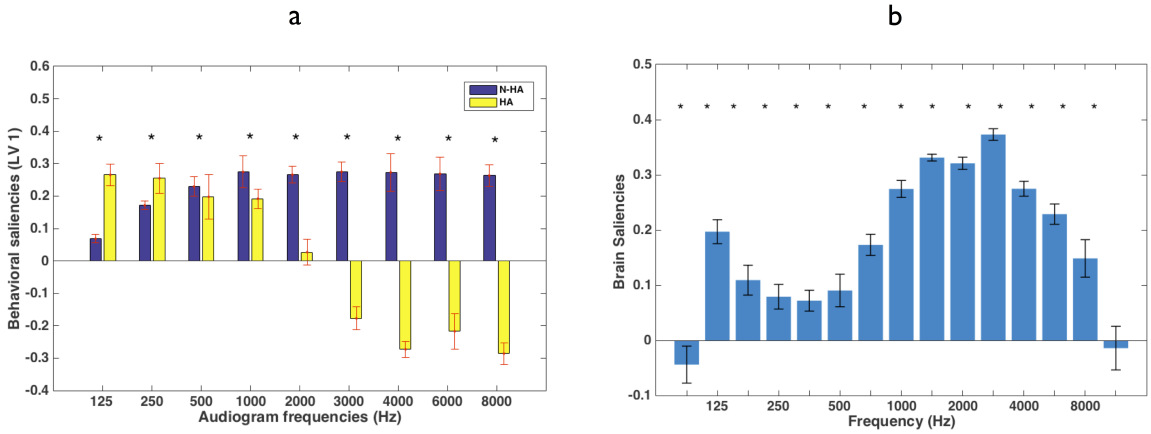

Figure 2. Results for the significant PLSC latent variable. (a) Behavioral saliences for hyperacusis (HA) and non-hyperacusis (N-HA) groups. (b) Brain saliences for tonotopy experiment frequencies. The asterisk (*) indicates significant bootstrap ratios ($p < 0.05$).

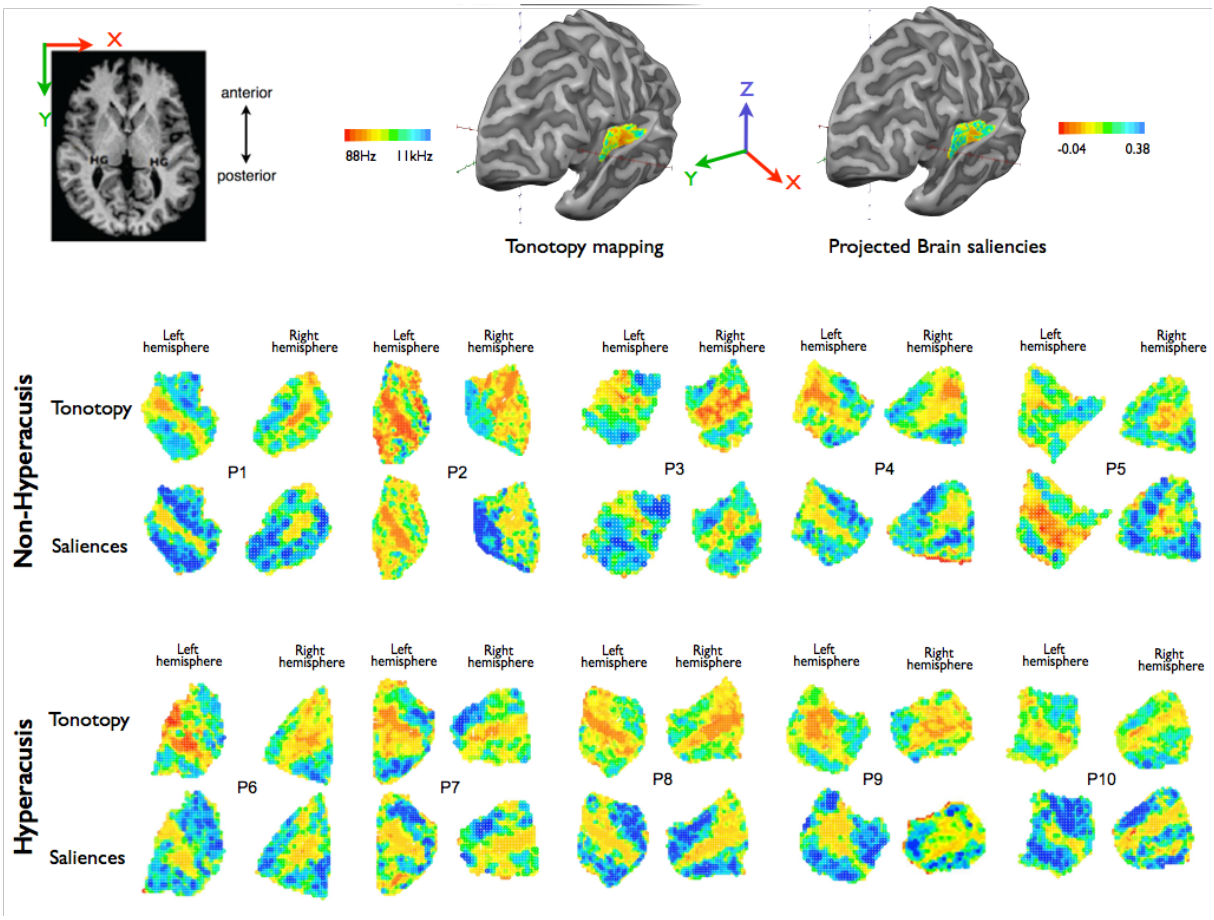

Figure 3. For all the Individual subjects projection of the saliencies and tonotopic map on the flattered cortical mesh in auditory cortex are shown. For patients without hyperacusis in the middle and with hyperacuis in the bottom row. The upper-left inset is provided as a reference of the anatomical orientation of all the plots (HG=Heschl's gyrus) and the upper right insets are the tonotopic map and brain saliencies projections on 3D mesh of left hemisphere for a sample subject.

5 Subject-specific parcellation of auditory cortex based on resting state fMRI functional and effective connectivity

This article is in preparation for submission to Journal of Neuroscience.

Subject-specific parcellation of auditory cortex based on resting state fMRI functional and effective connectivity.

Naghmeh Ghazaleh[a,b,*], Adeel Razi[d,e], Kumar Sukhbinder[d,c], Maria Giulia Pretti[a,b], Karl Friston[d], Melissa Saenz[a], Dimitri Van De Ville[a,b]

[a] *Medical image processing Laboratory (MIPLAB), Institute of Bioengineering, Ecole Polytechnique Federale de Lausanne (EPFL), Geneva , Switzerland*
[b] *Department of Radiology and Medical Informatics, University of Geneva, Geneva, Switzerland*
[c] *Institute of Neuroscience, Medical School, Newcastle University, Newcastle, UK*
[d] *The Wellcome Trust Centre for Neuroimaging, University College London, London, UK*
[e] *Department of Electronic Engineering, NED University of Engineering and Technology, Karachi, Pakistan*

Abstract

The segmentation of auditory cortex based on anatomical atlases is usually inaccurate because of the large differences in the topography of auditory cortex across individuals. In this paper, we investigate the use of the pattern of extrinsic connectivity of auditory cortex as the segmentation feature. As measures of brain connectivity, we use two popular methods in literature namely: effective connectivity and functional connectivity. We will use dynamic causal modeling (DCM) for measuring effective connectivity. In this work, we aim to develop an accurate parcellation of auditory cortex into its two main parts of primary and the secondary auditory cortex. We will first divide auditory cortex into smaller auditory patches (or subregions). For each auditory patch ,we create a network comprising of three regions of interest (ROIs): an auditory patch in the auditory cortex and the two source regions outside the auditory cortex namely baso-lateral amygdala and hippocampus. Baso- lateral amygdala and hippocampus have been shown to have discriminative connections with both primary and secondary auditory cortex. We will use spectral clustering for classification of auditory cortexs two subregions of primary and secondary auditory cortex. We show that we can achieve 74% accuracy using DCM connectivity features and 71% for functional connectivity features for segmentation of auditory cortex - on average for both hemispheres. This new segmentation method built upon (effective) connectivity takes advantage of the information about directed causal interaction in our network model

*Naghmeh Ghazaleh
Email address: naghmeh.ghazaleh@epfl.ch (Naghmeh Ghazaleh)

in comparison to the functional (symmetric) connectivity which is a measure of statistical dependencies and leads to the lower clustering accuracy. This new data driven segmentation method is not only efficient in defining the subregions of the auditory cortex for studying healthy brain but is also a potentially powerful tool for characterizing the changes in functional anatomy of auditory cortex as a result of hearing disorders like tinnitus.

Keywords: DCM, Auditory cortex, Effective connectivity, Segmentation, Spectral clustering, Resting state fMRI

1. Introduction

Cortical parcellation, i.e. the subdivision of the brain cortex into meaningful sub-regions, is an important step needed in many neuroimaging analysis methods, and is therefore an active area of research in neuroscience[1, 2, 3, 4, 5]. In particular, auditory cortex parcellation represents a demanding application due to the diversity in this region topography among individuals[6, 7, 8]. For this reason, the definition of auditory cortex sub-regions based on a brain atlas, usually created from one individual brain or an average of different brains, does not represent a reliable reference. Most auditory studies require a precise subdivision of the auditory cortex into its two main segments; i.e. the primary auditory cortex located on the superior temporal gyrus in the temporal lobe - and secondary auditory cortex - the rostral part of the temporal lobe. In [9, 10], a tonotopic map captured using functional magnetic resonance imaging (fMRI) was used for better identifying the boundaries of the primary auditory cortex (PAC), however a limitation of this map is the capability of defining the boundaries of the auditory cortex only in one axis in the direction of frequency change. Other studies [11, 6] also used, in addition to a tonotopic map, the data of myelination of the auditory cortex to define the borders of PAC. The high dependency of these parcellations on the experimental design parameters encourage us to find a more reproducible and data-driven method for the parcellation of the auditory cortex. Brain connectivity features have been extensively used to guide the whole brain parcellation [12, 13, 14, 15]. For this purpose, two types of connectivity models are usually deployed: structural connectivity, based on the anatomical data of the brain as measured using diffusion MRI [15, 16] and functional connectivity (FC), which is broadly defined as the statistical dependencies between the brain regions time series obtained from resting-state functional MRI (rsfMRI)[17, 18, 19, 20, 21, 22, 23, 24, 16]. In rsfMRI, the subject is not doing an explicit task, and thus the blood oxygenation level dependent (BOLD) signal is reflective of the spontaneous fluctuations in the absence of an exogenous (experimental) input. FC-driven parcellations are based on the notion that the patterns of brain connectivity are consistent in the same cortical area. However, no study so far has attempted to specifically

parcellate the auditory cortex based on resting-state (functional) connectivity. The reason might be that resting-state FC does not have sufficiently discriminative features for neighboring small regions therefore a more precise model is required for segmentation on smaller scale. Compared to functional connectivity that shows the statistical dependencies of neurophysiological responses among different regions of the brain, effective connectivity provides us with a more informative way of characterizing connectivity of brain networks by estimating the causal (directed) influence of different brain regions on each other. The framework of dynamic causal modeling (DCM) is used for measuring effective connectivity (Friston et al. 2003). Primary auditory cortex is composed of neuronal populations that decode the sound frequencies and represent the tonotopic structure of sound stimuli whereas the secondary auditory cortex has less tonotopic structure and is responsible for more complex sound processing such as language processing, localization and auditory memory. Because of their different functional roles, primary and secondary auditory cortices have discriminative directed connections with other regions of the brain. Latero-basal amygdala and hippocampus are among the regions that have functional specificity in terms of their interaction with primary and secondary auditory cortices. There are several studies in both animals and humans that show the strong connection of secondary auditory cortex with amygdala in emotional sound memory and fear conditioning [25], the role of hippocampus in long-term memory formation for sounds [26, 27, 25] and the impact of primary auditory cortex in settling long-term illustration of specific auditory experiences. Previous work in [28, 29, 30] therefore constructed a network composed of the aforementioned regions of interests (ROIs) (i.e. latero-basal amygdala, hippocampus and auditory cortex), producing valuable features for the segmentation of auditory cortex. With the aim of providing a new and objective way to parcellate the auditory cortex, we explored the utility of using functional connectivity and effective connectivity using rsfMRI data. We used the pattern of connectivity as the features for distinguishing between different regions of the auditory cortex and used spectral clustering for the division of primary and secondary cortex.

2. Material and methods

2.1. fMRI data

Resting-state fMRI data of 25 healthy control subjects from the Human Connectome Project (HCP) database[31] have been used with the specification of gradient echo EPI as TR$\bar{7}$20 ms, TE=33.1 ms, flip angle = 52, FOV = [208 × 180], voxel size= 2 mm isotropic and structural data as3D MPRAGE T1-weighted, TR=2400 ms, TE=2.14 ms, TI=1000 ms, flip angle = 8, FOV

$= [224 \times 224]$, voxel size= 0.7 mm isotropic. The provided images already underwent standard preprocessing[32] and registration to MNI coordinates[33]. In addition to that, the first 10 volumes of the original acquisition were discarded, resulting in T = 1190 time points. The functional (EPI) volumes were smoothed (using Gaussian kernel of 5mm FWHM). The T1 image was linearly registered to the mean functional images and segmented into white matter, gray matter and Cerebrospinal fluid. The functional images were then detrended and nuisance variables were regressed out (that include 6 head motion parameters, cerebrospinal fluid (CSF) and white matter signal computed in standard masks mapped to the subjects space and masked with individual segmentation maps).

2.2. Dynamic causal modeling of effective connectivity

Dynamic casual modeling is a method for modeling fMRI data that describes how activity in one area of the brain affects the activity in another part of the brain, based on biophysical model of neuronal dynamics. The state space model is built using (ordinary) differential equations that describe the changes in neural activity [34, 35, 36]. With the recent extension of DCM [37, 38], it is possible to model spontaneous fluctuations of the brain in the resting state condition (using stochastic differential equations) as

$$\hat{x} = (Ax + Eu + v) \tag{1}$$

where A is the effective connectivity matrix in the absence of the fluctuations v and u serves as exogenous input, that will be zero for resting-state fMRI. This method is called stochastic DCM. However, stochastic DCM is computationally expensive method because we not only have to estimate the effective connectivity (A) but also the time varying states as well. Recently, a new method was introduced which models the spontaneous fluctuations (v) in spectral domain. This new method is called spectral DCM [37, 39]. It was shown that spectral DCM is computationally faster, accurate and more sensitive to group differences than stochastic DCMs,

2.3. ROI selection

As mentioned in the previous section, primary and secondary auditory cortices have distinctive interactions with basolateral amygdala [40] and hippocampus (extracted using Neuromorphometrics Inc. toolbox). We divide the auditory cortex (consisting of both primary and secondary auditory cotices) into 90 small (and similar sized) sub-regions of neighboring voxels, using $k - means$ clustering of the voxels coordinates. We will refer to these

sub-regions as auditory patches for the rest of this paper. We then constructed 90 networks where each network consisted of latero-basal amygdala, hippocampus and one of the 90 auditory patches. This step is shown in figure1.a for the case of effective connectivity. The time course of each ROI is computed as the principal eigenvector (eigenvector corresponding to the highest eigenvalue). This DCM connectivity network is described with a fully connected 3×3 matrix D. Matrix D represents the vectorized form of this matrix and is used for spectral clustering of the auditory cortex in the next step.

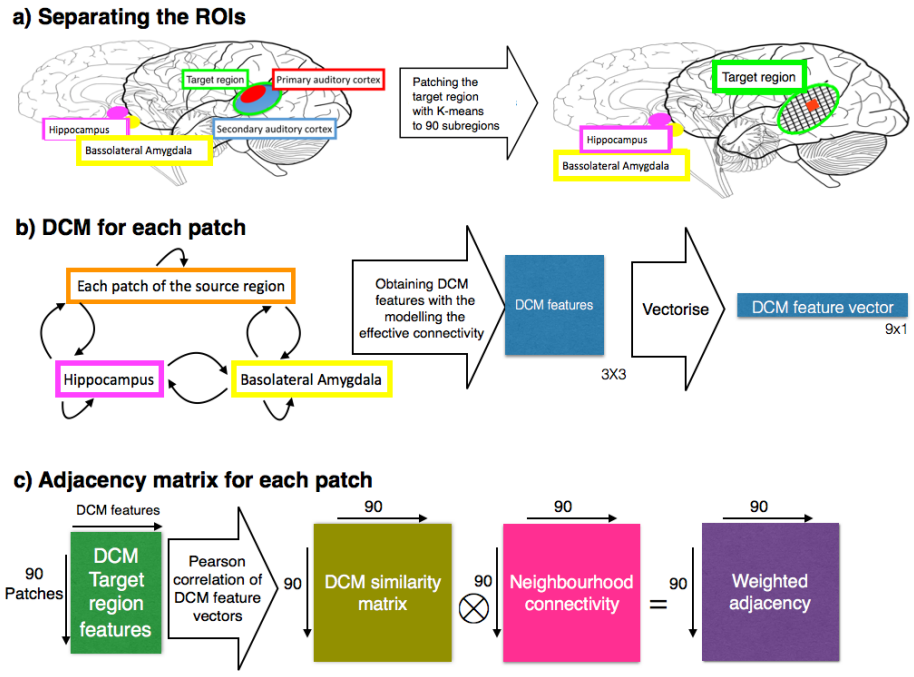

Figure 1: Pipeline of preparing the adjacency matrix for the spectral clustering of the auditory cortex with DCM. a) Defining nodes of the DCM network and patching of the auditory cortex. b) Extracting effective connectivity features for each auditory patch. c) Building the adjacency matrix for the graph of auditory cortex. Using DCM features and spatial proximity

2.4. Functional connectivity

For each auditory patch, we also calculated the functional connectivity using Pearson correlations with the two other ROIs namely the latero-basal amygdala and Hippocampus, which makes 2 features (i.e. the functional connectivity values) per auditory patch in the matrix D, as the connectivity

feature matrix. The time course of each ROI is defined as the average time course of all the voxels inside it.

2.5. Spectral clustering

We modeled the auditory cortex as a weighted graph, $G = (V, E)$, with V nodes - that is 90 auditory patches - and E edges. The weight of the edges between two connected nodes i and j is defined as w_{ij}. The procedure of calculating the weighted adjacency matrix of W is shown in Figure 1(c) using DCM connectivity matrix of the size 90 x 9. Pearson correlation between all rows of the matrix D is calculated, yielding a connectivity similarity matrix C of the size 90 x 90. For both DCM and FC, affinity in neuronal activity and also the spatial proximity in the brain were considered important in the construction of the graph adjacency matrix. We therefore took into account two measures: similarity of node connectivity feature vectors and spatial closeness between nodes. To model the spatial closeness, we used k-means clustering on the centre of the coordinate of each of the 90 auditory patches and divided them into 30 clusters. Using clustering we created a neighborhood binary matrix N that has non-zero values only in correspondence of neighboring patches. The final weighed adjacency matrix is calculated as $W = C. \times N$ where .x represents element by element multiplication. We finally computed graph Laplacian $L = D - W$, where D is the weight matrix. We then used eigenvalue decomposition on the matrix L and the eigenvector corresponding to the largest non-negative eigenvalue is chosen. Binary clustering of the corresponding eigenvector defines the label of each auditory patch by separating negative values and positive or zero values.

3. Results

The algorithm for DCM and FC based segmentation of auditory cortex was successfully applied on all the subjects as has been discussed in the previous sections. The validation of clustering was obtained by comparing the defined ROI to primary AC in [41] and secondary AC as is defined in Neuromorphometrics, Inc. The accuracy of clustering, corrected for the sample size of each cluster, is 74% and 75%for the left and right hemisphere when done separately for DCM based features and 73.1% and 70% for the left and right hemisphere separately using FC based features. Our results show that clustering based on asymmetric connectivity features calculated using DCM has higher accuracy when compared to symmetric connectivity features using FC. This accuracy comes from using more features nine compared to three FC features from DCM because of the causal nature of this modeling method which provides better characterization of the network connectivity.

. Figure 2 shows the averaged result of clustering . The left top panel shows the results for DCM based segmentation of auditory cortex using axial view and bottom left panels using saggital and coronal views. The right panel shows the segmentation of auditory cortex using functional connectivity (top left axial and bottom left saggital and coronal views). The reference atlas is shown in the middle panel in the same format as the DCM and FC as we can see the detected primary auditory cortex has been placed on Heschl's gyrus and secondary auditory cortex on planum temporale as expected. For validation purpose, for each method, two separate models consisting of one of obtained ROIs and Basolateral amygdala and Hippocampus are made. The difference between the two models is calculated as the Euclidian distance between the vectorised connectivity matrix of the networks for each ROI. The difference between the connectivity matrix of the network containing PAC and the network containing secondary AC in both method of effective and functional connectivity and for left and right hemisphere is significant ($p < 0.002$).

4. Discussion

In this paper, we presented for the first time a data-driven method for parcellation of auditory cortex based on rsfMRI data of the human connectome project. The pattern of connectivity of sub regions of auditory cortex has been investigated in previous studies. As in [42] where diffusion spectrum imaging (DSI) is used for comparing the structural connectivity of the sub regions of auditory cortex locally and also with other ROIs outside auditory cortex and this features has been used for modularity clustering of auditory cortex. In [43] employing a task based fMRI experiment, it has been shown that there is a significantly different pattern of intrinsic functional connectivity among the voxels inside the auditory cortex. Here we have used the pattern of extrinsic functional connectivity of the voxels of the auditory cortex for parcellation. As in Previous works has shown that functional connectivity based connectivity features can be useful in guiding cortical parcellation, for example the parcellation of medial frontal cortex into its subregions [24] using k-means clustering and the whole brain parcellation based on rsfMRI data using graph-theory [18] have been shown to be useful for segmentation. The parcellation of primary cerebral cortices [16] is another example of employing the pattern of local FC for cortical parcellation. However, it remained unclear if functional connectivity can also be useful in terms of delineating subregions of the auditory cortex . The auditory cortex is a relatively small area in the brain which is also functionally diverse and its parcellation into smaller subregions will require more informative features

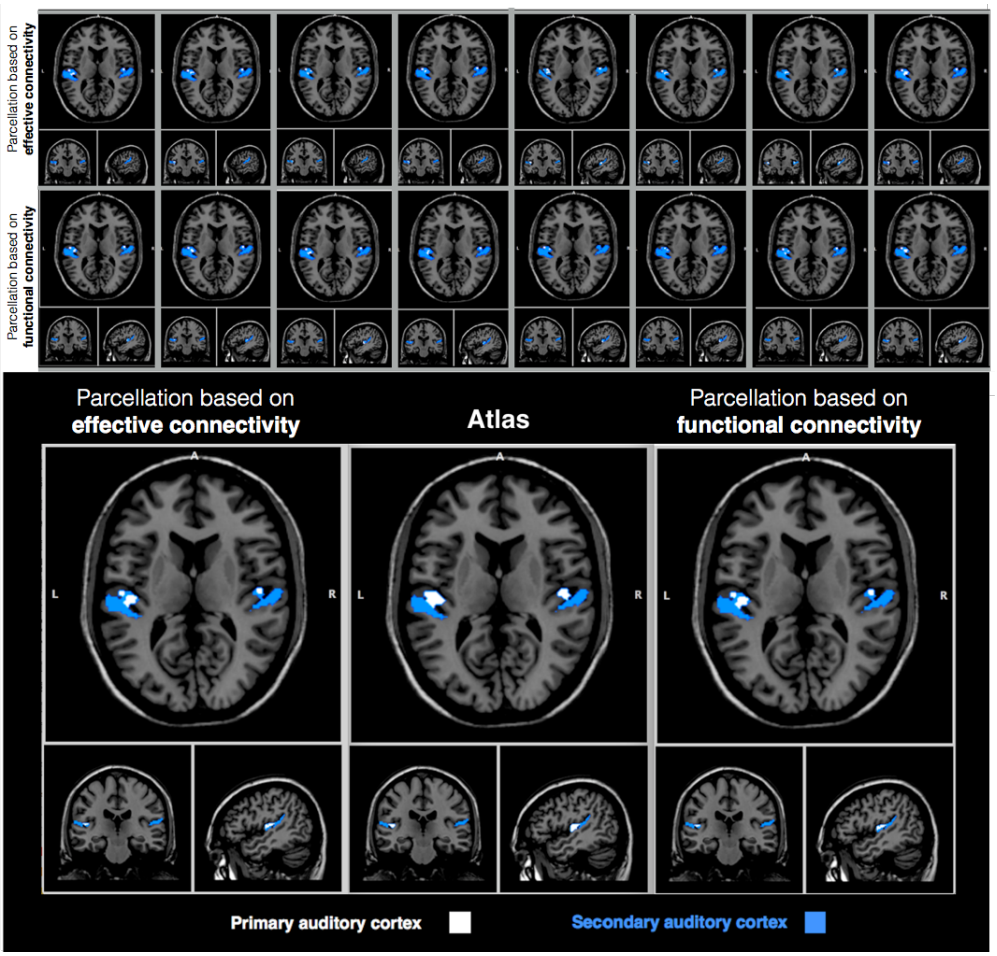

Figure 2: Auditory cortex segmentation result, averaged on all the subjects on the left with DCM features, on the right with FC features and in the middle the reference using atlas (extracted using Neuromorphometrics Inc. toolbox). Axial views on top and sagittal and coronal views on the bottom

comparing to larger scale whole brain segmentations which have been done previously based on functional connectivity In this work, in addition to the FC, we also investigated the utility of effective connectivity based on DCM as for connectivity-driven parcellation of the auditory cortex into primary and secondary cortices using resting state fMRI data. Our results show that using the connectivity features based on DCM has higher accuracy than the when using connectivity features using FC. DCM is a method that gives directed (causal) connectivity which is asymmetric hence provides more connectivity features when compared to the FC for the same size network. This data driven segmentation method can potentially be used for investigation of the cortical reorganization in auditory disorders as tinnitus that influences the

extrinsic connectivity of primary auditory cortex.

5. Acknowledgment

This work was supported by Swiss National Science Foundation Grant 320030_143989 and Ecole Polytechnique Federale de Lausanne school of engineering. Data were provided [in part] by the Human Connectome Project, WU-Minn Consortium (Principal Investigators: David Van Essen and Kamil Ugurbil; 1U54MH091657) funded by the 16 NIH Institutes and Centers that support the NIH Blueprint for Neuroscience Research; and by the McDonnell Center for Systems Neuroscience at Washington University.

References

[1] K. Zilles, K. Amunts, Receptor mapping: architecture of the human cerebral cortex, Current opinion in neurology 22 (4) (2009) 331–339.

[2] N. Tzourio-Mazoyer, B. Landeau, D. Papathanassiou, F. Crivello, O. Etard, N. Delcroix, B. Mazoyer, M. Joliot, Automated anatomical labeling of activations in spm using a macroscopic anatomical parcellation of the mni mri single-subject brain, Neuroimage 15 (1) (2002) 273–289.

[3] H.-J. Park, M. Kubicki, C.-F. Westin, I.-F. Talos, A. Brun, S. Peiper, R. Kikinis, F. A. Jolesz, R. W. McCarley, M. E. Shenton, Method for combining information from white matter fiber tracking and gray matter parcellation, American Journal of Neuroradiology 25 (8) (2004) 1318–1324.

[4] D. Zhang, L. Guo, G. Li, J. Nie, F. Deng, K. Li, X. Hu, T. Zhang, X. Jiang, D. Zhu, et al., Automatic cortical surface parcellation based on fiber density information, in: Biomedical Imaging: From Nano to Macro, 2010 IEEE International Symposium on, IEEE, 2010, pp. 1133–1136.

[5] B. Fischl, A. Van Der Kouwe, C. Destrieux, E. Halgren, F. Ségonne, D. H. Salat, E. Busa, L. J. Seidman, J. Goldstein, D. Kennedy, et al., Automatically parcellating the human cerebral cortex, Cerebral cortex 14 (1) (2004) 11–22.

[6] M. Moerel, F. De Martino, E. Formisano, An anatomical and functional topography of human auditory cortical areas, Frontiers in neuroscience 8 (2014) 225.

[7] T. Hackett, Organization and correspondence of the auditory cortex of humans and nonhuman primates-4.06.

[8] T. A. Hackett, Information flow in the auditory cortical network, Hearing research 271 (1) (2011) 133–146.

[9] N. Ghazaleh, W. Van der Zwaag, S. Clarke, D. Van De Ville, R. Maire, M. Saenz, High-resolution fmri of auditory cortical map changes in unilateral hearing loss and tinnitus, Brain topography (2017) 1–13.

[10] M. Schönwiesner, P. Dechent, D. Voit, C. I. Petkov, K. Krumbholz, Parcellation of human and monkey core auditory cortex with fmri pattern classification and objective detection of tonotopic gradient reversals, Cerebral Cortex (2014) bhu124.

[11] F. Dick, A. T. Tierney, A. Lutti, O. Josephs, M. I. Sereno, N. Weiskopf, In vivo functional and myeloarchitectonic mapping of human primary auditory areas, The Journal of Neuroscience 32 (46) (2012) 16095–16105.

[12] L. Nanetti, L. Cerliani, V. Gazzola, R. Renken, C. Keysers, Group analyses of connectivity-based cortical parcellation using repeated k-means clustering, Neuroimage 47 (4) (2009) 1666–1677.

[13] S. B. Eickhoff, D. Bzdok, A. R. Laird, C. Roski, S. Caspers, K. Zilles, P. T. Fox, Co-activation patterns distinguish cortical modules, their connectivity and functional differentiation, Neuroimage 57 (3) (2011) 938–949.

[14] B. Deen, N. B. Pitskel, K. A. Pelphrey, Three systems of insular functional connectivity identified with cluster analysis, Cerebral cortex 21 (7) (2011) 1498–1506.

[15] G. Battistella, E. Najdenovska, P. Maeder, N. Ghazaleh, A. Daducci, J.-P. Thiran, S. Jacquemont, C. Tuleasca, M. Levivier, M. B. Cuadra, et al., Robust thalamic nuclei segmentation method based on local diffusion magnetic resonance properties, Brain Structure and Function (2016) 1–14.

[16] Q. Li, M. Song, L. Fan, Y. Liu, T. Jiang, Parcellation of the primary cerebral cortices based on local connectivity profiles, Frontiers in neuroanatomy 9.

[17] J. Damoiseaux, S. Rombouts, F. Barkhof, P. Scheltens, C. Stam, S. M. Smith, C. Beckmann, Consistent resting-state networks across healthy

subjects, Proceedings of the national academy of sciences 103 (37) (2006) 13848–13853.

[18] X. Shen, X. Papademetris, R. T. Constable, Graph-theory based parcellation of functional subunits in the brain from resting-state fmri data, Neuroimage 50 (3) (2010) 1027–1035.

[19] S. Chen, T. J. Ross, W. Zhan, C. S. Myers, K.-S. Chuang, S. J. Heishman, E. A. Stein, Y. Yang, Group independent component analysis reveals consistent resting-state networks across multiple sessions, Brain research 1239 (2008) 141–151.

[20] M. De Luca, C. Beckmann, N. De Stefano, P. Matthews, S. M. Smith, fmri resting state networks define distinct modes of long-distance interactions in the human brain, Neuroimage 29 (4) (2006) 1359–1367.

[21] Y. Golland, P. Golland, S. Bentin, R. Malach, Data-driven clustering reveals a fundamental subdivision of the human cortex into two global systems, Neuropsychologia 46 (2) (2008) 540–553.

[22] S. Achard, R. Salvador, B. Whitcher, J. Suckling, E. Bullmore, A resilient, low-frequency, small-world human brain functional network with highly connected association cortical hubs, Journal of Neuroscience 26 (1) (2006) 63–72.

[23] K. A. Barnes, A. L. Cohen, J. D. Power, S. M. Nelson, Y. B. Dosenbach, F. M. Miezin, S. E. Petersen, B. L. Schlaggar, Identifying basal ganglia divisions in individuals using resting-state functional connectivity mri, Resting state brain activity: Implications for systems neuroscience (2010) 7.

[24] J.-H. Kim, J.-M. Lee, H. J. Jo, S. H. Kim, J. H. Lee, S. T. Kim, S. W. Seo, R. W. Cox, D. L. Na, S. I. Kim, et al., Defining functional sma and pre-sma subregions in human mfc using resting state fmri: functional connectivity-based parcellation method, Neuroimage 49 (3) (2010) 2375–2386.

[25] S. Kumar, H. M. Bonnici, S. Teki, T. R. Agus, D. Pressnitzer, E. A. Maguire, T. D. Griffiths, Representations of specific acoustic patterns in the auditory cortex and hippocampus, Proceedings of the Royal Society of London B: Biological Sciences 281 (1791) (2014) 20141000.

[26] J. Poppenk, G. Walia, A. McIntosh, M. Joanisse, D. Klein, S. Köhler, Why is the meaning of a sentence better remembered than its form?

an fmri study on the role of novelty-encoding processes, Hippocampus 18 (9) (2008) 909–918.

[27] S. Teki, S. Kumar, K. von Kriegstein, L. Stewart, C. R. Lyness, B. C. Moore, B. Capleton, T. D. Griffiths, Navigating the auditory scene: an expert role for the hippocampus, The Journal of Neuroscience 32 (35) (2012) 12251–12257.

[28] W. Clapp, I. Kirk, J. Hamm, D. Shepherd, T. Teyler, Induction of ltp in the human auditory cortex by sensory stimulation, European Journal of Neuroscience 22 (5) (2005) 1135–1140.

[29] N. M. Weinberger, Specific long-term memory traces in primary auditory cortex, Nature Reviews Neuroscience 5 (4) (2004) 279–290.

[30] N. M. Weinberger, Auditory associative memory and representational plasticity in the primary auditory cortex, Hearing research 229 (1) (2007) 54–68.

[31] D. C. Van Essen, S. M. Smith, D. M. Barch, T. E. Behrens, E. Yacoub, K. Ugurbil, W.-M. H. Consortium, et al., The wu-minn human connectome project: an overview, Neuroimage 80 (2013) 62–79.

[32] M. F. Glasser, S. N. Sotiropoulos, J. A. Wilson, T. S. Coalson, B. Fischl, J. L. Andersson, J. Xu, S. Jbabdi, M. Webster, J. R. Polimeni, et al., The minimal preprocessing pipelines for the human connectome project, Neuroimage 80 (2013) 105–124.

[33] M. Jenkinson, P. Bannister, M. Brady, S. Smith, Improved optimization for the robust and accurate linear registration and motion correction of brain images, Neuroimage 17 (2) (2002) 825–841.

[34] K. J. Friston, L. Harrison, W. Penny, Dynamic causal modelling, Neuroimage 19 (4) (2003) 1273–1302.

[35] A. C. Marreiros, K. E. Stephan, K. J. Friston, Dynamic causal modeling, Scholarpedia 5 (7) (2010) 9568.

[36] J. Kahan, T. Foltynie, Understanding dcm: ten simple rules for the clinician, Neuroimage 83 (2013) 542–549.

[37] K. J. Friston, J. Kahan, B. Biswal, A. Razi, A dcm for resting state fmri, Neuroimage 94 (2014) 396–407.

[38] A. Razi, K. J. Friston, The connected brain: Causality, models, and intrinsic dynamics, IEEE Signal Processing Magazine 33 (3) (2016) 14–35.

[39] A. Razi, J. Kahan, G. Rees, K. J. Friston, Construct validation of a dcm for resting state fmri, Neuroimage 106 (2015) 1–14.

[40] K. Amunts, O. Kedo, M. Kindler, P. Pieperhoff, H. Mohlberg, N. Shah, U. Habel, F. Schneider, K. Zilles, Cytoarchitectonic mapping of the human amygdala, hippocampal region and entorhinal cortex: intersubject variability and probability maps, Anatomy and embryology 210 (5-6) (2005) 343–352.

[41] P. Morosan, J. Rademacher, A. Schleicher, K. Amunts, T. Schormann, K. Zilles, Human primary auditory cortex: cytoarchitectonic subdivisions and mapping into a spatial reference system, Neuroimage 13 (4) (2001) 684–701.

[42] L. Cammoun, J. P. Thiran, A. Griffa, R. Meuli, P. Hagmann, S. Clarke, Intrahemispheric cortico-cortical connections of the human auditory cortex, Brain Structure and Function 220 (6) (2015) 3537–3553.

[43] K. Cha, R. J. Zatorre, M. Schönwiesner, Frequency selectivity of voxel-by-voxel functional connectivity in human auditory cortex, Cerebral Cortex (2014) bhu193.

6 Conclusion

Studying the function and plasticity of the human auditory cortex have been the subject of this dissertation. In this frame, three studies have been conducted. In the first study, we successfully employed high spatial resolution fMRI data to study the functional changes in primary auditory cortex related to hearing loss and tinnitus. A very common condition in tinnitus patients is hyperacusis that has overlapping symptoms with tinnitus, therefore detecting this condition in tinnitus patient can increase the accuracy and specificity of the result that is obtained for this condition. Following this goal, the second study focuses on detecting the hyperacusis condition in tinnitus patients based on their primary cortical maps responses. In these two described studies, parcellation of PAC is done by using tonotopic mapping as the reference of the border in one axis and manual parcelation on the other axis on the surface. The result In both described studies could get improved with parcellation of auditory cortex in a data driven approach. The third chapter introduces a segmentation method to define the area of primary and secondary auditory cortex in a data-driven way, to address the challenge of automatic parcellation of the auditory cortex.

6.1 Summary

High-Resolution fMRI of Auditory Cortical Map Changes in Unilateral Hearing Loss and Tinnitus. We used ultra-high field MRI scanner and acquired high-resolution

fMRI data to perform tonotopic mapping in primary auditory cortex on patients with unilateral hearing loss and tinnitus, compared to normal-hearing controls. Based on animal studies, it appears likely that tinnitus is associated with alteration of the tonotopic maps of primary auditory cortex, although the exact pattern of changes to expect is unclear. Some animal studies support a maladaptive reorganization hypothesis which posits that overrepresentation of the hearing loss or hearing-loss edge frequencies causes tinnitus (analagous to the leading hypothesis concerning phantom pain following the loss of a limb). More recent studies, quite differently, describe a broader pattern of distortions in primary auditory cortex that favor hyperactivity in low-frequency map areas, notably away from the hearing loss and presumed tinnitus range. Further, these studies are limited by the difficult of assessing subjective tinnitus perception in animal (primarily rodent) models, which contributes to the challenge of relating these findings to human patients. The value of our study is that it confirms, for the first time, that plastic map changes do indeed exist in individual human patients with hearing loss and tinnitus. It is precisely the individual subject mapping, enabled by high-resolution imaging at 7T, which allowed to identify a map distortions (hyperactivity and overrepresentation) which localize to a specific low-frequency region of the map, peaking at approximately 300 Hz. Such a result was, in principle, not obtainable by previous fMRI imaging studies of tinnitus, which relied on more standard inter-subject brain averaging for data analysis. This is because the high anatomical variability of the temporal plane, including Heschl's gyrus, leads to rather poor alignment of the tonotopic maps in inter-subject analysis. Additionally in the previous studies the data was acquired at lower field scanners that leads to acquision of data with lower signal to noise ratio. Also of considerable interest is that the map distortions occurred in the low frequency map region, irrespective of the patient's hearing loss and tinnitus frequency range. In light of this frequency mismatch, these results do not support the maladaptive plasticity hypothesis for tinnitus, but do corroborate findings form other recent animal studies. We interpret the findings to suggest that, in the human patients, gross plastic map distortions do exist but are not the likely cause of tinnitus. Rather, these distortions may be a co-occurring consequence of peripheral hearing loss, and could be related to other hearing-loss

related pathologies such as hyperacusis. Tinnitus disorder is very heterogeneous. Having access to a larger group of patients could make it possible to cluster them in groups with the same specification of their tinnitus condition and therefore be able to interpret the obtained result more specifically.

Detection of hyperacusis condition in tinnitus patients based on PLSC features that link audiogram and fMRI tonotopy responses. Here, we tested the hypothesis that the primary auditory cortex activity in our patients relates, at least in part, to hyperacusis, a hearing disorder commonly co-occuring with tinnitus. Hyperacusis is characterized by increased loudness discomfort and decreased tolerance to normal sound levels, and is a common symptom of age-related hearing loss. Little is known about the neural origin of hyperacusis, although cortical hyperexcitibility appears to be a strong candidate hypothesis. Interestingly, in our data, neither the patient's audiograms (behavioral measure) nor the neuroimaging data alone were sufficient to classify the presence or absence of hyperacusis (as assessed by clinical diagnosis of subject loudness report) in the tinnitus patient cohort. To explore further, we developed a partial least square correlation analysis (PLCS) which classifies based on the cross-covariance information between the audiogram and the fMRI data. This PLCS analysis provided a classification accuracy of 80%. The novelty of this study is the unique combination of behavioral (audiogram) data and fMRI data for diagnosis. Importantly this study provides new information regarding the neural origin hyperacusis, providing evidence for involvement of the primary auditory cortex.

Subject-specific parcellation of auditory cortex based on resting state fMRI functional and effective connectivity. Non-invasive mapping of the human auditory cortex remains challenging and is an area of active research. Here, we tested the use of effective connectivity of resting-state fMRI date for parcellation of auditory cortex. The value of such a method would be to provide a data-driven approach to primary and secondary auditory cortex identification in cases when tonotopic mapping data is not available. We employed dynamic causal modelling (DCM) to make a model of effective connectivity of auditory cortex with two other brain regions, the hippocampus and basolateral amygdala, that shows the influence of these regions

on each other in a directed graph representation. This modelling of resting state fMIR data resulted in a segmentation of primary and secondary auditory cortices with 74% accuracy, compared to atlas models. This work indicates a novel avenue for data-driven parcellation of auditory cortex in human neuroimaging data. Moreover, this data driven segmentation method can potentially be used for investigation of the cortical reorganization in auditory disorders as tinnitus that influences the extrinsic connectivity of primary auditory cortex.

6.2 Outlooks

Categorising tinnitus patients for better prediction of the obtained result: Tinnitus disorder is very heterogeneous. Having access to a larger group of patients could make it possible to cluster them in groups with the same specification of their tinnitus condition. This could specify the obtained result

Effective connectivity in tinnitus: To better understand the underlying mechanism of tinnitus and the interactions of high-level cognitive brain systems on auditory cortex processing as a result of this disorder, we could model the effective connectivity within a network of carefully selected brain regions [Elgoyhen et al., 2015]. Such a model could potentially detect subtle changes in the intrinsic rorganization of spontaneous activity measured with resting-state fMRI. This can be done, by applying state-of-the-art spectral dynamic causal modeling (DCM) of resting-state fMRI data [Friston et al., 2014]. As DCM is a unique Bayesian network modeling approach that can provide information about both excitatory and inhibitory influences between regions, the fitted model opens a unique window on these interregional interactions that goes beyond conventional correlational analyses that are the basis of conventional functional connectivity.

Measuring the inhibition: A promising animal study of hearing loss and tinnitus has shown different changes in low vs. high frequency regions of the tonotopic map. That study showed an increase in excitatory and inhibitory synaptic transmission in the low-frequency range (resulting in a prominent low-frequency hyperactivity, as in our

study), and also showed down-regulation of inhibitory synaptic transmission and unaffected excitatory synaptic transmission in the high-frequency part of a tonotopic map. [Yang et al., 2011]. The down-regulation of inhibition in the hearing loss range is a strong candidate as a tinnitus mechanism. However, testing for neural inhibition in human BOLD fMRI data is very challenging since any negative BOLD responses due to inhibition may be counteracted by positive metabolic responses driving inhibitory transmission. Thus in our experiment, we are potentially missing an important tinnitus mechanism, namely that changes in inhibitory synaptic transmission in high-frequency neurons. In order to investigate this, we suggest designing an experiment based on repetition priming, a protocol shown to be applicable for the measurement of inhibition [Henson and Rugg, 2001, Noppeney et al., 2006, Harms and Melcher, 2002]. Sounds of different frequency are played randomly followed by repetition of the same frequency or presentation of a different frequency. It is expected that neural inhibition (associated with habitation) decreases the response to the second stimulus in the case of repetition, but not when a novel stimulus is presented. It is expected that the down-regulation of inhibition in the high-frequency (hearing loss region) of the tonotopic map in tinnitus patients would inhibit the habituation. Therefore, we expect to capture a relatively higher BOLD response amplitude, for repeated high-frequency tones, in tinnitus patients compared to healthy controls.

Tinnitus treatment based on sensory integration: Finally, we offer thoughts regarding a potential non-invasive tinnitus treatment. In sensory impairments, the rehabilitation process may based on the ability of the brain to link an existing sensory input with the lost sensory input [Hillary et al., 2002, Naumer and Kaiser, 2010]. Additionally, Based on metamodal processing theory [Naumer and Kaiser, 2010], each brain region is specific for a particular function regardless of the modality of the input, thus cross-sensory stimulation may be an effective means of targeting and resetting the activity of tinnitus-frequency specific neurons. This points towards a treatment idea for tinnitus patients, particularly in the case of unilateral hearing loss like our patient cohort. We suggest to train the patients, using their normal hearing ear, to pair visual stimuli of varying visual spatial or temporal frequencies with sound stimuli

of varying frequencies. The figure illustrates a disc flashing at different temporal frequencies paired with sound stimuli of varying frequencies Fig.6.1. After multiple training sessions, the patient is asked to follow, with the hearing impaired ear, a series of paired visual and sound stimuli, containing the hearing loss sound frequency range. The patients are asked to imagine the frequency tone that they can not hear. As the link between the visual and sound stimuli is built in the brain, viewing the visual stimuli equivalent to the sound stimuli with hearing loss frequency tone, could potentially stimulate neurons in the auditory cortex repressing that frequency the tinnitus frequency leading to a renormalization of its response.

The advantage of this suggested means of stimulation is the possibility to target a specific part of the auditory cortical map. In comparison, existing stimulation methods based on transcranial electrical stimulation [Vanneste et al., 2013b, Vanneste et al., 2013a, Theodoroff and Folmer, 2013] have been tested for tinnitus treatment. However, these techniques suffer from poor spatial resolution and cannot reliably target the primary auditory cortex and, thus far, have not succeeded in eliminating tinnitus permanently.

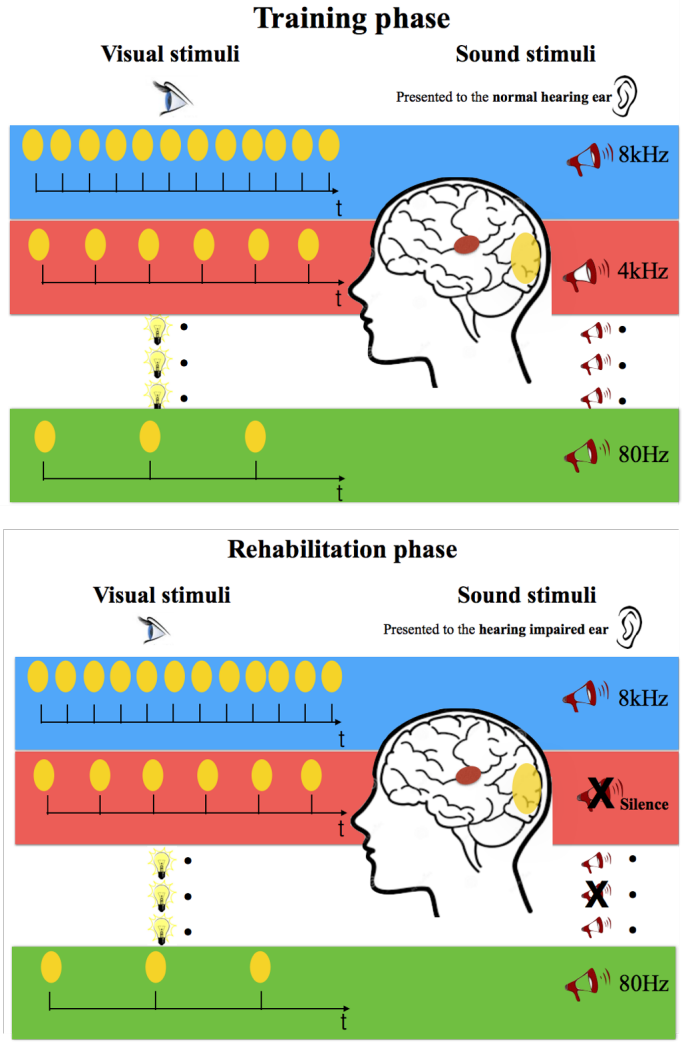

Figure 6.1 – Tinnitus treatment based on sensory integration suggested paradigm. At the top, training phase for linking visual and auditory stimuli. At the bottom, rehabilitation phase, where the patient should imagine hearing the dropped sound stimuli corresponding to its paired visual stimuli.

A Supplementary material for Chapter 3

Journal article: ***Study of tonotopic brain changes with functional MRI and FDG-PET in a patient with unilateral objective cochlear tinnitus*** A.-C. Guinchard, Naghmeh Ghazaleh, M. Saenz, E. Fornari, J.O. Prior, P. Maeder, S. Adib, R. Maire, Hearing research 341 (2016): 232-239.

Contribution: Data analysis, text edition, and revision.

Hearing Research 341 (2016) 232–239

Contents lists available at ScienceDirect

Hearing Research

journal homepage: www.elsevier.com/locate/heares

Research Paper

Study of tonotopic brain changes with functional MRI and FDG-PET in a patient with unilateral objective cochlear tinnitus

A.-C. Guinchard [a], Naghmeh Ghazaleh [b], M. Saenz [b, c], E. Fornari [d], J.O. Prior [e], P. Maeder [d], S. Adib [e], R. Maire [a, *]

[a] Department of Otorhinolaryngology, Head and Neck Surgery, Lausanne University Hospital, Lausanne, Switzerland
[b] Institute of Bioengineering, École Polytechnique Fédérale de Lausanne (EPFL), Lausanne, Switzerland
[c] Department of Clinical Neurosciences, Lausanne University Hospital, Lausanne, Switzerland
[d] Department of Radiology, Centre Imagerie Biomédicale, Lausanne University Hospital, Lausanne, Switzerland
[e] Department of Nuclear Medicine and Molecular Imaging, Lausanne University Hospital, Lausanne, Switzerland

ARTICLE INFO

Article history:
Received 1 June 2015
Received in revised form
11 May 2016
Accepted 7 September 2016
Available online 20 September 2016

Keywords:
Objective tinnitus
Human neuroimaging
Auditory cortex
Tonotopy

ABSTRACT

We studied possible brain changes with functional MRI (fMRI) and fluorodeoxyglucose positron emission tomography (FDG-PET) in a patient with a rare, high-intensity "objective tinnitus" (high-level SOAEs) in the left ear of 10 years duration, with no associated hearing loss. This is the first case of objective cochlear tinnitus to be investigated with functional neuroimaging.

The objective cochlear tinnitus was measured by Spontaneous Otoacoustic Emissions (SOAE) equipment (frequency 9689 Hz, intensity 57 dB SPL) and is clearly audible to anyone standing near the patient. Functional modifications in primary auditory areas and other brain regions were evaluated using 3T and 7T fMRI and FDG-PET.

In the fMRI evaluations, a saturation of the auditory cortex at the tinnitus frequency was observed, but the global cortical tonotopic organization remained intact when compared to the results of fMRI of healthy subjects. The FDG-PET showed no evidence of an increase or decrease of activity in the auditory cortices or in the limbic system as compared to normal subjects.

In this patient with high-intensity objective cochlear tinnitus, fMRI and FDG-PET showed no significant brain reorganization in auditory areas and/or in the limbic system, as reported in the literature in patients with chronic subjective tinnitus.

1. Introduction

Tinnitus is characterized by the perception of auditory signals in the absence of any external sound source. It affects about 10–15% of the population (Rauschecker et al., 2010), and in 1-3% of adults it adversely affects quality of life. There are two types of tinnitus: objective and subjective. Subjective tinnitus is more common and may contribute to depression, insomnia and anxiety. The pathophysiology of subjective tinnitus is still poorly understood, but is most often associated with sensorineural hearing loss of various origins. As a consequence of damage to the peripheral auditory system, reduced auditory input reaches the central auditory neurons within the affected frequency range, which in turn leads to compensatory changes in the central auditory system. Therefore, subjective tinnitus is a phantom perception of sound that may be due to aberrant plastic reorganization within the auditory centers of the brain. There is currently no standard treatment for the management of subjective tinnitus, however behavioral therapies are considered the most effective. Earlier studies of human brain imaging using fMRI in patients with subjective tinnitus have suggested reorganization in the auditory cortex (Rauschecker et al., 2010; Melcher et al., 2000; Lockwood et al., 1998; Plewnia et al., 2007; but see Langers et al., 2012). Furthermore, stress and emotion can modulate tinnitus with brain imaging studies showing

Abbreviations: BOLD, blood oxygenation level dependant; dB SPL, decibel sound pressure level; EPI, Echo Planar Imaging; FDG-PET, ^{18}F-fluorodeoxyglucose positron emission tomography; Hz, Hertz; LYSO, lutetium-yttrium-orthosilicate; OHCs, Outer hair cells; OSEM, ordered-subset expectation maximization; PFL, paraflocculus of the cerebellum; SOAEs, Spontaneous otoacousitc emissions; SPM, Statistical parametric mapping; 3T fMRI, 3 T functional MRI; 7T fMRI, 7 T functional MRI

* Corresponding author.
E-mail address: raphael.maire@chuv.ch (R. Maire).

http://dx.doi.org/10.1016/j.heares.2016.09.005
0378-5955/

functional and anatomical differences in the limbic system between tinnitus patients and controls (Rauschecker et al., 2010).

Objective tinnitus is much less common and corresponds to a physical noise produced in the body and is audible to others. The etiology is most often vascular and, more rarely, is related to other causes such as palatal myoclonus, myoclonus of the tensor tympani, tubal patency or cochlear damage. Objective tinnitus of cochlear origin is due to a highly localized anomaly of the basilar membrane at high frequencies with spontaneous activity of the outer hair cells (OHCs) and it can be measured by Spontaneous Otoacoustic Emissions (SOAEs). Some authors have described the correlation between tinnitus pitch and SOAEs frequency (Prasher et al., 2001; Roberts et al., 2010).

This article considers the case of a 30 year-old man who presented with a rare left ear objective cochlear tinnitus, of over 10 years duration, which is clearly audible to others standing near the patient as a continuous high-pitched tone. Using functional magnetic resonance imaging (fMRI) and ^{18}F-fluorodeoxyglucose positron emission tomography (FDG-PET), we investigated possible reorganization of the auditory cortex and limbic system in this patient, as compared to healthy control subjects. The results of three experiments (3T fMRI, 7T fMRI, and FDG-PET) showed no large-scale reorganization of auditory brain areas, revealing a case of overall resiliency to pathological sound exposure.

2. Materials and methods

2.1. Case report

The patient in this study was a 30-year-old male, in good general health, with no previous history of acoustic trauma, presenting with a left continuous objective tinnitus of over 10 years duration. The tinnitus was non-pulsatile and of high intensity and frequency. The patient was bothered by the symptom and looked for possible treatment. Validated French versions of the Subjective Tinnitus Severity Scale (STSS) (Meric et al., 1996), the Hospital Anxiety and Depression Scale (HADS) (Lepine et al., 1985), and the Tinnitus Handicap Inventory (THI) (Ghulyan-Bédikian et al., 2010), were used to evaluate the impact of the tinnitus. On the STSS, the patient's score was 8/16 indicating a moderate tinnitus discomfort. On the HADD, the global score was 23/42 revealing moderate anxiety (14/21) and slight depression (9/21) symptoms. The THI score was 74 points indicating a severe handicap (severe is more than 58 points). Finally, using a Visual Analogic Scale (VAS), the patient evaluated at 9/10 the intensity and suffering of his tinnitus.

The otoscopy showed normal tympanic membranes bilaterally. Weber's test was central and Rinne's test was positive on both sides. CT-scan of the temporal bone followed by a cerebral and angio-MRI failed to reveal any abnormality.

Otherwise, the patient underwent a complete neurovestibular evaluation including caloric testing, video-head impulse test and videonystagmography, which were normal.

2.2. Audiological assessment

2.2.1. Audiometry and impedancemetry

Pure tone audiograms were normal on both sides at all frequencies, except for a rapid drop on the left side of up to 50 dB at 8 kHz, probably due to the tinnitus interfering with hearing thresholds (Fig. 1).

Impedancemetry (objective test of middle-ear function evaluating the mobility of the tympanic membrane and ossicular chain) was normal (type A) on both sides.

2.2.2. Otoacoustic emissions recording

Otoacoustic emissions are produced by the outer hair cells activity in the cochlea, either spontaneously (Spontaneous Otoacoustic Emissions – SOAEs) or in response to an acoustic stimulus (Transitory Evoked Otoacoustic Emissions – TEOAEs) and can be recorded with an intra-auricular probe. To measure the otoacoustic emissions, we used the Madsen Celesta 503 device, Madsen Celesta logiciel, NOHA system 3.6, GN Otometrics. SOAEs were recorded bilaterally from 125 to 10,000 Hz and TEOAEs from 1000 to 4000 Hz. In the right ear, physiologic SOAEs were present with small peaks of 8 dB SPL recorded at 5200 Hz and 7500 Hz. In the left ear, pathological SOAEs were present with a highly abnormal significant peak of 57 dB SPL at 9689 Hz, producing an audible sound (Fig. 1).

2.2.3. Functional neuroimaging

To test for possible brain reorganization, we performed three neuroimaging experiments with the patient: (1) whole-brain assessment of response to sound stimulation at the tinnitus frequency with 3T-fMRI, (2) high-resolution assessment of the tonotopic organization of the primary auditory cortex with 7T fMRI, (3) evaluation of whole-brain metabolic activity with FDG-PET.

2.3. 3 T fMRI

We looked for changes in the activity in the auditory cortex bilaterally and in the limbic system by comparing sound stimulation at the SOAEs frequency with rest and with stimulation two octaves lower in a silent event-related design protocol (for details see Maeder et al., 2001).

2.3.1. Scanning methods and analysis

The MRI protocol was performed on a Siemens 3T Tim Trio scanner and included a sagittal T1-weighted gradient-echo sequence (MPRAGE, 160 contiguous slices, 1 mm isotropic voxel, TR = 2300 ms, TE = 2.98 ms, FoV = 256 mm) and the fMRI acquisition. Functional scans were acquired with an EPI sequence (TR = 1500 ms, TE = 30 ms, flip angle = 90°, FoV = 256 mm). The 28 axial slices (matrix size 128*128 with 4 mm slice thickness) were aligned with the anterior commissure-posterior commissure line. During the experiment, we collected 20 vol for each condition. MRI data were pre-processed and analyzed using Statistical Parametric Mapping (SPM8, Wellcome Department of Imaging Neuroscience, London, England; www.fil.ion.ucl.ac.uk/spm/software/spm8/). Functional images were corrected for motion along the experiment by means of rigid-body transformation and then co-registered to the high-resolution T1w acquisition. The anatomical images were then normalized to the MNI T1 template and the normalization parameters were applied to the functional images, which were finally smoothed with a 6-mm Gaussian kernel. All the preprocessing steps mentioned minimized the non task-related variability. Single-subject statistics were performed according to the General Linear Model and contrasts of interest were thresholded for peak height at $p = 0.001$ (uncorrected), with an extent threshold (k) of 50 voxels.

2.3.2. Sound stimulation methods

During the active condition, the patient received binaural stimulation (on/off) for 5 s followed by EPI acquisition (silent event-related paradigm, Hall, et al., 1999; Maeder et al., 2001) every 15 s. The 5 s stimulation included 16 pulsed sounds (pure tone bursts of 150 ms, the amplitude multiplied with half sine-wave function) either at the SOAEs frequency (9689 Hz, 90 dB SPL) or two octaves below (2422 Hz, 75 dB SPL, for a perception of similar loudness to the SOAEs frequency). The tone stimuli were sampled at 44.1 kHz

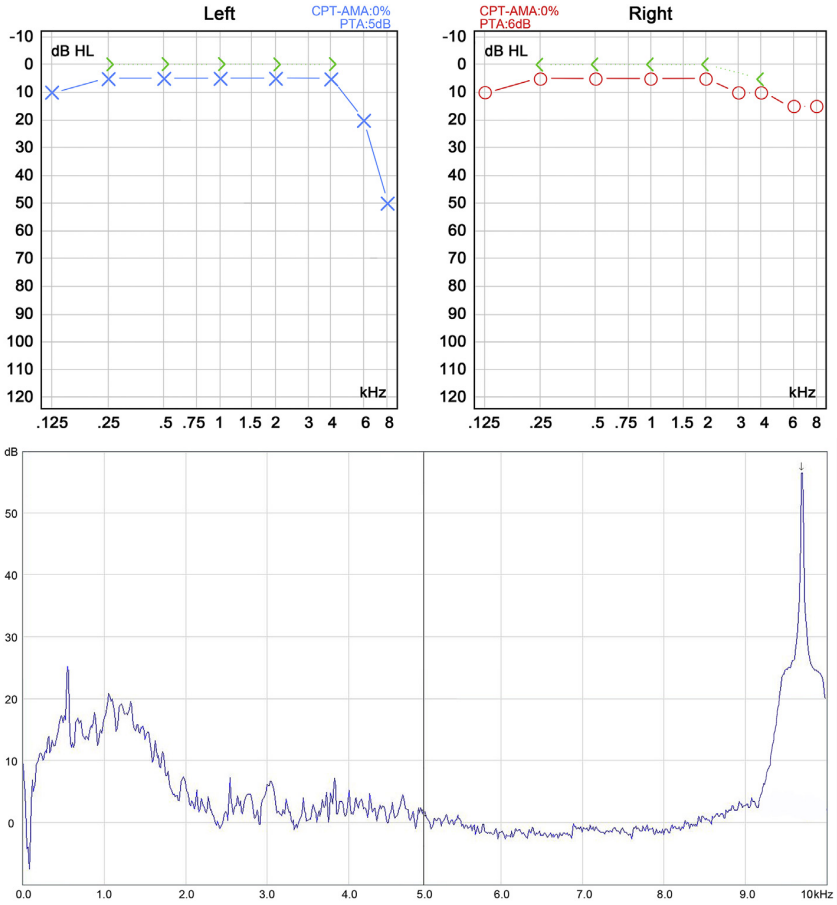

Fig. 1. Pure tone audiogram: Normal hearing on both sides except for a rapid fall in the very high frequency range on the left ear up to 50 dB at 8 kHz (Masking by the high-level SOAE is a probable explanation). Spontaneous otoacoustic emissions (SOAEs): left ear shows a pathological peak of 57 dB SPL at 9689 Hz (arrow) corresponding to the audible tinnitus.

and were delivered by MR-compatible earplug headphones (AudioSystem, Nordic NeuroLab Bergen, Norway). The 5 s stimulation was repeated 5 times for each condition and followed by five rest acquisitions; this cycle was repeated four times.

The stimulus was not masked by scanner noise. During fMRI, following the sparse sampling technique (Hall et al., 1999; Edmister et al., 1999), the stimulus was not presented during the scanner noise and the tinnitus could be heard normally. The use of stimulation earphones did not alter the perception of the tinnitus.

2.4. 7 T fMRI

High-resolution tonotopic maps of the primary auditory cortex were obtained with functional 7T MRI. Normally, neurons of primary auditory cortex are arranged in spatial gradients according to their preferred sound frequencies from low to high. Previous studies from our laboratory (Da Costa et al., 2011; Da Costa et al., 2013) have demonstrated the consistency with which we can measure cortical tonotopic maps with high-resolution 7T imaging in human subjects with normal hearing. The human primary auditory cortex is situated bilaterally on the transverse temporal plane centered on Heschl's gyrus. Moving from the posterior to the anterior end, we normally observe two complete tonotopic gradients ("high to low" followed by "low to high") that correspond to the primary cortical regions A1 and R (Fig. 2). Both of these regions correspond to the primary core region and this organization is largely homologous to that observed in non-human primates (Saenz and Langers, 2014).

2.4.1. Scanning methods

Blood oxygenation level-dependent (BOLD) functional imaging was performed with an actively shielded 7T Siemens MAGNETOM scanner (Siemens Medical Solutions) located at the Centre d'Imagerie BioMedicale (CIBM) in Lausanne, Switzerland. fMRI data were acquired using an eight-channel head volume rf-coil (RAPID Biomedical) and an EPI pulse sequence with sinusoidal readout (1.5 × 1.5 mm in-plane resolution, slice thickness = 1.5 mm, TR = 2000 ms, TE = 25 ms, flip angle = 47°, slice gap = 0.07 mm, matrix size = 148 × 148, field of view 222 × 222, 30 oblique slices covering the superior temporal plane. The first three EPI images of each BOLD sequence were discarded).

BrainVoyager QX software v2.3 was used for standard fMRI data analysis. The tonotopic maps follow the convoluted cortical surface and are most easily viewed on cortical surface renderings. Cortical surface meshes were generated for the patient based on his own high-resolution 3D anatomical brain scan (1 x 1 × 1 mm, MPR2AGE T1-weighted sequence).

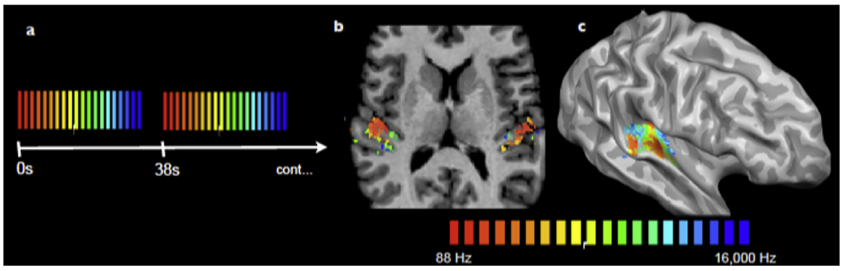

Fig. 2. Tonotopic mapping in auditory cortex with 7T fMRI. *(a)* Sound stimuli were pure tone bursts presented in cycled progressions from low to high frequencies: 88 to 16,000 Hz in half-octave steps. Each 32 s progression from low to high (red-to-blue color scale) was followed by a 4 s stimulus pause. Sound stimuli were designed to induce a traveling wave of response across cortical tonotopic maps: fMRI responses peak sooner in map regions preferring low frequencies and progressively later in regions preferring higher frequencies. *(b and c)* Resulting color-coded frequency maps are projected onto the subject's cortical surface meshes, as shown here in a normal hearing control subject. Surfaces were minimally inflated to expose the auditory cortex on the temporal plane (adapted from Da Costa et al., 2011).

2.4.2. Sound stimulation methods

The tonotopic mapping stimulus follows a "phase-encoded" mapping paradigm. Also know as the "traveling wave" technique, this paradigm has been shown to be highly efficient for mapping visual retinotopy and auditory tonotopy (Engel et al., 1994; Sereno et al., 1995; Talavage et al., 2004; Engel, 2012). Briefly, the mapping stimulus is designed to generate a wave of response across the tonotopic maps of the cortex, peaking earliest at low frequency endpoints and progressively later in parts of the map preferring higher sound frequencies. Hence, the time-to-peak of the response (i.e. the response phase) reveals the preferred frequency of each responsive voxel.

The auditory stimuli were pure tones of 16 distinct frequencies presented in increasing order from low to high: 88, 125, 177, 250, 354, 500, 707, 1000, 1414, 2000, 2828, 4000, 5657, 8000, 11,314, and 16,000 Hz (half-octave steps). The transition from low to high frequencies occurred over 32 s (2 s presentation of each frequency) followed by a 4 s of silence. This 36 s period was cycled 15 times during a continuous 9 min scan run. The tone stimuli were generated with a sampling rate of 44.1 kHz and were delivered via MRI-compatible headphones (AudioSystem, Nordic NeuroLab). The sound intensity of each frequency was chosen between 82 and 97 dB SPL to equate perceived loudness according to standard equal-loudness curves (ISO226, 85 phon). To minimize exposure to scanner noise, the patient (and controls) wore earplugs during the experiment which reduced background noise by about 24 dB. This means that a significant amount of scanner noise remains, of which it is difficult to assess the impact. However, it is controlled for in the sense that the background noise is the same for both the patient and the control subjects. According to the patient's self-report, the tinnitus remained hearable during the scanning session. Subjects (the patient and 5 normal hearing control subjects) were instructed to keep eyes closed during scanning. Linear cross-correlation analysis was used to determine the temporal delay that best fit the measured fMRI response time course of each voxel and to assign a corresponding best frequency. Briefly, the measured fMRI time courses were correlated with model time courses of 16 different delays corresponding to each sound frequency, and frequency-preferences were assigned according to the corresponding delay of highest correlation value. Model time courses were constructed by convolution with a standard two gamma hemodynamic response function (HRF) assuming a 5 s time to response-peak in the BOLD response (Glover, 1999). Response amplitudes (in % fMRI signal change) were determined as the maximal signal change of voxels assigned to each sound frequency, as in Da Costa et al., 2015. Response amplitudes were compared between the patient and controls.

2.5. FDG-PET

A fasting period of more than 6 h was respected by the patient before the PET study. The patient received an intravenous injection of 200 MBq of ^{18}F -FDG after resting comfortably in a quiet, dimmed room. He was instructed not to speak or move. The patient wore earplugs and phonic isolation headphones during the initial resting phase (20 min) before radiotracer injection and PET acquisition starting immediately after. A PET/CT scanner (Discovery-690 time-of-flight scanner. GE Healthcare, Milwaukee, WI) combining lutetium-yttrium-orthosilicate (LYSO) block detectors with a 64-slice CT scanner was used for image acquisition and 3D iterative reconstruction was performed using ordered-subset expectation maximization (OSEM) using a 256 × 256 pixels matrix, with a final image resolution of about 4–6 mm FWHM. The PET data was analyzed with the 3D-Stereotactic Surface Projections Neurostat Software (3D-SSP, Department of Radiology, University of Washington, Seattle, WA, USA, http://128.208.140.75/~Download/). A subsequent analysis compared to a database of 20 healthy persons of the same mean age using SPM8 with a p-value < 0.001, corrected for cluster size (Guedj et al., 2010).

3. Results

In the patient, we identified pathological SOAEs on the left ear with a significant peak of 57 dB SPL recorded at 9689 Hz. This highly abnormal spontaneous activity of OHCs generates a continuous tonal tinnitus at 57 dB SPL that is clearly audible to others standing near the patient.

First, we looked for brain reorganization in the auditory pathways and the limbic system with 3T fMRI. Results did not reveal any activation of primary auditory cortex when comparing stimulation at the SOAEs frequency with rest. There was no asymmetry of the response to the stimulus at the tinnitus frequency since no response at all could be obtained. The comparison of the lower frequency (two octaves lower, see Method for details) with the SOAEs frequency showed bilateral activation of the middle Hechl's gyrus with a slight predominance in the left hemisphere (Fig. 3). No activation in the limbic areas was observed.

Secondly, we tested using 7T fMRI for a change in the tonotopic maps of primary auditory cortex, with the hypothesis that a long-term noise at the same frequency could create a change in the auditory area. We observed that the tonotopic mapping results of the patient were in the normal range (Fig. 4a) based on qualitative

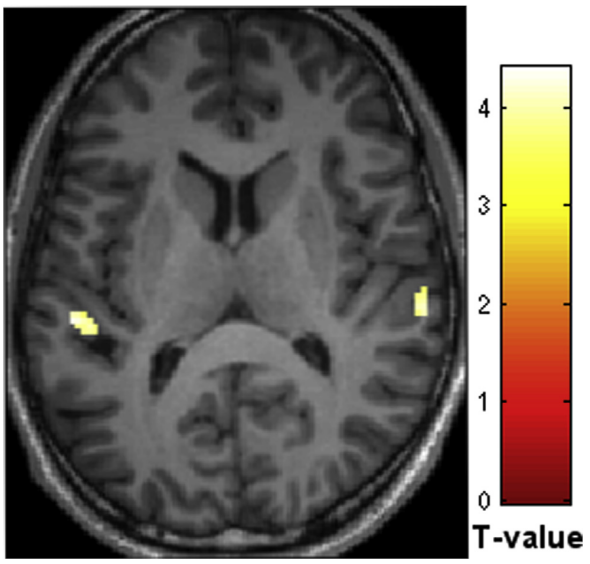

Fig. 3. 3T fMRI results. Image represents clusters more active during stimulation at 2422 Hz (two octaves lower than SOAE frequency) than at 9689 Hz (SOAE frequency). The slice is located at z = 12 mm in MNI space. Map is thresholded at $p < 0.001$, $k = 20$ voxels. Colorbar represents T-values.

comparison to 20 individual hemispheres of healthy young adults without tinnitus (Da Costa et al., 2011). In both left and right brain hemispheres of the patient, mappings of sound frequency preference ("high-to-low" followed by "low-to-high") corresponding to primary auditory regions A1 and R appeared normal (see Da Costa et al., 2011). These tonotopic maps appeared normal in terms of location (centered on Heschl's gyrus of the temporal lobe of each hemisphere) and orientation (overall posterior-to-anterior). Fig. 4b displays the preferred frequency as a function of distance along the cortical surface in each hemisphere. Note the distinct "V-shape" indicative of the two continuous and gradual tonotopic transitions. We did not observe a gross overrepresentation of sound frequencies in any frequency range. The x,y,z Talairach coordinates of the patient's estimated left and right map endpoints (left: [-39 -22 5], [-45 -25 3]; right: [40 -21 6], [46 -29 12]) were in the range of five normal-hearing control subjects (mean ± sd; left: [-38.8 ± 4.0–21.4 ± 2.7 3.0 ± 6.8], [-44.0 ± 5.6–27.2 ± 4.8 3.8 ± 3.3]; right: [41.2 ± 4.1–18.2 ± 4.7 4.4 ± 3.8], [49.0 ± 4.7–28.2 ± 6.2 9.2 ± 4.1]). Fig. 5 shows response amplitudes to each sound frequency in the patient compared to the five normal-hearing control subjects. The response amplitudes of the patient were within the range of the control subjects and were not significantly different from controls at any frequency (*t-tests*, $p > 0.05$). Finally, we investigated for evidence of hypermetabolism in the brain with the FDG-PET. This examination revealed no abnormalities. Images were compared to a database of normal, age-matched control subjects using the 3D-Stereotactic surface projections software 3DSSP Neurostat, which showed no significant abnormalities. Furthermore, The PET data were subsequently compared to a database of 20 healthy persons of the same mean age using SPM8 and p-value < 0.001, corrected for cluster size (Guedj et al., 2010). This analysis did not further identify any area of abnormally increased or decreased glucose metabolism.

4. Discussion

Spontaneous otoacoustic emissions (SOAEs) are thought to arise as a response to random perturbations in cochlear mechanisms due

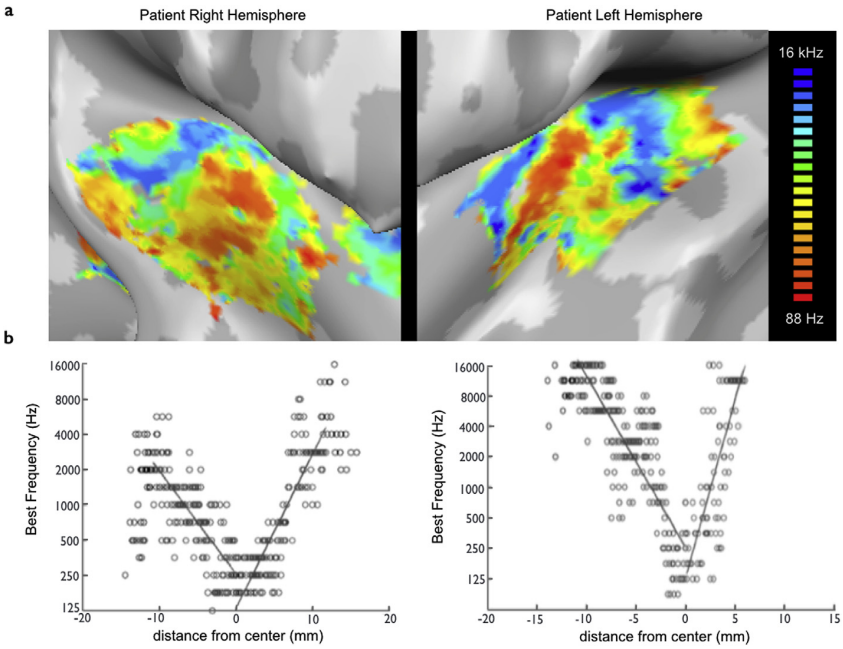

Fig. 4.. (a) Tonotopic maps in the patient with objective tinnitus: tonotopic maps sound frequency preference ("high-to-low" followed by "low-to-high") corresponding to primary auditory regions A1 and R were observed in each brain hemisphere. These tonotopic maps appeared normal in terms of location (centered on Heschl's gyrus on the temporal plane of each hemisphere) and orientation (overall posterior-to-anterior), suggesting that the global tonotopic organization of the patient remains intact. (b) Plots of preferred frequency within a posterior-to-anterior strip across the surface Heschl's gyrus in right and left hemispheres, respectively: the distinct "V-shape" shows two continuous and gradual tonotopic transitions in each hemisphere corresponding to regions A1 and R.

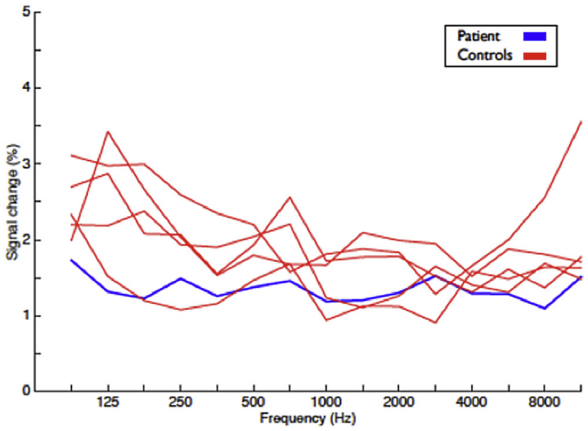

Fig. 5.. Plot of response amplitudes (in % fMRI signal change) to each sound frequency in the patient compared to normal-hearing control subjects (no difference at any frequency, $p > 0.05$). Overall, the results suggest that the global tonotopic organization of the patient remains within the normal range.

to irregularities in the OHC arrangement or due to a highly localized anomaly of the basilar membrane at high frequencies (Prasher et al., 2001). Small peaks across the frequency spectrum in the cochlea (generally not exceeding 20 dB SPL) can be recorded, inconsistently, in normal hearing subjects. Very rarely and exceptionally, more severe SOAEs can be recorded as audible sounds classifiable as objective non-pulsatile tinnitus. Only nine cases of objective tinnitus measured by SOAE equipment have been previously described in the literature (Glanville et al., 1971; Huizing and Spoor, 1973; Mathys et al., 1991; Yamamoto et al., 1987), but the tinnitus frequency and loudness were lower than in our patient. In Glanville et al., there was a familial history of high frequency tinnitus and the authors suggested a genetic defect in the cochlea associated to a venous abnormalities at the base of the skull. The others studies described 6 people with high-intensity SOAEs measured in normally hearing ears and emission failed to synchronize to external click stimuli (TEOAEs). They hypothesized that high-intensity SOAEs are associated with damage to the cochlea. In these studies, the associated hearing loss observed in five patients was explained by a masking effect due to the high intensity SOAEs.

Here we studied a rare case of objective tinnitus associated with clearly audible SOAEs. Given the continuous tonal quality of our patient's objective tinnitus, we hypothesize that it is generated by activity of the outer hair cells, in contrast to myogenic or vascular origins which produce pulsatile, non-tonal sounds. In the cochlea, only outer hair cells are contractile and would appear to be capable of emitting pure tone sounds. To our knowledge, this is the first case report of objective tinnitus to be studied with neuroimaging. We considered the possibility of changes in auditory brain centers, particularly in the cortex and in the limbic system, based on the findings of previous studies of auditory plasticity and of subjective tinnitus in both humans and animal models.

Firstly, animal studies of auditory plasticity have shown that repeated exposure to a particular sound frequency can alter the tonotopic maps of auditory cortex, resulting in overrepresentation of that frequency (Recanzone et al., 1993). However, the map reorganization depended on pairing the sounds with an attentive task requiring the animal to focus on the frequency content (Recanzone et al., 1993; Polley et al., 2006). Tonotopic map alterations may also be possible following long-term passive sound exposure (Noreña et al., 2006). In our patient, the duration of sound exposure largely exceeds those studies and the specific attentional state afforded to the sound is unknown.

Second, previous studies of subjective tinnitus in both animal models and humans report a number of associated changes in the auditory cortex. Subjective tinnitus is often associated with sensorineural hearing loss. Nerve deafferentation due to the destruction of hair cells induces changes in the central auditory pathways leading to the perception of a phantom tinnitus (Rauschecker et al., 1999). Usually, the pitch or the tinnitus corresponds to the hearing loss range (Roberts et al., 2010; Mühlau et al., 2006; Melcher et al., 2000, 2009). Animal models of subjective tinnitus consistently show elevated responses throughout the central auditory system including elevated spontaneous and stimulus driven activity, increased bursting and neural synchrony, as well as down-regulation of inhibition (Noreña and Eggermont, 2003; Mulders and Robertson, 2009; Seki and Eggermont, 2003). Others have reported tonotopic changes including expansion of lesion-edge frequency areas (Seki and Eggermont, 2003; Noreña and Eggermont, 2005) or more global distortion pervading the entire tontotopic map organization (Engineer et al., 2011; Yang et al., 2011). Earlier studies of human brain imaging with fMRI and FDG-PET have shown abnormal responses in central auditory brain regions in patients suffering from chronic subjective tinnitus (Rauschecker et al., 2010; Melcher et al., 2000; Lockwood et al., 1998; Plewnia et al., 2007) with some suggesting cortical tonotopic map distortion (Muhlnickel et al., 1998; Wienbruch et al., 2006). However, in most studies of subjective tinnitus it is difficult to disentangle the effects of tinnitus from more general consequences of hearing loss. Notably, Langers et al., 2012 tested subjective tinnitus patients with only minimal hearing loss and, like us, reported a lack of macroscopic changes in the tonotopic maps.

Finally, neuroimaging studies have also described changes in the limbic-related brain areas in subjective tinnitus patients, including alterations in some parts of the limbic networks and significant grey matter decreases in the right inferior colliculus and in the left hippocampus, when compared to controls (Lockwood et al., 1998; Mühlau et al., 2006; Landgrebe et al., 2009; Schlee et al., 2009). Leaver et al., 2011, suggested that interactions between the limbic corticostriatal network and primary auditory cortex may be key to understanding the pathophysiology of chronic subjective tinnitus. This interaction may be an important gateway to centers mediating emotional control and memory. In addition, the limbic system may participate in the suppression of the tinnitus signal. If this “noise cancellation system” works properly, the tinnitus is transient (Rauschecker et al., 2010). If this mechanism fails, patients become aware of their tinnitus. Recently, functional imaging in rats with tinnitus showed evidence of elevated neural activity in the paraflocculus of the cerebellum (PFL), which was not observed in normal rats. This suggests that plastic changes in the PFL may also serve as a tinnitus generator (Bauer et al., 2013).

Based on these observations in animal models and in patients with subjective tinnitus, we investigated whether our objective tinnitus patient would have aberrant brain reorganization in the auditory cortex, reorganization in the tonotopy of the auditory cortex and/or activation in non-auditory areas (i.e. limbic and paralimbic areas), which would reflect an emotional reaction to tinnitus. Functional imaging and FDG-PET in this patient failed to reveal any major changes. The 3T fMRI experiment showed no activation in the primary auditory cortex when comparing stimulation at the SOAEs frequency with rest, but revealed bilateral activation or the Hechl's gyrus when comparing the SOAEs frequency with lower frequencies. This observation is compatible with a saturation of the measurable auditory cortex response at the tinnitus frequency due to continuous SOAE stimulation. Saturation effects have been previously described in fMRI responses in

auditory cortex (Talavage and Edmister, 2004). Except for this probable saturation effect in the primary auditory cortex at the SOAEs frequency, neither gross reorganization of the central auditory system nor changes in the limbic-related brain areas were observed.

Testing with 7T fMRI revealed overall normal tonotopic maps of primary auditory cortex in terms of location and orientation as shown in Fig. 4. While these findings do not exclude the possibility of finer scale reorganization, they do suggest that the global tonotopic organization of the patient's primary auditory cortex remained intact. It should be noted that a methodological limitation in our tonotopic mapping is that sound frequencies were presented only in increasing order. Previous applications of phase-encoded mapping emphasize the importance of presenting mapping stimuli also in the reverse direction, to confirm responses do not depend on stimulus order (Talavage et al., 2004). In particular, responses at map endpoints could be influenced by sound offsets and onsets, as opposed to strict frequency-dependence. In our previous tonotopic mapping study, both stimulus directions were applied and we observed that the two major gradients of primary auditory cortex were largely stable, irrespective of stimulus order (Da Costa et al., 2013, Fig. 3). Future tonotopic mapping experiments should ideally apply both stimulus directions each time.

The FDG-PET examination did not identify any abnormal metabolic activity in the auditory cortex and limbic areas, also suggested an absence of brain changes in this patient. A possible limitation of FDG-PET imaging is its intrinsic spatial resolution (4–6 mm), where low-intensity metabolic changes in small-sized brain structures could be missed due to partial volume effects. The difference in findings between our patient and those with subjective tinnitus may be due to the fact that objective cochlear tinnitus is peripheral in origin, producing a continuous neural excitation from the labyrinth, while subjective tinnitus might be maintained by cortical reorganization as a consequence of sensorineural hearing loss.

5. Conclusions

Functional and metabolic imaging in our patient with chronic cochlear objective tinnitus showed no gross distortions in auditory cortical organization and/or in limbic system responses, as observed in patients with chronic subjective tinnitus, despite the presence of chronic objective tinnitus of over 10 years duration. Subjective tinnitus seems to be maintained by cortical reorganization as a consequence of sensorineural hearing loss. On the contrary, objective cochlear tinnitus is peripheral in origin and, while finer-scale neural changes may exist, the results of our three experiments suggest an overall resilience of the central auditory system, despite long-term pathological sound exposure.

Conflicts of interest

No conflict of interest.

Financial disclosures

No financial disclosures.

Acknowledgments

This work was supported by Swiss National Science Foundation Grant 320030_143989 and by the Centre d'Imagerie BioMédicale (CIBM) of the Université de Lausanne, Université de Genève, Hôpitaux Universitaires de Genève. Lausanne University Hospital, École Polytechnique Fédérale de Lausanne, and the Leenaards and Louis-Jeantet Foundations. We thank Sandra Da Costa and Wietske van der Zwaag for assistance with 7T fMRI data collection.

References

Bauer, C.A., Kurt, W., Sybert, L.T., et al., 2013. The cerebellum as a novel tinnitus generator. Hear Res. 295, 130–139.
Da Costa, S., Van der Zwaag, W., Marques, J., Saenz, M., et al., 2011. Human primary auditory cortex follows the sape of Heschel's gyrus. J. Neurosci. 31 (40), 14067–14075.
Da Costa, S., Van der Zwaag, W., Miller, L., Clarke, S., Saenz, M., 2013. Tuning in to sound: frequency-selective attentional filter in human primary auditory cortex. J. Neurosci. 33 (5), 1858–1863.
Da Costa, S., Saenz, M., Clarke, S., Van der Zwaag, W., 2015. Tonotopic gradients in human primary auditory cortex: concurring evidence from high-resolution 7T and 3T fMRI. Brain Topogr. 28, 66–69.
Edmister, W.B., Talavage, T.M., Ledden, P.J., Weisskoff, R.M., 1999. Improved auditory cortex imaging using clustered volume acquisition. Hum. Brain Mapp. 7, 89–97.
Engel, S.A., Rumelhart, D.E., Wandell, B.A., Lee, A.T., Glover, G.H., Chichilnisky, E.J., Shadlen, M.N., 1994. fMRI of human visual cortex. Nature 369, 525.
Engel, S.A., 2012. The development and use of phase-encoded functional MRI designs. Neuroimage 62, 373–382.
Engineer, N.D., Riley, J.R., Seale, J.D., Vrana, W.A., Shetake, J.A., Sudanagunta, S.P., Borland, M.S., Kilgard, M.P., 2011. Reversing pathological neural activity using targeted plasticity. Nature 470, 101–106.
Ghulyan-Bédikian, V., Paolino, M., Giorgetti-D'Esclercs, F., Paolino, F., 2010. Psychomtric properties of french adaptation of tinnitus handicap inventory. L'Encéphale 36, 390–396.
Glanville, J., Coles, R., Sullivan, B., 1971. A family with high-tonal objective tinnitus. J. Laryngology Otology.
Glover, G.H., 1999. Deconvolution of impulse response in event-related BOLD fMRI. Neuroimage 9, 416–429.
Guedj, E., Aubert, S., McGonigal, A., Mundler, O., Bartolomei, F., 2010. Deja-vu in temporal lobe epilepsy: metabolic pattern of cortical involvement in patients with normal brain MRI. Neuropsychologia 48 (7), 2174–2181.
Hall, D.A., Haggard, M.P., Akeroyd, M.A., Palmer, A.R., Summerfield, A.Q., Eliott, M.R., et al., 1999. "Sparse" temporal sampling in auditory fMRI. Hum. Brain Mapp. 7, 213–223.
Huizing, E., Spoor, A., 1973. An Unusual Type of tinnitus. Production of a high tone by the ear. Arch. Otolaryngol. 98.
Landgrebe, M., Langguth, B., Rosengarth, K., Braun, S., Koch, A., Kleinjung, T., May, A., de Ridder, D., Hajak, G., 2009. Structural brain changes in tinnitus: greymatter decrease in auditory and non-auditory brain areas, 15 Neuroimage 46 (1), 213–218.
Langers, D.R., de Klein, E., van Dijk, P., 2012. Tinnitus does not require macroscopic tonotopic map reorganization. Front. Sys. Neurosci. 6, 2.
Leaver, A.M., Renier, L., Chevillet, M., et al., 2011. Dysregulation of limbic and auditory networks in tinnitus. Neuron 69 (1), 33–43.
Lepine, J.P., Goldcheau, M., Brun, P., Lempérière, T., 1985. Evaluation de l'anxiété et de la dépression chez les patients hospitalisés dans un service de médecine interne. Ann. Médico-psychologiques 143 (2), 175–189.
Lockwood, A.H., Salvi, R.J., Coad, M.L., et al., 1998. The functional neuroanatomy of tinnitus: evidence for limbic system links and neural plasticity. Neurology 50 (1), 114–120.
Maeder, P.P., Meuli, R.A., Adriani, M., Bellmann, A., Fornari, E., Thiran, J.P., Pittet, A., Clarke, S., 2001. Distinct pathways involved in sound recognition and localization: a human fMRI study. Neuroimage 14 (4), 802–816.
Mathys, A., Probst, R., De Min, N., Hauser, R., 1991. A child with an unusually high-level spontaneous otoacoustic emission. Arch. Otolaryngol. Head. Neck Surg. 117.
Melcher, J., Sigalovsky, S., Guinan, J., et al., 2000. Lateralized tinnitus studied with fonctionnal magnetic resonance Imaging: abnormal inferior Colliculus Activation. AJP-JN Physiol. 83 (2), 1058–1072.
Melcher, J., Levine, R., Bergevin, C., et al., 2009. The auditory midbrain of people with tinnitus: abnormal sound-evocked activity revisited. Hear Res. 257, 63–74.
Meric, C., Pham, E., Cery-Croze, S., 1996. Traduction et validation de l'échelle subjective de mesure de la séverité de l'acouphène (Subjective Tinnitus Severity Scale, Halford, et al. 1991). J. français d'oto-rhino-laryngologie 45 (6), 409–412.
Mühlau, M., Rauschecker, J., Oestreicher, E., et al., 2006. Structural brain changes in tinnitus. Cereb. Cortex 16, 1283–1288.
Muhlnickel, W., Elbert, T., Taub, E., Flor, H., 1998. Reorganization of auditory cortex in tinnitus. PNAS 95 (17), 10340–10343.
Mulders, W.H., Robertson, D., 2009. Hyperactivity in the auditory midbrain after acoustic trauma: dependence on cochlear activity. Neuroscience 164 (2), 733–746.
Noreña, A.J., Eggermont, J.J., 2003. Changes in spontaneous neural activity immediately after an acoustic trauma: implications for neural correlates of tinnitus. Hear Res. 183 (1–2), 137–153.
Noreña, A.J., Eggermont, J.J., 2005. Enriched acoustic environment after noise trauma reduces hearing loss and prevents cortical map reorganization. J. Neurosci. 25, 699–705.
Noreña, A.J., Gourévitch, B., Aizawa, N., Eggermont, J.J., 2006. Spectrally enhanced acoustic environment disrupts frequency representation in cat auditory cortex.

Nat. Neurosci. 9 (7), 932–939.
Plewnia, C., Reimold, M., Najib, A., Brehm, B., Reischl, G., Plontke, S.K., Gerloff, C., 2007. Dose-dependent attenuation of auditory phantom perception (tinnitus) by PET-guided repetitive transcranial magnetic stimulation. Hum. Brain Mapp. 28 (3), 238–246.
Polley, D.B., Steinberg, E.E., Merzenich, M.M., 2006. Perceptual learning directs auditory cortical map reorganization through top-down influences. J. Neurosci. 26 (18), 4970–4982.
Prasher, D., Ceranic, B., Sulkowski, W., et al., 2001. Objective evidence for tinnitus from spontaneous emission variability. Noise Health 3, 61–73.
Rauschecker, J., et al., 1999. Auditory cortical plasticity: a comparison with other sensory systems. Trends Neurosci. 22 (2), 74–80.
Rauschecker, J., Leaver, A., Mühlan, M., 2010. Tuning out the noise: limbic-auditory interactions in tinnitus, 24 Neuron 66 (6), 819–826.
Recanzone, G.H., Schreiner, C.E., Merzenich, M.M., 1993. Plasticity in the frequency representation of primary auditory cortex following discrimination training in adult owl monkey. J. Neurosci. 13, 87–103.
Roberts, L.E., Eggermont, J.J., Caspary, D.M., Shore, S.E., Melcher, J.R., Kaltenbach, J.A., 2010. Ringing ears: the neuroscience of tinnitus, 10 J. Neurosci. 30 (45), 14972–14979.
Saenz, M., Langers, D., 2014. Tonotopic mapping of human auditory cortex. Hear Res. 307, 42–52.
Schlee, W., Mueller, N., Hartmann, T., Keil, J., Lorenz, I., Weisz, N., 2009. Mapping cortical hubs in tinnitus. BMC Biol. 23, 7–8.
Seki, S., Eggermont, J.J., 2003. Changes in spontaneous firing rate and neural synchrony in cat primary auditory cortex after localized tone-induced hearing loss. Hear. Res. 180 (1–2), 28–38.
Sereno, M.I., Dale, A.M., Reppas, J.B., Kwong, K.K., Belliveau, J.W., Brady, T.J., Rosen, B.R., Tootell, R.B., 1995. Borders of multiple visual areas in humans revealed by functional magnetic resonance imaging. Science 268, 889–893.
Talavage, T.M., Sereno, M.I., Melcher, J.R., Ledden, P.J., Rosen, B.R., Dale, A.M., 2004. Tonotopic organization in human auditory cortex revealed by progressions of frequency sensitivity. J. Neurophysiol. 91 (3), 1282–1296.
Talavage, T.M., Edmister, W.B., 2004. Nonlinearity of fMRI responses in human auditory cortex. Hum. Brain Mapp. 22 (3), 216–228.
Wienbruch, C., Paul, I., Weisz, N., Elbert, I., Roberts, L.E., 2006. Frequency organization of the 40-Hz auditory steady-state response in normal hearing and in tinnitus. Neuroimage 33 (1), 180–194.
Yamamoto, E., Takagi, A., Hirono, Y., et al., 1987. A case of Spontaneous otoacoustic emission. Arch. Otolaryngol. Head. Neck Surg. 113.
Yang, S., Weiner, B.D., Zhang, L.S., Cho, S.-J., Bao, S., 2011. Homeostatic plasticity drives tinnitus perception in an animal model. PNAS 108 (36), 14974–14979.

B Supplementary material for Chapter 4

This work has been presented as this poster in the Annual Meeting of Organization For Human Brain Mapping June. 2016, Geneva.

Relating audiogram measures and fMRI tonopic responses in tinnitus patients with and without hyperacusis

Summary: Here we used partial least squares correlation (PLSC) to investigate the relationship between audiogram measures and fMRI tonotopic response for comparing tinnitus patients with and without the hyperacusis condition. We found that allowing PLSC to split the audiogram measures reveals group differences at different (higher) frequency tones that if we allow PLSC to split the fMRI tonotopic responses. The reason could be that the functional changes of hyperacusis in response to different frequency tones at the cortex level are more general because of the homeostatic plasticity that doesn't get limited to separate set of voxels, representing specific frequency tone. Our results not only reveal this difference in relationship between audiogram and brain signals depending on the hyperacusis condition, but also open new avenues to study the underlying neural mechanisms.

Relating audiogram measures and fMRI tonopic responses in tinnitus patients with and without hyperacusis

Naghmeh Ghazaleh[1,2], Wietske van der Zwaag [3], Raphael Maire [4], Melissa Saenz [5], Dimitri Van De Ville [1,2]

1 Medical Image processing Laboratory, Ecole Polytechnique Fédérale de Lausanne (EPFL), University of Geneva, Switzerland
2 Department of Radiology & Medical Informatics, University of Geneva
3 Center for Biomedical Imaging, Ecole Polytechnique Fédérale de Lausanne (EPFL), Switzerland
4 Clinic of Otolaryngology, Head & Neck surgery, Lausanne University Hospital, Switzerland
5 Dept of Clinical Neurosciences, Lausanne University Hospital

INTRODUCTION and objectives

- Tinnitus is the chronic perception of ringing or other phantom sounds. Some tinnitus patients additionally suffer from **loudness hyperacusis** that is the **over-sensitivity** to environmental **sounds** [1].
- We **used partial least squares correlation (PLSC) to investigate the relationship between audiogram measures and fMR**I tonotopic response **for comparing tinnitus patients with and without the hyperacusis condition.**

Data

- 10 patients with **unilateral hearing loss and tinnitus** were recruited among which five also have loudness **hyperacousis**.
- The recruitment of patients with **unilateral hearing loss** allows us to **deliver sound via the unaffected ear**, bypassing any abnormal responsiveness at the peripheral level.
- **Audiogram** was acquired by measuring the audible thresholds for 9 frequency presentations in the range 125Hz-8kHz with steps of half an octave, **making 10 in 9 matrix of audiogram measurements**.
- The **fMRI data** was recorded on a 7T MRI (resolution of 1.5mm^3). The experimental paradigm was according to the **tonotopic mapping experiment** [2] (presenting a sequence of 15 pure frequency tones in 14 cycles (88Hz-11340Hz)).
- Voxels from the auditory cortex are then extracted and their timecourses are fitted to the sine/cosine with the period of the block-based paradigm, which gives access to the amplitude and the phase of the response.
- Voxels are labeled using the relationship between the phase and the presented frequency, and then amplitudes of voxels with similar labels are averaged resulting into **15 fMRI features/subject making 10 in 15 matrix of fMRI measurements.**

PLS analysis

- We used **PLSC** [2] **to establish the relation between audiogram measures and fMRI responses** with known groups (hyperacusis and non-hyperacusis).
- **Classical PLSC** decomposes the data in latent variables (LVs) where there is **a single saliency vector for the high-dimensional imaging data, and several saliency vectors (according to number of groups) for the low-dimensional behavioral data.**
- Since **our fMRI responses are low-dimensional**, this choice is not a priori obvious here .
- **We applied PLSC in two forms** where **either the audiogram measures or the fMRI responses were split per group**. We refer to these models as **PLSC-1 and PLSC-2**.
- The **significance of the LVs** is assessed using **permutation testing**, and the **confidence intervals** of the weights of the saliency vectors using **bootstrapping**.

Results

- We found evidence that **one LV is significant (p<0.05) in both PLSC forms**.
- Fig. 1 shows the results for **PLSC-1**: in 1a the audiogram saliences for both groups and in 1b the fMRI tonotopy saliences. Both groups share the same fMRI saliency vector, but the **audiogram one shows group differences for three frequency tones** (4kHz, 6kHz and 8kHz). The projection of brain saliencies on the brain of one sample subject is shown in Fig 1c; it can be compared against the tonotopic map of this same subject in Fig. 3.
- Fig 2. shows the results for **PLSC-2**: in 2a the fMRI tonotopy saliences for both groups and in 2b the audiogram saliences. This time, **the fMRI saliency vectors reveals group differences for one frequency tone at 88Hz**.

PLSC1

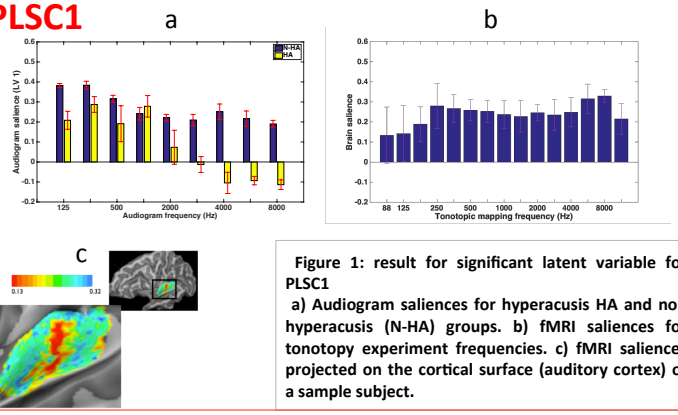

Figure 1: result for significant latent variable for PLSC1
a) Audiogram saliences for hyperacusis HA and non hyperacusis (N-HA) groups. b) fMRI saliences for tonotopy experiment frequencies. c) fMRI saliences projected on the cortical surface (auditory cortex) of a sample subject.

PLSC2

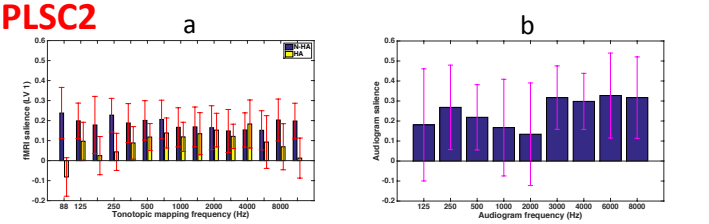

Figure 2: Result for significant latent variable for PLSC2
a) fMRI saliences for hyperacusis HA and non hyperacusis (N-HA) groups. b) Audiogram saliences for audiogram measured frequencies.

Tonotopic map

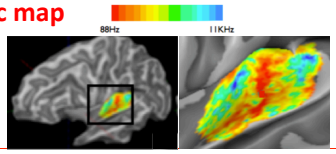

Figure 3: Tonotopic map of a sample subject

Conclusions

- We established **a link between behavioral (audiogram measures) and brain signals (fMRI tonotopy responses)** in tinnitus patients with and without hyperacusis.
- We found that allowing **PLSC** to **split the audiogram** measures **reveals group differences** at **higher and more frequency tones** that if we allow **PLSC to split the fMRI** tonotopic responses. The reason could be that the **functional changes of hyperacusis** in response to different frequency tones at the **cortex level are more general** because of the **homeostatic plasticity** that **doesn't get limited to separate set of voxels**, representing specific frequency tone [4].
- Our results not only reveal this difference in relationship between audiogram and brain signals depending on the hyperacusis condition, but also open new avenues to study the underlying neural mechanisms.

References
[1] D.M Baguley, "Hyperacusis," *Journal of the Royal Society of Medicine*, pp. 582-585, 2003.
[2] S Da Costa et al., "Human Primary Auditory Cortex Follows the Shape of Heschl's Gyrus," *Journal of Neuroscience*, 2011.
[3] AR McIntosh, A Bookstein, F Haxby, and CL Grady, "Spatial pattern analysis of functional brain images using partial least squares," *NeuroImage*, pp. 143-157, 1996.
[4] M Knipper, P Van Dijk, I Nunes, and L Rüttige, "Advances in the neurobiology of hearing disorders: recent developments regarding the basis of tinnitus and hyperacusis," *Progress in neurobiology* , pp. 17-33, 2013.

Acknowledgement
This work was supported by Swiss National Science Foundation, grant number 320030_143989.

Abstract online

Bibliography

[Achard et al., 2006] Achard, S., Salvador, R., Whitcher, B., Suckling, J., and Bullmore, E. (2006). A resilient, low-frequency, small-world human brain functional network with highly connected association cortical hubs. *Journal of Neuroscience*, 26(1):63–72.

[Ashburner, 2009] Ashburner, J. (2009). Preparing fmri data for statistical analysis. *Functional MRI Techniques. Humana Press. Filippi M (ed.)*.

[Axelsson and Ringdahl, 1989] Axelsson, A. and Ringdahl, A. (1989). Tinnitus—a study of its prevalence and characteristics. *British Journal of Audiology*, 23(1):53–62.

[Baguley, 2003] Baguley, D. M. (2003). Hyperacusis. *Journal of the Royal Society of Medicine*, 96(12):582–585.

[Bandettini, 2015] Bandettini, P. A. (2015). The birth of functional mri at the medical college of wisconsin. In *fMRI: From Nuclear Spins to Brain Functions*, pages 11–18. Springer.

[Barnes et al., 2010] Barnes, K. A., Cohen, A. L., Power, J. D., Nelson, S. M., Dosenbach, Y. B. L., Miezin, F. M., Petersen, S. E., and Schlaggar, B. L. (2010). Identifying basal ganglia divisions in individuals using resting-state functional connectivity MRI. *Frontiers in systems neuroscience*, 4:7–11.

[Beckmann et al., 2005] Beckmann, C. F., DeLuca, M., Devlin, J. T., and Smith, S. M. (2005). Investigations into resting-state connectivity using independent component analysis. *Philosophical transactions of the Royal Society of London. Series B, Biological sciences*, 360(1457):1001–13.

[Beisteiner et al., 2011] Beisteiner, R., Robinson, S., Wurnig, M., Hilbert, M., Merksa, K., Rath, J., Höllinger, I., Klinger, N., Marosi, C., Trattnig, S., et al. (2011). Clinical fmri: evidence for a 7t benefit over 3t. *Neuroimage*, 57(3):1015–1021.

[Biswal et al., 1995] Biswal, B., Zerrin Yetkin, F., Haughton, V. M., and Hyde, J. S. (1995). Functional connectivity in the motor cortex of resting human brain using echo-planar mri. *Magnetic resonance in medicine*, 34(4):537–541.

[Breakspear, 2008] Breakspear, L. K. (2008). Nonlinear Dynamic Causal Models for {FMRI}. 42(2):649–662.

[Buxton, 2009] Buxton, R. B. (2009). *Introduction to functional magnetic resonance imaging: principles and techniques*. Cambridge university press.

[Chen et al., 2008] Chen, S., Ross, T. J., Zhan, W., Myers, C. S., Chuang, K.-S., Heishman, S. J., Stein, E. A., and Yang, Y. (2008). Group independent component analysis reveals consistent resting-state networks across multiple sessions. *Brain research*, 1239:141–151.

[Cordes et al., 2000] Cordes, D., Haughton, V. M., Arfanakis, K., Wendt, G. J., Turski, P. A., Moritz, C. H., Quigley, M. A., and Meyerand, M. E. (2000). Mapping functionally related regions of brain with functional connectivity mr imaging. *American Journal of Neuroradiology*, 21(9):1636–1644.

[Da Costa et al., 2011] Da Costa, S., van der Zwaag, W., Marques, J. P., Frackowiak, R. S. J., Clarke, S., and Saenz, M. (2011). Human Primary Auditory Cortex Follows the Shape of Heschl's Gyrus. *The Journal of Neuroscience*, 31(40):14067–14075.

[Daunizeau et al., 2011] Daunizeau, J., David, O., and Stephan, K. E. (2011). Dynamic causal modelling: a critical review of the biophysical and statistical foundations. *Neuroimage*, 58(2):312–322.

[De Luca et al., 2006] De Luca, M., Beckmann, C. F., De Stefano, N., Matthews, P. M., and Smith, S. M. (2006). fMRI resting state networks define distinct modes of long-distance interactions in the human brain. *NeuroImage*, 29(4):1359–1367.

[De Martino et al., 2015] De Martino, F., Moerel, M., Xu, J., van de Moortele, P.-F., Ugurbil, K., Goebel, R., Yacoub, E., and Formisano, E. (2015). High-Resolution Mapping of Myeloarchitecture In Vivo: Localization of Auditory Areas in the Human Brain. *Cerebral Cortex (New York, N.Y.: 1991)*, 25(10):3394–3405.

[Dick et al., 2012] Dick, F., Tierney, A. T., Lutti, A., Josephs, O., Sereno, M. I., and Weiskopf, N. (2012). In vivo functional and myeloarchitectonic mapping of human primary auditory areas. *The Journal of Neuroscience: The Official Journal of the Society for Neuroscience*, 32(46):16095–16105.

[Dougherty et al., 2008] Dougherty, D. D., Rauch, S. L., and Rosenbaum, J. F. (2008). *Essentials of neuroimaging for clinical practice*. American Psychiatric Pub.

[Eggermont and Komiya, 2000] Eggermont, J. J. and Komiya, H. (2000). Moderate noise trauma in juvenile cats results in profound cortical topographic map changes in adulthood. *Hearing research*, 142(1-2):89–101.

[Eggermont and Tass, 2015] Eggermont, J. J. and Tass, P. A. (2015). Maladaptive neural synchrony in tinnitus: origin and restoration. *Neuro-otology*, 6:29.

[Elgoyhen et al., 2015] Elgoyhen, A. B., Langguth, B., De Ridder, D., and Vanneste, S. (2015). Tinnitus: perspectives from human neuroimaging. *Nature Reviews Neuroscience*, 16(10):632–642.

[Engel, 2012] Engel, S. A. (2012). The development and use of phase-encoded functional MRI designs. *NeuroImage*, 62(2):1195–1200.

[Engineer et al., 2011] Engineer, N. D., Riley, J. R., Seale, J. D., Vrana, W. A., Shetake, J. A., Sudanagunta, S. P., Borland, M. S., and Kilgard, M. P. (2011). Reversing pathological neural activity using targeted plasticity. *Nature*, 470(7332):101–104.

[Faro and Mohamed, 2010] Faro, S. H. and Mohamed, F. B. (2010). *BOLD fMRI: A guide to functional imaging for neuroscientists*. Springer Science & Business Media.

[Flor et al., 2006] Flor, H., Nikolajsen, L., and Jensen, T. S. (2006). Phantom limb pain: a case of maladaptive cns plasticity? *Nature Reviews Neuroscience*, 7(11):873–881.

[Friston et al., 2003] Friston, K. J., Harrison, L., and Penny, W. (2003). Dynamic causal modelling. *NeuroImage*, 19(4):1273–1302.

[Friston et al., 2014] Friston, K. J., Kahan, J., Biswal, B., and Razi, A. (2014). A dcm for resting state fmri. *Neuroimage*, 94:396–407.

[Ghazaleh et al., 2017] Ghazaleh, N., Van der Zwaag, W., Clarke, S., Van De Ville, D., Maire, R., and Saenz, M. (2017). High-resolution fmri of auditory cortical map changes in unilateral hearing loss and tinnitus. *Brain topography*, pages 1–13.

[Golland et al., 2008] Golland, Y., Golland, P., Bentin, S., and Malach, R. (2008). Data-driven clustering reveals a fundamental subdivision of the human cortex into two global systems. *Neuropsychologia*, 46(2):540–553.

[Greicius et al., 2007] Greicius, M. D., Flores, B. H., Menon, V., Glover, G. H., Solvason, H. B., Kenna, H., Reiss, A. L., and Schatzberg, A. F. (2007). Resting-state functional connectivity in major depression: abnormally increased contributions from subgenual cingulate cortex and thalamus. *Biological psychiatry*, 62(5):429–437.

[Greicius et al., 2009] Greicius, M. D., Supekar, K., Menon, V., and Dougherty, R. F. (2009). Resting-state functional connectivity reflects structural connectivity in the default mode network. *Cerebral cortex*, 19(1):72–78.

[Guinchard et al., 2016] Guinchard, A.-C., Ghazaleh, N., Saenz, M., Fornari, E., Prior, J., Maeder, P., Adib, S., and Maire, R. (2016). Study of tonotopic brain changes with functional mri and fdg-pet in a patient with unilateral objective cochlear tinnitus. *Hearing research*, 341:232–239.

[Hampson et al., 2002] Hampson, M., Peterson, B. S., Skudlarski, P., Gatenby, J. C., and Gore, J. C. (2002). Detection of functional connectivity using temporal correlations in mr images. *Human brain mapping*, 15(4):247–262.

[Harms and Melcher, 2002] Harms, M. P. and Melcher, J. R. (2002). Sound repetition rate in the human auditory pathway: representations in the waveshape and amplitude of fMRI activation. *Journal of neurophysiology*, 88(3):1433–50.

[Heeger and Ress, 2002] Heeger, D. J. and Ress, D. (2002). What does fmri tell us about neuronal activity? *Nature Reviews Neuroscience*, 3(2):142–151.

[Henson and Rugg, 2001] Henson, R. and Rugg, M. D. (2001). Effects of stimulus repetition on latency of bold impulse response. *NeuroImage*, 13(6):683.

[Hillary et al., 2002] Hillary, F. G., Steffener, J., Biswal, B. B., Lange, G., DeLuca, J., and Ashburner, J. (2002). Functional magnetic resonance imaging technology and traumatic brain injury rehabilitation: guidelines for methodological and conceptual pitfalls. *The Journal of head trauma rehabilitation*, 17(5):411–430.

[Huettel et al., 2004] Huettel, S. A., Song, A. W., and McCarthy, G. (2004). *Functional magnetic resonance imaging*, volume 1. Sinauer Associates Sunderland.

[Kaltenbach, 2011] Kaltenbach, J. A. (2011). Tinnitus: Models and mechanisms. *Hearing Research*, 276(1–2):52–60.

[Kim et al., 2010] Kim, J.-H., Lee, J.-M., Jo, H. J., Kim, S. H., Lee, J. H., Kim, S. T., Seo, S. W., Cox, R. W., Na, D. L., Kim, S. I., and Saad, Z. S. (2010). Defining functional SMA and pre-SMA subregions in human MFC using resting state fMRI: functional connectivity-based parcellation method. *NeuroImage*, 49(3):2375–2386.

[Langers et al., 2012] Langers, D. R. M., de Kleine, E., and van Dijk, P. (2012). Tinnitus does not require macroscopic tonotopic map reorganization. *Frontiers in Systems Neuroscience*, 6.

[Li et al., 2015] Li, Q., Song, M., Fan, L., Liu, Y., and Jiang, T. (2015). Parcellation of the primary cerebral cortices based on local connectivity profiles. *Frontiers in neuroanatomy*, 9.

[Li, 2014] Li, X. (2014). *Functional magnetic resonance imaging processing*. Springer.

[Lowe et al., 1998] Lowe, M., Mock, B., and Sorenson, J. (1998). Functional connectivity in single and multislice echoplanar imaging using resting-state fluctuations. *Neuroimage*, 7(2):119–132.

[Margulies et al., 2007] Margulies, D. S., Kelly, A. C., Uddin, L. Q., Biswal, B. B., Castellanos, F. X., and Milham, M. P. (2007). Mapping the functional connectivity of anterior cingulate cortex. *Neuroimage*, 37(2):579–588.

[Melcher et al., 2000] Melcher, J. R., Sigalovsky, I. S., Guinan, J. J., and Levine, R. A. (2000). Lateralized tinnitus studied with functional magnetic resonance imaging: abnormal inferior colliculus activation. *Journal of Neurophysiology*, 83(2):1058–1072.

[Naumer and Kaiser, 2010] Naumer, M. J. and Kaiser, J. (2010). *Multisensory object perception in the primate brain*. Springer.

[Newman, 2006] Newman, M. E. (2006). Modularity and community structure in networks. *Proceedings of the national academy of sciences*, 103(23):8577–8582.

[Noppeney et al., 2006] Noppeney, U., Penny, W., et al. (2006). Two approaches to repetition suppression. *Human brain mapping*, 27(5):411–416.

[Noreña and Eggermont, 2003] Noreña, A. J. and Eggermont, J. J. (2003). Changes in spontaneous neural activity immediately after an acoustic trauma: implications for neural correlates of tinnitus. *Hearing Research*, 183(1-2):137–153.

[Noreña and Eggermont, 2005] Noreña, A. J. and Eggermont, J. J. (2005). Enriched acoustic environment after noise trauma reduces hearing loss and prevents cortical map reorganization. *The Journal of Neuroscience: The Official Journal of the Society for Neuroscience*, 25(3):699–705.

[Palacios et al., 2013] Palacios, E. M., Sala-Llonch, R., Junque, C., Roig, T., Tormos, J. M., Bargallo, N., and Vendrell, P. (2013). Resting-state functional magnetic resonance imaging activity and connectivity and cognitive outcome in traumatic brain injury. *JAMA neurology*, 70(7):845–851.

[Roberts et al., 2010] Roberts, L. E., Eggermont, J. J., Caspary, D. M., Shore, S. E., Melcher, J. R., and Kaltenbach, J. A. (2010). Ringing Ears: The Neuroscience of Tinnitus. *The Journal of Neuroscience*, 30(45):14972–14979.

[Robitaille and Berliner, 2007] Robitaille, P.-M. and Berliner, L. (2007). *Ultra high field magnetic resonance imaging*, volume 26. Springer Science & Business Media.

[Salloum et al., 2016] Salloum, R., Sandridge, S., Patton, D., Stillitano, G., Dawson, G., Niforatos, J., Santiago, L., and Kaltenbach, J. A. (2016). Untangling the effects of tinnitus and hypersensitivity to sound (hyperacusis) in the gap detection test. *Hearing research*, 331:92–100.

[Salloum et al., 2014] Salloum, R. H., Yurosko, C., Santiago, L., Sandridge, S. A., and Kaltenbach, J. A. (2014). Induction of enhanced acoustic startle response by noise exposure: dependence on exposure conditions and testing parameters and possible relevance to hyperacusis. *PloS one*, 9(10):e111747.

[Schaette, 2014] Schaette, R. (2014). Tinnitus in men, mice (as well as other rodents), and machines. *Hearing Research*, 311:63–71.

[Schaette and McAlpine, 2011] Schaette, R. and McAlpine, D. (2011). Tinnitus with a Normal Audiogram: Physiological Evidence for Hidden Hearing Loss and Computational Model. *The Journal of Neuroscience*, 31(38):13452–13457.

[Schnupp et al., 2011] Schnupp, J., Nelken, I., and King, A. (2011). *Auditory neuroscience: Making sense of sound*. MIT press.

[Seeley et al., 2007] Seeley, W. W., Menon, V., Schatzberg, A. F., Keller, J., Glover, G. H., Kenna, H., Reiss, A. L., and Greicius, M. D. (2007). Dissociable intrinsic connectivity networks for salience processing and executive control. *Journal of Neuroscience*, 27(9):2349–2356.

[Seki and Eggermont, 2003] Seki, S. and Eggermont, J. J. (2003). Changes in spontaneous firing rate and neural synchrony in cat primary auditory cortex after localized tone-induced hearing loss. *Hearing Research*, 180(1-2):28–38.

[Shen et al., 2010] Shen, X., Papademetris, X., and Constable, R. T. (2010). Graph-theory based parcellation of functional subunits in the brain from resting-state fmri data. *Neuroimage*, 50(3):1027–1035.

[Stephan et al., 2004] Stephan, K. E., Harrison, L. M., Penny, W. D., and Friston, K. J. (2004). Biophysical models of fmri responses. *Current opinion in neurobiology*, 14(5):629–635.

[Theodoroff and Folmer, 2013] Theodoroff, S. M. and Folmer, R. L. (2013). Repetitive transcranial magnetic stimulation as a treatment for chronic tinnitus: a critical review. *Otology & Neurotology*, 34(2):199–208.

[Thirion et al., 2006] Thirion, B., Dodel, S., and Poline, J.-B. (2006). Detection of signal synchronizations in resting-state fmri datasets. *Neuroimage*, 29(1):321–327.

[Triantafyllou et al., 2005] Triantafyllou, C., Hoge, R., Krueger, G., Wiggins, C., Potthast, A., Wiggins, G., and Wald, L. (2005). Comparison of physiological noise at 1.5 t, 3 t and 7 t and optimization of fmri acquisition parameters. *Neuroimage*, 26(1):243–250.

[Van Den Heuvel and Pol, 2010] Van Den Heuvel, M. P. and Pol, H. E. H. (2010). Exploring the brain network: a review on resting-state fmri functional connectivity. *European neuropsychopharmacology*, 20(8):519–534.

[Vanneste et al., 2013a] Vanneste, S., Fregni, F., and De Ridder, D. (2013a). Head-to-head comparison of transcranial random noise stimulation, transcranial ac stimulation, and transcranial dc stimulation for tinnitus. *Frontiers in psychiatry*, 4:158.

[Vanneste et al., 2013b] Vanneste, S., Walsh, V., Van De Heyning, P., and De Ridder, D. (2013b). Comparing immediate transient tinnitus suppression using tacs and tdcs: a placebo-controlled study. *Experimental brain research*, 226(1):25–31.

[Wang et al., 2006] Wang, L., Zang, Y., He, Y., Liang, M., Zhang, X., Tian, L., Wu, T., Jiang, T., and Li, K. (2006). Changes in hippocampal connectivity in the early stages of alzheimer's disease: evidence from resting state fmri. *Neuroimage*, 31(2):496–504.

[Weishaupt et al., 2008] Weishaupt, D., Köchli, V. D., and Marincek, B. (2008). *How does MRI work?: an introduction to the physics and function of magnetic resonance imaging*. Springer Science & Business Media.

[Wienbruch et al., 2006] Wienbruch, C., Paul, I., Weisz, N., Elbert, T., and Roberts, L. E. (2006). Frequency organization of the 40-Hz auditory steady-state response in normal hearing and in tinnitus. *NeuroImage*, 33(1):180–94.

[Yang et al., 2011] Yang, S., Weiner, B. D., Zhang, L. S., Cho, S.-J., and Bao, S. (2011). Homeostatic plasticity drives tinnitus perception in an animal model. *Proceedings of the National Academy of Sciences*, 108(36):14974–14979.

[Zeng, 2013] Zeng, F.-G. (2013). An active loudness model suggesting tinnitus as increased central noise and hyperacusis as increased nonlinear gain. *Hearing Research*, 295:172–179.

[Zwaag et al., 2015] Zwaag, W., Schäfer, A., Marques, J. P., Turner, R., and Trampel, R. (2015). Recent applications of uhf-mri in the study of human brain function and structure: a review. *NMR in Biomedicine*.

Naghmeh Ghazaleh

✉ naghmeh.ghazaleh@gmail.com

Education

12.2012-3.2017 **PhD, Neuroscience, EPFL**, Medical Image Processing Laboratory (MIPLAB), Geneva, campus Biotech, Switzerland

- Neuroimaging of human auditory cortex: data analysis and applications

7.2016-8.2016 Exchange, UCL, Functional imaging laboratory London, UK

9.2008-10.2010 **M.Sc, Communication systems, University of Tabriz**, Image processing laboratory, Tabriz, Iran

5.2010-9.2010 Exchange, University of Tehran, Tehran, Iran

9.2003-10.2007 **B.Sc, Electrical engineering-Communications, K.N.Toosi university of technology**, Tehran, Iran

Experiences

12.2012-03.2017 **EPFL, Doctoral assistant,** Medical Image Processing Laboratory (MIPLAB), Geneva, Switzerland

- **Studying high-resolution fMRI of Auditory Cortical Map Changes in Unilateral Hearing Loss and Tinnitus**, In collaboration with CHUV University Hospital.

Tasks: . fMRI experimental designing and data acquisition with 7T MRI scanner

. Studyng the fMRI activity and tonotopic map organization in tinnitus patients

Achievements: - Acquring high resulotion fMRI data set of healthy control and tinnitus patients for task and resting-state fMRI

- Discovering fine organization of the auditory cortex that get altered as result of tinnitus

- Advanced multivariate data analysis.

- **Detection of hyperacusis condition in tinnitus patients based on partial least square correlation (PLSC) features that link audiogram and fMRI tonotopy responses**

Tasks: . Extracting the information from combining fMRI brain data and behavioral audiogram measurement data to detect hyperacusis condition

. Data driven detection of hyperacusis condition in tinnitus patients

Achievements: - Detecting different discrete audiogram measures that can discriminate fMRI data between the two groups of hyperacusis and non-hyperacusis patients

- Designing a preciese classifier for data driven detection of hyperacusis condition, based on the features driven from applying PLSC method

- Obtaining significant and stable results with permutation testing and bootstrapping

7.2016-8.2016 **UCL, Academic visitor**, Welcome Trust Centre for Neuroimaging, Functional Imaging Laboratory, prof.Karl Friston, London, UK

- **Data-driven segmentation of auditory cortex based on brain effective connectivity using resting state fMRI data.**

Tasks: . Discovering the effective connectivity network of the auditory cortex with the other regions in the brain

. Data driven segmentation of the auditory cortex

Achievements: . Successfully estimation of effective connectivity network of auditory cortex with the other regions of the brain using dynamical causal modeling (DCM) of resting state fMRI

. Extracting meaningful features of DCM effective connectivity

. Accurate segmentation of auditory cortex, using graph spectral clustering method

1.2012-10.2012 **CIBM, Research assistant,** Eleonora Fornari group, CHUV, Lausanne, Switzerland

- **Brain thalamus segmentation using diffiusion tensor MRI data and connectivity mapping**

Tasks: . Diffusion MRI analysis of brain thalamus

. Brain thalamus segmentation to find it's different sub-regions

Achievements: . Extracting significant diffusion MRI features of brain thalamus

. Successful data driven segmentation of brain thalamus based on the features derived from diffusion tensor imaging

3.2011-6.2011 **EPFL, Internship,** Signal processing laboratory 4 (LTS4), Lausanne, Switzerland

- **Video motion estimation with regularization using graph cut energy minimization**

Tasks: . Video motion estimation

. Applying graph cut energy minimization algorithm

Achievements: . Successful estimation of motion in video frames based on spatio-temporal regularization method

7.2011-10.2011 **EPFL, Internship,** Signal processing laboratory 2 (LTS2), Lausanne, Switzerland

- **Graph classification with optimization and semi supervised learning**

Tasks: . Design a semi-supervised classifier to learn from a limited number of labeled data

Achievements: . Successful classification of graph with applying optimization and spectral clustering algorithm on graph

7.2011-10.2011 **University of Tabriz, Master project,** Tabriz, Iran

- **Watermarking and visual cryptography for images of visual sensor networks**

Tasks: . Designing a secure method to share images in a visual sensor network

Achievements: . Successful design a secure image sharing method using watermarking of the owner signature and visual cryptography

1.2008-7.2008 **Pouyandan Company, Research engineer,** Tehran, Iran

- **Exploring the application of variable speed drives for gas and oil pumps of Tehran oil refining company**

Tasks: . Preparing a scientific report about the state of the art applications of variable speed drive motors in oil industry

Achievements: . The report got prepared and Tehran oil refining company took a great advantage of it and was a great success for Pouyandan company

9.2003-10.2007 **K.N.Toosi university of Technology, Bachelor project,** Tehran, Iran

- **Voice over IP (VOIP) software designing to transfer voice signal via Internet and recording and remotely replaying**

Tasks: . Designing a VOIP software

Achievements: . A reliable VOIP software has been designed using multi-thread visual C++ program with the option of recording and remotely replaying the voice

Achievements

8.2016 **Member of the winning team of Novartis International Biotechnology Leadership Camp 2106 .**

- Getting accepted to participate in 3 days Novartis International Biotechnology Leadership Camp 2016. 60 people got accepted among many applicants from around the world. We learned about trends and challenges in the biotech company. In parallel, working in groups, we have been provided by a real challenge that Novartis is dealing with and we were asked to design a business plan with the goal of solving this problem. Our team successfully won the competition for presenting the best business plan. My participation was with designing a machine learning based method to detect the strength of a disease to discover the effect of the drugs on improving the disorder.

10.2010 **M.Sc thesis honorably funded by the Iran Telecommunication Research Center (ITRC).**

Computer skills

Languages Matlab, R, Python, C, C++, Visual C++

Software FSL, Freesurfer, SPM, Brainvoyager, Latex, Microsoft office

Languages

Farsi Native *Mother Tongue*

English Fluent *Daily practice*

French Intermediate *B1/B2 level*

Teaching experience

2016-2017 Auditory Neuroscience (tinnitus session), lecturer

2012-2015 Image processing, Teacher Assistant

2012-2015 Signal processing for functional brain imaging, Teacher Assistant and lecturer

2015 Neuroscience for engineers, Teacher Assistant

Reference

Prof.Dimitri Van de ville
Associate Professor
MIPLAB, EPFL, Campus Biotech, H4
Ch. des Mines 9
CH-1202 Geneva, Switzerland
✉ dimitri.vandeville@epfl.ch

Dr.Raphael Maire
Head of audiology and otoneurology unit in university
hospital of Lausanne (CHUV)
CH-1011 Lausanne, Switzerland
✉ Raphael.maire@chuv.ch

Publications

Journals

2017 N. Ghazaleh, W. Van der Zwaag, R. Maire, D. Van De Ville S. Clarke and M. Saenz, *High-Resolution fMRI of Auditory Cortical Map Changes in Unilateral Hearing Loss and Tinnitus.* Brain topography, 1-13.

2016 A-C. Guinchard, N. Ghazaleh, M. Saenz, E. Fornari, J. O. Prior, P. Maeder, S. Adib, and R. Maire, *Study of tonotopic brain changes with functional MRI and FDG-PET in a patient with unilateral objective cochlear tinnitus.* Hearing Research 341.

2016 G. Battistella, E. Najdenovska, P. Maeder, N. Ghazaleh, A. Daducci, J. Thiran, S. Jacquemont, C. Tuleasca, M. Levivier, M. Bach Cuadra, E. Fornari, *Robust Thalamic Nuclei Segmentation Method Based on Local Diffusion Magnetic Resonance Properties.* Brain Structure and Function.

N. Ghazaleh, W. Van der Zwaag, R. Maire, M. Saenz and D. Van De Ville., *Detection of hyperacusis condition in tinnitus patients based on PLSC features that link audiogram and fMRI tonotopy responses.* Front. Syst. Neurosci, submitted.

N. Ghazaleh, A. Razi, K. Friston, M. Saenz and D. Van De Ville., *Data driven parcellation of auditory cortex based on brain effective connectivity using resting state fMRI data..* Journal of Neuroscience, in preparation.

Conferences

2016 N. Ghazaleh, W. Van der Zwaag, R. Maire, M. Saenz and D. Van De Ville., *Relating audiogram measures and fMRI tonopic responses in tinnitus with and without hyperacusis.* Organization for Human Brain Mapping, OHBM2016, Geneva, Switzerland, 2016.

2015 N. Ghazaleh, W. Van der Zwaag, R. Maire, M. Saenz and D. Van De Ville., *Detection of hyperacusis condition in tinnitus patients based on PLSC features that link audiogram and fMRI tonotopy responses.* Machine learning for health care workshop, NIPS2015, Montreal, December, 2015.

2014 N. Ghazaleh, W. Van der Zwaag, R. Maire and M. Saenz., *High-field functional MRI (7 Tesla) mapping of Tonotopy in Human primary auditory cortex in patients with unilateral hearing loss and tinnitus.* Society for Neuroscience, Washington, DC, November, 2014.

2014 N. Ghazaleh, W. Van der Zwaag, R. Maire and M. Saenz, *Lateralization of the primary auditory cortex, in patients with unilateral tinnitus.* 5th International Conference on Auditory Cortex, Magdeburg, Germany, September, 2014.

2013 O. Joly, N. Ghazaleh, S. Kumar, S. Baumann, G. Chapuis and M. Saenz , *Tonotopic organization in monkey and human auditory cortex using phase-encoded functional MRI.* The Tucker-Davis Technologies (TDT) Symposium on Advances and Perspectives in Auditory Neurophysiology (APAN), San Diego, USA, November, 2013.

2013 G. Battistella, N. Ghazaleh, E. Fornari, E. Najdenovska, M. Bach Cuadra, *A new approach for cerebello-thalamic motor network evaluation in asymptomatic premutation carriers at risk for FXTAS.* Organization for Human Brain Mapping, OHBM2013, Seattle, USA, 2013.

2011 N. Ghazaleh, A. Aghagolzadeh and H. Seyedarabi , *Watermarking based on Visual Cryptography and Discrete Wavelet Transform.* The 11th IEEE International Conference on Computer and Information Technology, Pafos, Cypros, September, 2011.